# THE EFFECTS OF ULTRASOUND, CHILLING AND ANNEALING TREATMENTS ON THE PHYSICOCHEMICAL PROPERTIES AND GLYCEMIC INDEX OF THAI RICE

**KANNIKA KUNYANEE**

**A DISSERTATION SUBMITTED IN PARTIAL FULFILLMENT**

**OF THE REQUIREMENTS FOR THE DEGREE OF**

**DOCTOR OF PHILOSOPHY IN FOOD SCIENCE**

**FACULTY OF FOOD INDUSTRY**

**KING MONGKUT'S INSTITUTE OF TECHNOLOGY LADKRABANG**

**2020**

**KMITL-2020-FI-D-051-361**

| | |
|---|---|
| **Dissertation Title** | The effects of ultrasound, chilling and annealing treatments on the physicochemical properties and glycemic index of Thai rice |
| **Student** | Miss Kannika Kunyanee |
| **Student ID.** | 57608001 |
| **Degree** | Doctor of Philosophy (Food Science) |
| **Program** | Food Science |
| **Year** | 2020 |
| **Thesis Advisor** | Assistant Professor Dr. Naphatrapi Lungsakul |

# ABSTRACT

Rice is an important economic crop of any country in Asian, especially, Thailand. Rice is important both for consumption (as main food of people) and export (as a major agricultural export product of Thailand). Rice is rich in carbohydrate, some protein, and minerals, and can have a high glycemic index (GI) values in a range from 75 to 83. Thus, it unsuitable for many people with diabetes. There have been the modification methods to reduce glycemic index by limits the accessibility of the digestive enzymes on starch molecules. Therefore, this study focused on to lower GI by ultrasound, chilling, and annealing treatments in three Thai rice cultivars: Glutinous rice (RD6), Khao Dawk Mali 105 (KDML105) and Chai-Nat1 (CN1). Their physicochemical properties (crystallinity, pasting properties, thermal properties) and *in vitro* digestibility were investigated. Three rice cultivars were modified with ultrasound for 15 and 30 min and at 40, 70, and 100% of ultrasound power levels. Then, all of the ultrasound treated rice were stored at $4^{o}$C for 24 h. The results showed that increase in sonication times and ultrasound power showed decreased crystallinity but were not changed FITR pattern and X-ray diffraction pattern. The decrease in peak viscosity was found in RD6 while KDML105 and CN1 showed increased peak viscosity as compared to native. Moreover, increase in sonication times and ultrasound power levels induced the kinetic rate constant (k-value), hydrolysis index (HI) and expected glycemic index (eGI) increased with longer time and higher power. The chilled rice after ultrasound treatments demonstrated that the ratio of crystalline to amorphous, and $\Delta$H increased, while k-value, HI and

eGI decreased compared to their ultrasound treatment. Thus, the conditions of ultrasound before chilling treatments were selected to produce the lower glycemic index for further study, which were 15 min at 100% of ultrasound power for RD6, 15min at 70% of ultrasound power for KDML105 and CN1 rice cultivars with chilling treatment, respectively.

For the annealing treatments (at 45, 50 or 55$^{o}$C) were used after ultrasound-chilled rice of three rice cultivars. The samples were then evaluated for their crystallinity, pasting properties gelatinization properties and *in vitro* glycemic index (k-value, HI, and eGI). The increased annealing temperatures contributed to change in properties of starch, which increased relative crystallinity had direct effect on increased pasting temperature, onset temperature, and gelatinization enthalpy of ultrasound-chilled followed annealing treatments (UC+ANN) in all rice cultivars. In addition, UC+ANN significance ($p$<0.05) decrease in k-value, hydrolysis index and promoted a decrease in their glycemic index. The combination of these treatments reduced glycemic index to 76.78 for RD6, which is ranked as high. But the reduced glycemic index to 63.18 and 54.03 for KDML105 and CN1, respectively, which are ranked as intermediate. However, reduction of eGI for three rice cultivars of this study depends on conditions and cultivars. Therefore, modified rice condition to lower glycemic index of RD6, KDML105 and CN1 rice was UC+ANN45, UC+ANN50 and UC+ANN55, respectively.

# ACKNOWLEDGEMENTS

There are so many people who deserve my most sincere gratitude. Their support and encouragement have been tremendous strength for me throughout my studies at King Mongkut's Institute of Technology Ladkrabang. First of all, I wish to express my sincere appreciation to my thesis supervisor Asst. Prof. Dr. Napathrapi Luangsakul for her support, expert supervision, encouragement, and advice throughout my studies and thesis writing.

I would like to appreciate my committee members: Asst. Prof. Dr. Suched Samuhasaneetoo, Asst. Prof. Dr. Yuporn Puechkamut, Asst. Prof. Dr. Soraya Kerdpiboon and Dr. Weerachat Sompong for their valuable advising, suggesting, and reviewing my thesis.

I greatly appreciate Professor Dr. Anthony Keith Thompson for his helps and suggests my manuscripts. Thanks, are also extended to Asst. Prof. Dr. Kallayanee Tengpongsathon for her guides and teaches in statistical analysis.

I also thanks to Onvara Ritudomphol, Chanakarn Jancila, Waleeporn Vacikarat, Kalyalak Phuruen, Patinya Virulchatapan, Kodchawan Chaturattanachaiporn, and Nialmas Samuela (graduate students) for their friendship and support during my stay in the department.

The author also wishes to express sincere appreciation to my family, especially my dad (Narawut Kunyanee), mom (Vantana Kunyanee), sister (Chanikarn Kunyanee), and Satit Pracomethai, who continuously give me love and supports, which serve as inspiration throughout my life.

Kannika Kunyanee

# TABLE OF CONTENTS

**PAGE**

# TABLE OF CONTENTS (Cont.)

**PAGE**

# TABLE OF CONTENTS (Cont.)

**PAGE**

# TABLE OF CONTENTS (Cont.)

**PAGE**

# TABLE OF CONTENTS (Cont.)

**PAGE**

# LIST OF TABLES

**TABLE** **PAGE**

# LIST OF TABLES (Cont.)

**TABLE** **PAGE**

# LIST OF TABLES (Cont.)

**TABLE** **PAGE**

# LIST OF FIGURES

**FIGURE** **PAGE**

# LIST OF TABLES (Cont.)

**TABLE** **PAGE**

# CHAPTER 1

# INTRODUCTION

## 1.1 General background

World Health Organization (WHO) (2018) reported an increase in prevalent of diabetes in recent years associated with chronic disease. It is estimated that the number of diabetes sufferers in the world will increase from the current figure of 190 million to 420 million during the next 25 years. Consumption of high carbohydrates food is a factor develop risk of type II diabetes (Mohan et al., 2010; Kaur, B. et al., 2016). This draws a lot of researcher's attention to find ways to prevent diabetes. Dietary intervention methods are the cornerstone of diabetes prevention and management which aims primarily at maintaining a low and stable blood glucose level after consumption of carbohydrate foods (Kaur, B. et al., 2016). Therefore, the concept of glycemic index (GI) is a scale that ranks carbohydrate foods by how much they raise blood glucose levels. The GI scale ranks as a high GI (≥70), medium GI (55-69), and low GI (≤ 55), based on their glucose raising potential compared to the reference known as glucose solution or white bread (Jenkins et al., 1981). Many studies reported that consumption of low GI food has beneficial effects on glucose control which could be helpful in reducing and preventing the risk of diabetes (Chen et al., 2010; Kaur, Bhupinder et al., 2016). Although a high consumption of simple carbohydrates, such as glucose and maltose, have historically been regarded as the greater development risk of type II diabetes, recent data conclusively shows that carbohydrates, such as starches, can produce high blood glucose levels (Willett et al., 2002; Kayode et al., 2009).

Rice (*Oryza sativa*) is the most widely consumed staple in the world. Ninety percent of rice contains starch, which is the main energy source. Asia has the highest consumption of rice. White rice is the most popular eaten form as compared to brown rice that is regularly consumed in some area. Additionally, white rice is one of the main foods and source of carbohydrates for a large segment of Thai population with around 10 million tons of white rice. However, high consumption of white rice can affect blood glucose levels and is not considered suitable for diabetics since it may be a factor in the prevalence of type II diabetes in humans. (Miller et al., 1992; Silva et al.,

2017). The GI of rice have been reported that in a range from medium to high GI (Frei et al., 2003; Guo et al., 2015). Normally, amylose content of rice relates to the GI and its impacts on the GI. Rice with high amylose content (25-33 %) is presents low GI. Some of the most common types consumed of rice in Thailand for consuming are Thai Jasmine rice (Hom Mali rice) and glutinous rice (Khao Neow), respectively, which have been reported to exhibit high GI in a range of 70.3 - 92.0 (Frei et al., 2003; Jaisut et al., 2008; Guo et al., 2015). However, the variability in the GI of rice can be attributed to various factors, including dietary fiber content, physical properties (particularly gelatinization properties), amylose-lipid complexes, and cooking (gelatinization) (Wani et al., 2012).

In order to reduce the GI of rice, the main idea is modifying the rice resistant to enzymatic hydrolysis. There are many techniques used to reduce the GI, such as genetical modifications (Fitzgerald et al., 2011), chemical modifications (Zieba et al., 2010), enzymatic modifications (Berry, 1986; Guraya, James, & Champagne, 2001; Shin et al., 2004; Shin, Kim, Ha, Lee and Moon, 2005), and physical modifications, such as gelatinization-retrogradation (Dundar & Gocmen, 2013), and hydrothermal treatment (Chung, H.-J. et al., 2009). Furthermore, a study reported by Wang et al. (2015) found that chilling rice at low temperature might arise more ordered structure of starch granule, resulting in a compact structure of starch granule. Zia et al. (2017) also reported that the suitable method used for modifying starch to reduce GI on food is the physical methods as it is simple and environmental-friendly. Mostly, physicochemical modification methods have applied to reduce the glycemic index in starch, including heat moisture treatment (HMT) and annealing treatment (ANN) (Zavareze & Dias, 2011; Afolabi et al., 2018; Xu, Saleh, Gong, et al., 2018). HMT is a modification method that involves at low moisture content (10-30%) at high temperatures (90-120$^{o}$C) for a period of time. Annealing (ANN) is a modification of starch with the presence of medium water content (40-55%) or higher water content (>60%) for an extended period of time and performed at a temperature above the glass transition but below the gelatinization temperature of starch (Gomes et al., 2005; Liu, Yu, et al., 2009; Dias et al., 2010). According to Gunaratne and Hoover (2002) reported that HMT treatment promoted the distribution of crystallinity in starch leading to enzyme can easily attract within starch granules. While ANN treatment changed the physicochemical properties of starch but did not destroy the structure of starch (Dias et al., 2010). ANN treatment changed the starch properties, including gelatinization

temperatures, especially onset temperature and changed in gelatinization enthalpy, and pasting properties, especially crystallinity improvement. (Gomes et al., 2004; Waduge et al., 2006; Wang et al., 2017). These effects made the starch granule more stable by strengthening the links between the molecules of amylopectin-amylose and/or amylose-amylose chain which leads to slow digestibility of starch (Chung et al., 2009).

Ultrasound is another physical modification method for starch modification that has been shown advantages in term of reduced chemical processing time, and safe. The term of ultrasound is the sound waves at a frequency above threshold of human hearing range (>16 kHz). The effect of ultrasound acoustic results from cavitation, which refers to the formation, growth, and rapid collapse of microbubbles. As a result of this treatment, the starch chains near the collapsing microbubbles lead to the breakage of macromolecular C-C bonds which impact on starch properties (Manchun et al., 2012; Monroy et al., 2018). Many studies have reported that the molecular structure and properties of starch changed after ultrasound treatment (Wang & Wang, 2004; Zuo et al., 2009; Polesi & Sarmento, 2011). Huang et al. (2007) reported that the increase in gelatinization temperatures increased gelatinization enthalpy of maize starch after ultrasound treatment. Jambrak et al. (2010) reported that ultrasound treatment affected on the properties of starch including solubility, swelling power, and viscosity. However, the effects of ultrasound on starch depend on its parameters such as power, frequency, amplitude, time, and temperature of ultrasonication. Nevertheless, using ultrasound is highly changed in physicochemical properties of starch, but does not help for lowering the glycemic index of starch. Some studies have used the combinations of ultrasound with others physical methods, such as annealing treatment. Previously, studies have used ultrasound and annealing treatments in starches which highly presented effect on crystallinity increased. Pinto et al. (2015) reported the increase in the crystallinity and gelatinization temperatures of pinhão starch with the combination of ultrasound-annealed pinhão starch. Babu et al. (2019) reported the combination of ultrasound-chilled foxtail millet (*Panicum italicum*) starch with annealing treatment showed a higher crystallinity than its native and increased the onset temperature ($T_o$), gelatinization enthalpy ($\Delta H$) and pasting temperature (PT) as compared to the native. However, there are limited information about the effect of the combination of ultrasound and annealing treatments on the glycemic index. Thus, the combination of the ultrasound and annealing treatment is interesting to apply on rice grains for lowering the rice glycemic index and

to study their effects on physicochemical properties and the glycemic index. Furthermore, the information about ultrasound and chilling treatment before annealing treatment on the glycemic index and physicochemical properties of rice is also limited.

Thus, the objective of this research aims to apply the combined physical modification methods of ultrasound, chilling, and annealing treatments for lowering the glycemic index of three types of rice differing in amylose content and to determine physicochemical properties of the modified rice.

## 1.2 Objectives

1.2.1 To study the effects of the combination of ultrasound and chilling treatment on physicochemical properties and *in vitro* glycemic index of Thai rice with differing amylose content.

1.2.2 To study the effects of the combination of physical modifications on physicochemical properties and in *vitro* glycemic index of Thai rice with differing amylose content.

## 1.3 Scopes of research

2.3.1 This research studied the effects of ultrasound treatment with or without chilling treatment on the physicochemical properties and *in vitro* glycemic index of rice grains. The rice grains were used in three different rice cultivars and different amylose content including with glutinous rice (RD6), Khao Dawk Mali 105 (KDML105) and Chai-Nat1 cultivar (CN1). Three rice cultivars were treated with ultrasound for 15 and 30 min at various amplitude frequency levels of 40%, 70% and 100% of ultrasound power (60 kHz). Then, a half of rice treated ultrasound sample of three rice cultivars was stored in 4$^{o}$C for 24 h. The ultrasound treated rice samples and ultrasound-chilled rice samples were dried to 11 ± 1% of moisture content. All rice samples were analyzed the ratio of crystalline to amorphous and their chemical compositions, relative crystalline and their crystalline structure, pasting properties, thermal properties, and *in vitro* glycemic index.

2.3.2 The rice sample of three rice cultivars was selected from the lowest glycemic index of each rice cultivars to improve the glycemic index using annealing treatment (ANN). Therefore, this part was studied the effects of ANN treatment on properties and *in vitro* glycemic index of three rice cultivars. Three rice cultivars were treated with ANN treatment in the different conditions at 45, 50, or 55$^{o}$C for 16 h. The annealed rice grains of three rice cultivars were analyzed relative

crystalline and their crystalline structure, pasting properties, thermal properties, and *in vitro* glycemic index.

# CHAPTER 2

# LITERTURE REVIEW

## 2.1 Rice

### 2.1.1 Definition and characteristic of rice

Rice is grass family (Gramineae) belong to the genus *Oryza.* There are numerous varieties of rice, but the two most cultivated species are *Oryza sativa* Linn (*O. sativa* Linn) and Oryza *glaberrima* Steud (*O. glaberrima* Steud) (Sitch, 1990; Juliano, 1993). Cultivars of these varieties can grow in a wide range of water and soil regimes, from deeply flooded land to dry, hilly slopes. In Thailand, rice is grown in the provinces which is found in the upper northern, lower northern, central, upper northeastern, lower northeastern and southern plains. Rice is a staple food of Asia, especially Thailand (Walter et al., 2008; Brand-Miller et al., 2009; Wani et al., 2012) which estimated consumption in 2017-2018 was 142.7 million tons. Moreover, rice is an important export product of Thailand which brings income to ten billion baht per year (Office of Agricultural Economics, 2018).

Rice classified into three types according to their phenotype appearance: 1) *Indica* long grains, 2) *Javanica* broad thick grains and 3) *Japonica* thick and short grains. There exist waxy and non-waxy types within each of these sub-species and they can be different base on their cooking characteristics. The physiological difference of rice grains subspecies as shown in Figure 2.1.


**Figure 2.1** Rice grains photograph of sub-species of Indica (a), Javanica (b) and Japonica (c).

**Source**: Ogawa (2016)

In addition, rice be able to classify in many categories based on their major characteristics such as kernel length, shape, and amylose content (Patindol et al., 2015). Furthermore, amylose content is used to classify and is positively correlated with hardness and negatively correlated with stickiness. Juliano (1992) reported that amylose content of rice is classified as waxy, very low amylose, low amylose, medium amylose, and high amylose (as showed in Table 2.1).

**Table 2.1** Classification of rice based on their amylose content.

| Types | Amylose content (%) | Appearance |
|---|---|---|
| Waxy | 0-2 | Most sticky |
| Very low amylose | 2-12 | Sticky and soft |
| Low amylose | 12-20 | Sticky and soft |
| Medium amylose | 20-25 | Rather not sticky |
| High amylose | 25-33 | Not sticky and hard |

**Source**: Juliano (1992) and Chairote (2009)

### 2.1.2 The structure of rice grain

Rice is harvested as paddy rice which varies in compositions with different cultivars, but it has the same basic structure as shown in Figure 2.2. The principal part of rice grain is composed of a hull and caryopsis. The hull is outer covering for the caryopsis. The hull helps as a protection against insect infestation and against rapid change in moisture content of rice grain. Hull is comprised of sterile lemmas, palea and lemma, and its presents for 16 - 28% of rough rice. The hull is low protein, fat and starch, but high crude fiber, crude ash, and dietary fiber (Juliano & Bechtel, 1985). The caryopsis is the edible part of rice grain and also known as brown rice which comprise of the pericarp (1-2%), seed coat and nucellus (4-6%), the embryo (2-3%), and endosperm (89-94%) (Zhou et al., 2002). The endosperm comprises the aleurone layer, sub-aleurone layer, and starchy endosperm. It can be removed as part of the bran fraction during milling. Most of the oil and protein are stored in this part. The starchy endosperm comprises the greatest proportion of the rice grain, containing most of starch and storage protein (Blakeney, 1984).

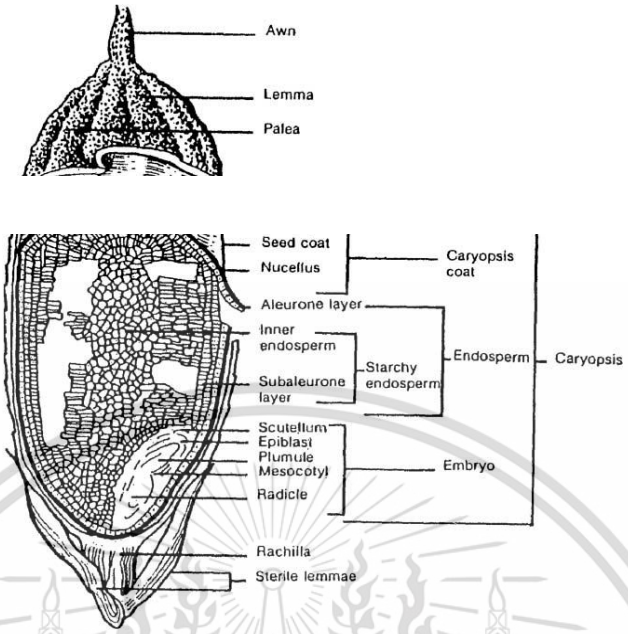


**Figure 2.2** General structure of rice grain.

**Source**: Blakeney (1984)

### 2.1.3 Rice grain composition

The chemical compositions of rice grain varies widely depends on cultivar, environment, soil, physical dimensions, growing area, harvesting dates and processing treatment (Webb, 1991; Champagne et al., 2005; Griglione et al., 2015). Milled rice is produced from removing the bran layer by milling. The degree of milling determines the amount of the nutrition of milled rice. The approximate nutrition of milled rice is composed of starch (77-90%), protein (6.3-7%), lipid (0.4-0.5%), ash (0.4-0.8%), and fiber (0.2-0.5%) at 14% of moisture content (Juliano & Bechtel, 1985; Champagne et al., 2005).

#### 2.1.3.1 Rice starch

Rice starch is the major component of the rice grain, accounting for about 90% dry weight of a milled rice grain at the moisture content of 14% (Juliano, 1985). The granular of rice starch are small with the size in the range of 2-7 μm (Vandeputte et al., 2003) and are smooth surface by polyhedral structure and irregular shape, which observed by scanning electron microscopy (SEM) (Hayakawa et al., 1980; Li & Yeh, 2001; Wani et al., 2012; Arns et al., 2015) as shown in Figure 2.3. Rice starch is composed of two polymers of glucose units that can be

amylose and amylopectin which are presented in various ratio (Lu et al., 1997; Nakamura et al., 2002).

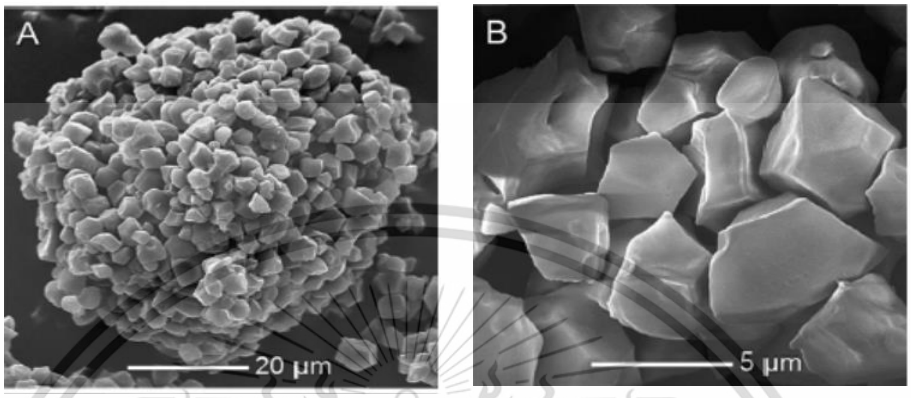


**Figure 2.3** Rice starch granules observed by scanning electron microscopy with a magifications of 1,000x (A) and 5,000x (B)

**Source**: Patindol et al. (2015)

Starch granule consists of semi-crystalline and amorphous areas packed in an alternating form that is similar to tree growth rings (Figure 2.4-A). Within each granules are many concentric light and dark ring (Waigh et al., 1996). The dark rings region consist of an ordered structure of double helices of amylopectin branches (crystalline lamella) embedded in an amorphous lamella (light ring) that consists of amylose chains and amylopectin branch points (Figure 4-B) (Patindol et al., 2015). The order semi-crystalline structure arranged in a radial direction is capable of rotating polarized light and displays birefringence (Bertoft, 2017) (as shown in Figure 2.5-B). Starch also shows a distinct X-ray diffraction pattern depending on its botanical source. Cereal starches such as rice starch present A-pattern (Patindol et al., 2015); tuber starches present B-pattern (Campos et al., 2017); bean starches are a mixture of A- and B-patterns as display C-pattern (Piecyk et al., 2018; Xu, Saleh, Liu, et al., 2018); V-pattern is complex formed by amylose and fatty acids or phospholipids (Shin et al., 2009).

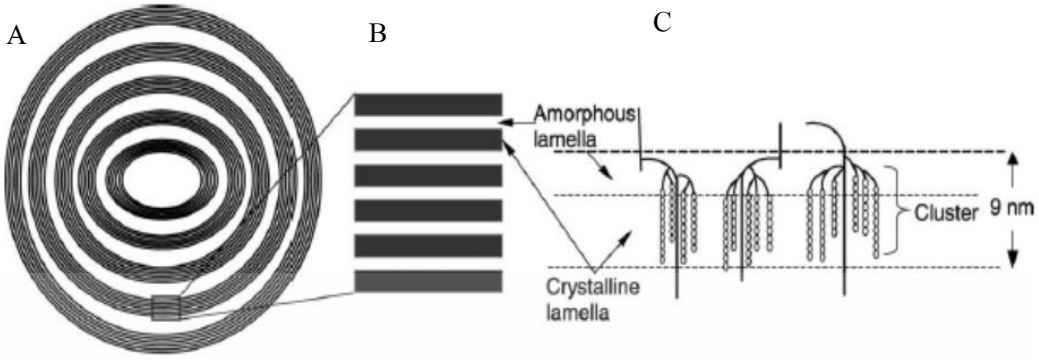


**Figure 2.4** Starch granular structure: the whole granule (A), the lamellae (B), and the double helices chain of amylopectin give rise to crystalline lamellae (C).

**Source**: Waigh et al. (1996)

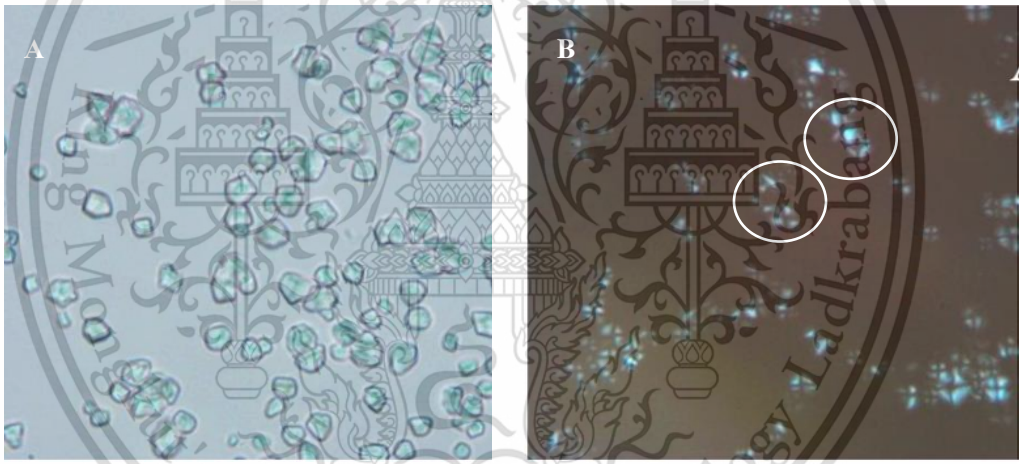


**Figure 2.5** Photomicrographs of rice starch (A) and polarized light micrograph of rice starch (B)

**Source**: Sittipod (2014)

Two majors structurally apparent compound of starch are amylose and amylopectin. Hence its composition, physicochemical characteristics and changes during cooking processing and storage will largely influence the physiological response to rice therefore they are discussed below.

1) Amylose

Amylose is a linear molecule that compose of glucose monomers bound by α-1,4 linkages (Figure 2.6). However, amylose has a few branches which are bounded by α-1,6

linkages (Juliano, 1985; Curá et al., 1995). Amylose forms a complex with iodine, changing the color of amylose to blue-black. This is the basis of commonly used colorimetric methods or determining the amylose content in a sample (Juliano, 1985; Frazier et al., 1997). Rice starch amyloses have degree of polymerization (DP) values of 920 to 1110, CL of 250 to 370 (Takeda et al., 2003). The molecular weight of amylose in rice starch also varies among varieties. Amylose contents in rice with varieties are classified in high (25-32%), medium (20-25%), low (10-20%), very low (2-10%) and waxy (0-2%)as determined by iodine colorimetry (Juliano, 1985).

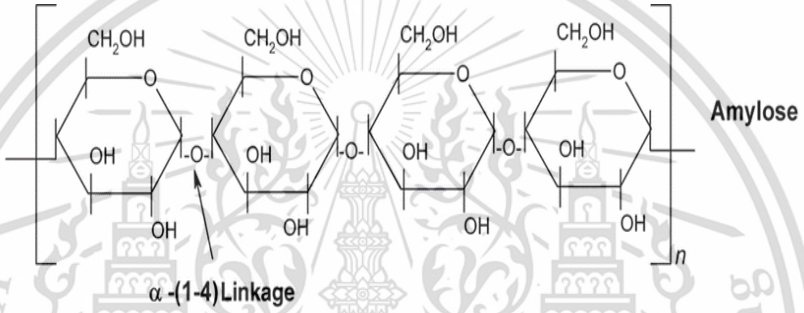


**Figure 2.6** Structure of amylose

**Source**: Liu, Xie, et al. (2009)

2) Amylopectin

Amylopectin is a larger molecule than amylose with a molecular weight of $1x10^7 – 1x10^9$ (Tester et al., 2004) and branched structure with glucose monomers bound built from 95% α-1,4 linkages and 5% branched points of α-1,6 linkages (Figure 2.7) which link from the first glucose molecule (Kainuma & French, 1972; Robin, 1974; Liu, Xie, et al., 2009). Amylopectin molecules of rice fall into three broad groups, with average degrees of polymerization (DP) of 700 – 2,100 (small), 4,400 – 8,400 (medium), and 13,400 – 26,500 (large) (Takeda et al., 2003). The structure of amylopectin can be classified in to three types of chain: A, B and C. The A chains are linear chain that link to the B and C chains though the reducing end with no other chains attached. The B chains are similarly linked but carries the A or other B chains. The C chain is the only chain of the amylopectin molecule which has a free reducing end (Hizukuri, 1986; Tester et al., 2004) (Figure 2.8).

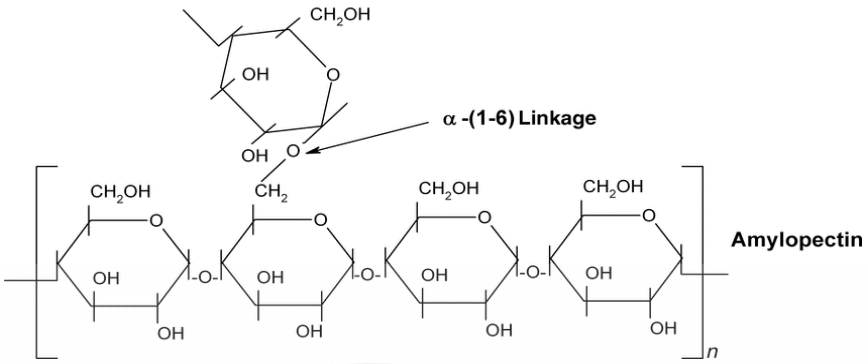


**Figure 2.7** Structure of amylopectin

**Source**: Liu, Xie, et al. (2009)

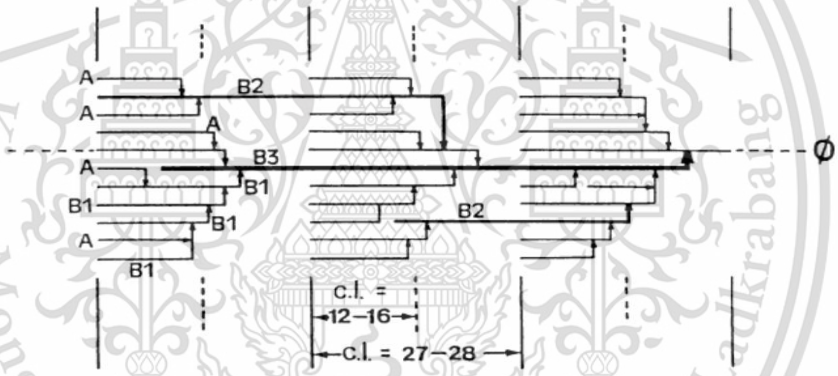


**Figure 2.8** A cluster model of amylopectin (Ø, reducing chain end; ——, α -(1,4)-D-glucan chain; ----, α-(1,6) linkage

**Source**: Hizukuri (1986)

#### 2.1.3.2 Protein

Proteins in rice are non-uniformly distributed in the rice grain which present in the aleurone layers, bran, and endosperm (Blakeney, 1984; Champagne et al., 2004). The protein content of milled rice varies widely depending on the rice variety as well as growing conditions such as soil, fertilization, and environment. On the average protein accounts are present only 4-9.5% of milled rice at 14% of moisture content (Gomez, 1979; Juliano, 1985). The two majors protein in the milled rice (endosperm) are mainly water-soluble protein which are mostly alkali-

soluble glutelin (up to 80%), globulin (10%), and two minor ones, albumin (5%) and prolamin (less than 3%) (Juliano, 1985; Huebner et al., 1990). Glutelin is the major protein which is reported to cross-link by both intra and inter disulfide bonding. The formation of disulfide bonds of glutelin was found to impact on the cooking quality of rice, which correlated with an increase in disulfide binding resulting in the decreased stickiness of cooked rice (Martin & Fitzgerald, 2002).

#### 2.1.3.3 Lipids

Lipids are present within starch and throughout the caryopsis which are controlled by cultivar and environment similar to protein. Lipids are reported to form up to 20% of rough rice, which are mostly triglycerides (68-71%), glycolipids (5-7%), phospholipids (3-4%) and free-fatty acids (2-3%) (Maningat & Juliano, 1980; Champagne et al., 2004). The lipids present in the starch granule are mainly phospholipids and free-fatty acids, which consist of palmitic and linoleic acid (Zhou et al., 2002). The degradation of rice lipids is strongly related to quality of rice during storage. During storage, lipids are hydrolyzed to free-fatty acid and/or further oxidized to peroxides which result in the qualities of rice such as taste and flavor (Juliano, 1977; Aibara et al., 1986).

#### 2.1.3.4 Minor compositions

Starches also contain small amount of minerals (less than 0.4% dry basis) such as calcium, magnesium, phosphorus, potassium, and sodium (Anjum et al., 2007). Phosphorus is the most dominant mineral in milled rice (0.8-1.5% of milled rice).

### 2.1.4 Functional properties of rice starch

During cooking, several stages occur to transform a raw grain into a cooked grain of textural attributes, including glass transition, gelatinization swelling, and pasting and leaching of amylose, and retrogradation.

#### 2.1.4.1 Glass transition

Before gelatinization of starch can occur the glassy (amorphous) regions of the starch must become soft and rubbery (Biliaderis et al., 1986; Slade & Levine, 1987). This process is called glass transition. Water depresses the glass transition temperature ($T_g$). In the

conditions required to cook rice, the rice is generally in excess water, so glass transition is always depressed. When rice is used as an ingredient in a process, the moisture content can be used to manage the glass transition and thereby the processing properties of food (Slade & Levine, 1988). For a synthetic polymer glass transition occurs when a glassy region is at a certain moisture content and temperature that allows it to become rubbery, and when those conditions are removed, the effects of glass transition are reversed. In terms of starch, though, the glassy or amorphous, areas contain the branch points of the amylopectin of subtend chains that traverse crystalline clusters on either side of the amorphous regions (Biliaderis et al., 1986; Slade & Levine, 1987), so reversing glass transition may not necessarily reverse the secondary effect of rubbery amorphous regions.

#### 2.1.4.2 Swelling and pasting

The phenomenon following the dissolution of starch, during the gelatinization process, is usually called pasting. Once starch gelatinizes, starch granules begin to swell, usually to many times their original volume, in the absence of shearing (Parker & Ring, 2001). Swelling of starch granules is accompanied with leaching of amylose molecules that influence the cooked product texture properties. During pasting measurements, in the presence of water and heating, the changes in the physicochemical properties of starch are usually manifested by an increase in the viscosity of the starch water slurry. Continued heating and agitation result in rupturing of starch granules releasing amylose molecule into the solution with complete solubilization of the starch granule (as shown in Figure 2.9) (Sowbhagya & Bhattacharya, 1979; Juliano, 1982).

Several factors are reported to influence the pasting properties of cereals. Amylose content, branch chain length distribution of amylopectin, amount and type of amylose and amylopectin leached out from the starch granule, amylose-amylose, amylose-amylopectin, lipid complexes, heating temperature, are heating rate are among these factors. For instance, indicated that starch granules that are high amylose content which presented elastic and stronger as compared to low amylose.

#### 2.1.4.3 Gelatinization temperatures

Gelatinization temperatures are an important property of rice starch due to its correlates strongly with the cooking time and the texture of cooked rice (Maningat & Juliano, 1978).

The cooking of starchy food such as rice results in the gelatinization and swelling of starch granules in the endosperm with absorption of water. When gelatinization occurs, the granules swell irreversibility and the birefringent are lost and loss of crystallinity. This is due to an irreversible breakdown in the order and crystallinity of the starch granules (Whistler & Danie, 1984; Juliano, 1982). When the heating is continuing, the starch molecules vibrate, breaking intermolecular bonds and allowing their hydrogen binding sites to involve more water molecules make granule swelling and amylose leaching. (Figure 2.9). The gelatinization properties (gelatinization temperature and enthalpy change) depend on the structure of the amylopectin, the amylose content, and the phosphate monoester derivatives of starch (Srichuwong & Jane, 2007). Gelatinization of starch granules usually occurs due to increase in starch water suspension that leads to excessive vibration and twisting of the molecules within starch granule forming intermolecular hydrogen bonds causing extensive hydration. Gelatinization temperature is an important property of the gelatinization process resulting in cooking time and the texture of cooked rice.

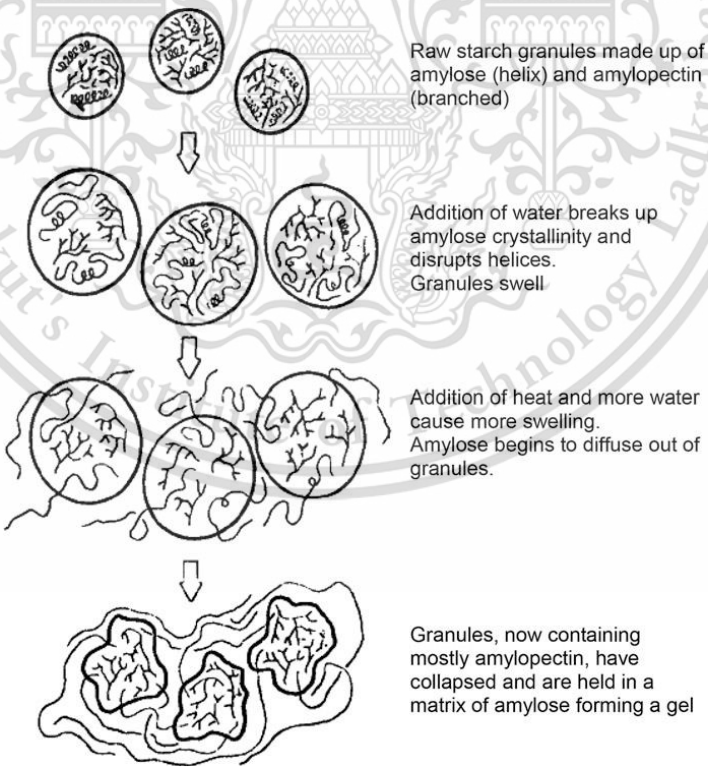


**Figure 2.9** Mechanism of starch gelatinization.

**Source**: Remsen and Clark (1978)

Normally, Starch gelatinization analysis is measured by differential scanning calorimeter (DSC). Starch is mixed with water at least the ratio 1:2 of starch to water and is heated using the DSC to measure gelatinization temperatures (onset temperature ($T_o$), peak temperature ($T_p$), and conclusion temperature ($T_c$)) and enthalpy change of gelatinization ($\Delta H$) (Biliaderis et al., 1980). Gelatinization properties of starch depend on the botanical sources, amylose content, amylose-lipid complex. In general, starch with high amylopectin shows a higher gelatinization temperature and enthalpy change of gelatinization because amylopectin is favorable in the crystalline region of the starch structure (Lu et al., 1997; J. l. Jane et al., 1999). Kraithong et al. (2018) also reported that rice with higher amylopectin showed increase in onset temperature and enthalpy change of gelatinization as compared with low amylopectin.

**2.1.4.4 Retrogradation**

Gelatinized starch under certain conditions of storage and temperature, starch molecules tend to re-associated to develop double helices. This re-association process is called as retrogradation (Morris, 1990; Baik et al., 1997). Retrogradation rate of starch depend on amylose/amylopectin ratio, amylopectin structure, lipid content, and storage conditions (Sievert & Pomeranz, 1989). Both amylose and amylopectin molecules can retrograde (Figure 2.10). The retrogradation of amylose is faster to forms crystalline than amylopectin because of the unbranched structure (Gidley, 1987; Wang et al., 2015). In stage of retrogradation, amylose requires a short time to recrystallize to form crystallites then amylopectin requires serval day or longer to forms crystallite at the temperature 40-60$^{o}$C (Karim et al., 2000). Similar to the reports of Sievert and Wuesch (1993) and Setiawan and Jane (2010), They also reported that the retrogradation of amylopectin requires longer time and form crystallites with a low temperature because of branched chain of amylopectin.

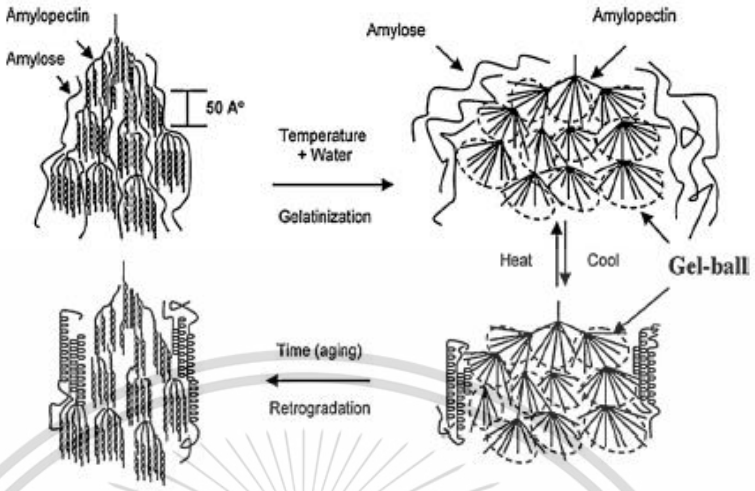


**Figure 2.10** Schematic representations of starch gelatinization and retrogradation form

**Source**: Keetels et al. (1996)

## 2.2 Carbohydrates digestion

In general, rice is the only cereal which can be consumed primarily in the form of whole grain. The most consumption of rice is in form of white rice. In Asia countries, white rice is usually eaten from the most meals (breakfast, lunch, and dinner) to dessert. Rice is prepared in many ways such as boiling, steaming and baking. Since carbohydrates in rice are major source of energy for human. Digestion of carbohydrates begin in the mouth. Chewing also known as mastication, crumbles the carbohydrate foods into smaller pieces. The salivary glands in the oral cavity secrete saliva that coats the food particles. Saliva contains the enzyme, salivary amylase. This enzyme breaks the bonds between the monomeric sugar units of disaccharides, oligosaccharides, and starches. The salivary amylase breaks down amylose and amylopectin into smaller chains of glucose, called dextrin and maltose. The increased concentration of maltose in the mouth that results from the mechanical and chemical breakdown of starches in whole grains is what enhances their sweetness. When carbohydrates reach the stomach no further chemical breakdown occurs because the amylase enzyme does not function in the acidic conditions of the stomach. After that, the chyme is gradually expelled into the upper part of the small intestine. Upon entry of the chyme into the small intestine, the pancreas releases pancreatic juice through a duct. This pancreatic juice contains the enzyme, pancreatic amylase, which starts again the breakdown of dextrin into shorter and shorter

carbohydrate chains. These enzymes, known collectively as disaccharidase, are sucrase, maltase, and lactase. Sucrase breaks sucrose into glucose and fructose molecules. Maltase breaks the bond between the two glucose units of maltose, and lactase breaks the bond between galactose and glucose. Once carbohydrates are chemically broken down into single sugar units they are then transported into the inside of intestinal cells. The cells in the small intestine have membranes that contain many transport proteins in order to get the monosaccharides and other nutrients into the blood where they can be distributed to the rest of the body. The first organ to receive glucose, fructose, and galactose is the liver. The liver takes them up and converts galactose to glucose, breaks fructose into even smaller carbon-containing units, and either stores glucose as glycogen or exports it back to the blood. How much glucose the liver exports to the blood is under hormonal control and you will soon discover that even the glucose itself regulates its concentrations in the blood (Gray, 1970).

## 2.3 Glycemic index (GI)

The glycemic index (GI) indicates the potential of a carbohydrate-rich foods to raise blood glucose level *after eating*. The scale of GI is used in a range of 0 to 100, where 100 is represented by white bread or pure glucose (Freeman & Lyons, 2008; Wordu & Banigo, 2013). The food can be classified into three groups including low GI (GI≤55), medium GI (56-69) and high GI (≥70) (Brand-Miller et al., 2009). Generally, the GI of food is calculated as the percentage of the total area under the curve (AUC) of glucose response in 2 hours after the consumption of 50 gram of carbohydrates as compared to the AUC after the consumption of a reference food as white bread or glucose. (Wolever et al., 1991; FAO, 1997; Brouns et al., 2005). Foods with a high GI are rapidly digested, absorbed and metabolized resulting in marked variations in blood glucose levels. Starchy foods, most rice, breakfast cereals, potato tend to have high GI. Rice is an important source of energy. It is comprised about 80% of carbohydrate and very easy to digest especially, white rice. The glycemic index of white rice was reported between 75-83 depending on the growing zone and cultivars (Chan et al., 2001; Frei et al., 2003). For this reason, rice or rice products when consumed in high amount result in a high GI, which is not appropriated to diabetics (Frei et al., 2003). With increasing concerns over diabetes development worldwide, there is a pressing need to find

techniques of rice and rice products to reduce starch hydrolysis rates and glycemic index (Reed et al., 2013).

### 2.3.1 Glycemic index (GI) determinations

Both *in vivo* and *in vitro* methods have been used to measure starch digestibility. Two methods of glycemic index measurement are used; *in vivo* glycemic index (FAO, 1997; Brouns et al., 2005) and *in vitro* glycemic index (Goñi et al., 1997) as follows:

#### 2.3.1.1 *In vivo* method

*In vivo* GI measurement by human subjects which is calculated by the blood glucose levels from the actual blood sample at periods of time (Wolever et al., 1991). Therefore, selection of human subjects is one of the most important aspects of the test and their affect the test result. Subjects should include an equal number of men and women with normal body mass index (BMI) in a rage of 18.5 to 22.9 kg/m$^2$ (Nuttall, 2015) and blood glucose levels in a range of 72 to 99 mg/dL (4.0 to 5.4 mmol/L) when fasting (Granfeldt et al., 1992; Tirosh et al., 2005; Güemes et al., 2016). The subjects are required to fast before the blood test to prevent possible interference with test results, and all foods and drink intake are controlled during the test period. After consumed the reference food (glucose or white bread) and/or food sample. The blood samples are monitored for 2 hours which are collected at 15,30, 45, 60, 90 and 120 min. Blood glucose levels are determined using glucose-oxidase method (Jeevetha et al., 2014) or glucose meter analyzer (Truong et al., 2014; Sun et al., 2015). However, there are instrument to glucose test on the market that provide immediate blood glucose level that are being used by diabetes patients and researchers (Granfeldt et al., 1992). Calculation of GI, the blood glucose levels of each time are plotted and the area under the curve (AUC) are calculated. The GI value for the food samples is then calculated for each person by dividing their AUC of glucose by their AUC of reference food as following the equation by Wolever and Jenkins (1986):

$$GI = \frac{\text{Area under the curve for 50 g of carbohydrate from the test food}}{\text{Area under the curve for 50 g of carbohydrate from the reference food}} \times 100$$

**2.3.1.2 *In vitro* method**

A growing need to reduce the cost and time requirement and more efficiently measure the GI has resulted in an alternative method for measuring the GI. This method is referred to as estimated GI (eGI) (Goñi et al., 1997). The eGI is the kinetics of *in vitro* starch. The method involves imitating the *in vivo* starch digestion in test tubes using enzymes. Since starch hydrolysis method of eGI analysis is relatively new, experimental procedure to determine, validate and improve eGI is needed. Further, the method and the investigation of factors that affect the rate of *in vitro* starch hydrolysis still continue today, the two most accepted *in vitro* methods are Englyst method and Goni method (Englyst et al., 1992; Goni et al., 1997).

1) Englyst method

Englyst et al. (1992) who developed a method using small beads and guar gum to measure rapidly digestible starch (RDS), slowly digestible starch (SDS) and resistant starch (RS). Because the actual chewing process would not break down the food structure as fine as milling, food samples were not milled at the sample preparation step, instead it was run through a mincer with a plate of 0.9 cm diameter holes (Englyst et al., 1992). However, the authors found that the particle size reduction was taking place after swallowing thus reducing particle size before hydrolysis by mincing the sample could falsely elevate the amount of RDS. This is important because the rate and extent of starch hydrolysis determine the eGI and these factors vary depending on the way a food sample is broken down (Englyst et al., 1992). In contrast, the authors reported that the glass balls with guar gum effectively facilitated the degradation of large particles thus increasing starch-enzyme contact in most types of food except legumes, in which the cell walls are relatively stronger than most food starches (Englyst et al., 1992).

2) Goni method

Goni et al. (1997) established the eGI using *in vitro* enzymatic starch hydrolysis and starch digestion rate over time. The method included treating the sample with pepsin to digest protein, α-amylase to hydrolyze starch and then amyloglycosidase to release glucose from starch (Goni et al., 1997). Results from eGI, GI from *in vivo* study and the reference GI were compared and a correlation of 0.894 was found between reference GI and eGI (Goni et al., 1997). The researchers found that legumes were digested at the slowest rate of all the food products

measured. This could be due to dietary fiber and protein content, but the authors did not provide valid explanation for the low GI of legumes (Goni et al., 1997). The estimate glycemic index (eGI) was calculated as follow; The first order equation is $C = C_\infty (1 - e^{-kt})$, where C is the percentage of starch hydrolyzed at time t (min), $C_\infty$ is the equilibrium percentage of starch hydrolyzed after 180 min, and k is the kinetic constant. The parameters, $C_\infty$ and k, were estimated for each treatment based on the data obtained from the in vitro starch digestion. The area under the hydrolysis curve (AUC) was calculated by the following equation: $AUC = C_\infty(t_f - t_0) - (C_\infty/k)[1 - \exp]$, where $C_\infty$ is the equilibrium percentage of starch hydrolyzed after 180 min, $t_f$ is the final time (180 min), $t_0$ is the initial time (0 min), and k is the kinetic constant. A hydrolysis index (HI) represents the rate of starch digestion, and estimated GI indicates the digestibility of the starch in oats in relation to the digestibility of starch in a reference material, white bread. The HI, a good predictor of glycemic response, was calculated by dividing the AUC of each treatment by the AUC of a reference (control, white bread). The GI was then estimated by using the following equation of Goni et al. (1992): $eGI_G = 39.71 + 0.549HI$. and another the estimated glycemic index (eGI) was calculated using the equation described by Granfeldt et al. (1992): $eGI_{Gr} = 8.198 + 0.862HI$.

### 2.3.2 Factors affecting glycemic index of rice

The major carbohydrates in rice is starch, which are about 80%. The consumption of carbohydrates is affected on human health, leading to increase in blood glucose levels (Nounmusig et al., 2018). Long-term consumption of carbohydrate as rice can be unhealthy to human health which associated with an increasing in rick of type II diabetes and insulin tolerance in Asia people (Panlasigui et al., 1991). The GI of rice or carbohydrates food is affected by its digestibility. Various factors are affected on glycemic index of rice such as amylose/amylopectin ratio, amylopectin structure, cooking methods, fiber content (Hu et al., 2004; Brand-Miller et al., 2009; Mohan et al., 2016).

#### 2.3.2.1 The ratio of Amylose to amylopectin

The nature of rice grain and rice starch compositions also affect the rate of glucose absorption in human. The ratio of amylose/amylopectin is important character in the way for cooking. High amylose rice content tends to be fluffy, separate grains after cooking and become hard when cooling (Chiu & Stewart, 2013). However, the ratio of amylose/amylopectin is also

correlated with the glycemic index of rice. In general, rice with high amylose content presented low glycemic index which produced a lower blood glucose level (Jeevetha et al., 2014; Kumar et al., 2018; Ritudomphol & Luangsakul, 2019). This is similar the research of Hu et al. (2004) reported that significant difference in glycemic index of high amylose rice with different amylose content. Whereas the high amylose rice presented lower glycemic index compared to the rice with low amylose content. This result could be explained that amylose is hard to break down contributing to strong structure of amylose which ensures a sustained release of sugar into blood. This result leading to high amylose rice has lower glycemic index. Similar to the finding with researches were also reported by Ranawana et al. (2009) and Dipnaik and Kokare (2017) showed that high amylose rice showed low glycemic index compared with low amylose rice.

#### 2.3.2.2 Degree of cooking rice

Rice is processed for consumption in various ways for cooking, such as boiling, steaming, and pressure-cooking (Juliano & Hicks, 1996). Cooking rice normally presents gelatinization of the starch granules. Cooking rice that gelatinize starch granules or disrupt starch structure due to the disruption of starch structure by gelatinization which increases its accessibility for enzymatic digestion and its availability for absorption in the small intestine (Jung et al., 2009). This is resulted in raising blood glucose levels that was reported with the consumption of cooked rice compared to uncooked rice (Polesi et al., 2017; Adedayo et al., 2018). As previous studies also reported that cooking rice caused increase in starch hydrolysis and glycemic index as compared with the uncooked rice (Madan et al., 2016; Adedayo et al., 2018). Moreover, cooking methods seem to be affected to perform the starch easily digestible resulting in high glucose responses. Thus, the level of resistant starches and glycemic index present in carbohydrate foods depends on cooking methods, cooking conditions, and rice/water ratios (Hsu et al., 2015; Polesi et al., 2017; Chusak et al., 2019).

#### 2.3.2.3 Dietary fiber content of rice

Some research reported that relationship between the dietary fiber and the glycemic index in rice. It was suggested that the dietary fiber as well as the amylose in rice has a significant role on the GI (Panlasigui & Thompson, 2006; Madan et al., 2016; You et al., 2016). Amylose has a linear structure and easily rearranges after cooking and then cooling. The resultant

resistant starch is then metabolized similarly to the dietary fiber in the large intestine or colon. In conclusion, the presence of amylose and dietary fiber in rice affects glucose response and the GI. The combined effect of amylose and dietary fiber contributes significantly to the low GI in rice. High dietary fiber was shown to produce lower blood glucose responses than low dietary fiber. The most important feature of the dietary fiber hypothesis is that its focused attention on events occurring in the gastrointestinal tract and provided a rationale for the relationship between the rate of starch digestion and the glycemic response. The low glycemic response to high dietary fiber was thought to be due to a reduced rate of gastric emptying and a reduced rate of small intestinal absorption.

## 2.4 Starch modifications to reduce the glycemic index in starch

Slow digestible starch and resistant starch will lead to slower glucose release resulting in the glycemic index. They as the indigestible starch portion in the stomach and digested in the small intestine, can provide functional control of the GI which prevent heart disease, bodyweight management, cancer, diabetes, and cardiovascular disease. It has attracted great interest in diabetes treatment (Shu et al., 2009). The rate of starch digestion in rice products, can be altered by modified starch such as hydrothermal treatment (heat- moisture, annealing, and gelatinization and retrogradation) as in many processing techniques (Rashmi & Urooj, 2003; Jaisut et al., 2008, 2009; Dupuis et al., 2014).

Two hydrothermal methods for modifying starch are heat-moisture treatment (HMT) and annealing treatment (ANN) that have been used to modify starch digestibility (Chung et al., 2009). Several authors have reported the impact of heat moisture treatment and annealing treatment on starch digestibility (Shin et al., 2005; Trung et al., 2017).

### 2.4.1 Hydrothermal modifications

In general, white rice has high glycemic index in a range from 75 to 83 depending on its cultivar, growing zone, amylose/amylopectin ratios, cooking processing. Rice with high glycemic index tends to make blood sugar rise quickly (Frei et al., 2003). Consequently, reducing the glycemic index can control the rate of digestibility and blood sugar levels. Hydrothermal treatments, including heat- moisture treatment ( HMT) and annealing (ANN) are physical

modification that changed the physicochemical properties, and also changed digestibility of starch (Lehmann & F. Robin, 2007; Zavareze Roa et al., 2010; Zeng et al., 2015).

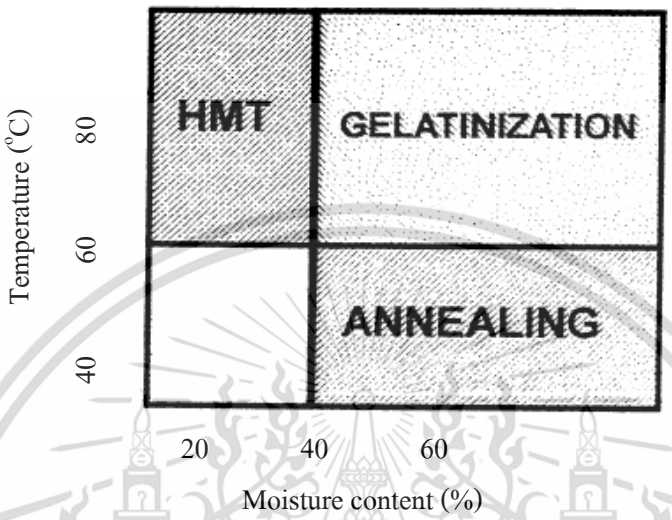


**Figure 2.11** Schematic representation of the temperature and moisture differences between gelatinization, annealing tretment and heat-moisture treatment (HMT).

**Source**: Manuel (1996)

#### 2.4.1.1 Heat-moisture treatment (HMT)

HMT is carried out at low moisture levels (below 35% of moisture content) and higher temperatures in a range of 60-120°C at above the glass transition temperature but below the gelatinization temperature during a certain time of period (15 min–16 hours) (Jacobs & Delcour, 1998; Maache-Rezzoug et al., 2008; Arns et al., 2015). HMT promotes the interaction of polymer chains by disrupting the crystalline structure and dissociating the double helical structure in the amorphous region, followed by the rearrangement of the disrupted crystals. (Gunaratne & Hoover, 2002). Furthermore, increase in gelatinization temperature range, decrease in granular swelling and amylose leaching and increase in thermal stability (Chung et al., 2009; Zavareze & Dias, 2011).

#### 2.4.1.2 Annealing treatment (ANN)

Annealing (ANN) is kwon as a physical modification method. The process of annealing treatment in presence of medium water content between 40-55% or high water content (above 60%) at an extended period of time (Gomes et al., 2005; Waduge et al., 2006; Dias et al.,

2010). Annealing treatment is performed at a temperature above the glass transition temperature, but below the gelatinization temperature (Waduge et al., 2006; Chung et al., 2009). The conditions of annealing treatment for modifying starches and starch digestibility as shown in the Table 2.2. Annealing treatment can modify the physicochemical properties of starch without destroying its granular structure. Especially, Annealing treatment changes the physicochemical properties by improving crystalline perfection, and facilitating interactions between starch chains during annealing treatment (Wang et al., 2017; Xu, Saleh, Liu, et al., 2018; Ji et al., 2019).

**Table 2.2** Annealing treatment conditions of starches and references.

| Starch sources | Temperature (°C) | Time (hs.) | Water content (%) | References |
|---|---|---|---|---|
| Rice | 45-55 | 8-24 | 1:3 (w/w) | Hormdok and Noomhorm (2007) |
| | 45-55 | 16 | 1:3 (w/w) | Dias et al. (2010) |
| | 7 and 15 | 16 | 1:2 (w/v) | Kiatponglarp et al. (2015) |
| | 50 and 55 | 4 -6 | 1:2 (w/w) | Li et al. (2018) |
| Bambara groundnut | 50 | 48 | 1:3 (w/w) | Afolabi et al. (2018) |
| potato | 55 | 24-96 | 1:3 (w/w) | Xu, Saleh, Gong, et al. (2018) |
| Red azuki bean | 55 | 12 | 1:3 (w/w) | Xu, Saleh, Liu, et al. (2018) |

2.4.1.2.1 Mechanism of annealing

In semi-crystalline polymers, annealing has been interpreted as: (1) sliding diffusion, which entails the movement of complete molecular sequences within a crystalline lattice (this mechanism being favored by high mobility of the chains in the crystalline structure), and/or (2) a complete or partial fusion of crystals and subsequent re-crystallization of the starch at the annealing temperature. Experimental evidence supports both mechanism (Matuscelli 1974). According to the side-chain liquid crystalline analogy of Waigh (1997), the rigid amylopectin double helices are attached to an amorphous backbone (Figure2.12-A). Waigh (1996) and Perry and Donald (2000) proposed that double helices of the unhydrated form of starch were

intact, but were not arranged regularly side by side, due to the differing lengths of radial and tangential branches (Figure 2.12-B) (Waigh 1996). This state is called a nematic, collapsed or a withered state. The amorphous region of the granule is the area most vulnerable to the initial water absorption and plasticization. Before hydration, the amorphous area is glassier and more immobile; hydration of the starch granule increases the mobility of the amorphous regions. This induces vibrational movement of tangential and radial chains in both amorphous and crystalline domains (Figure 2.12-B). An increase in annealing temperature and excess water accelerates the rate of hydration and increases glucan chain mobility (Figure 2.12-B). This dynamic nature allows limited side by side movement of the double helices resulting in the formation of the sematic-type structure (Figure 2.12-C). An amorphous lamella and, subsequently, the order of double helices of amylopectin (Tester, 1999). At this stage, molecules are closely aligned in a distinct series of layer with their axes lying perpendicular to the plane of the layers. With the progress of annealing the initially weaker or imperfect crystallites gradually disappear, while the rest of the crystallites become more perfect due to fusion and re-crystallization. The crystallite perfection on annealing was first suggested by Lorenz and Kulp (1980). Stute (1992) postulated that crystalline perfection may also occur due to: (1) larger crystal formation from smaller crystals, (2) a change of crystal shape, (3) a change in direction of crystal growth, (4) orientation of crystallites, (5) interactions between crystallites, and (6) changes within the amorphous regions. This clearly indicates that crystalline perfection does not necessarily correlate with an increase in crystallinity. Native starch contains crystallites of varying stabilities. However, annealing decreases the above variations resulting in more homogenous crystallites (Hoover & Vasanthan, 1994a; Jacobs et al., 1998b; Larsson & Eliasson, 1991; Paredes-Lopez & Hernández-Lopez, 1991; Tester & Debon, 2000; Tester, Debon, & Karkalas, 1998; Tester & Morrison, 1990; Yost & Hoseney, 1986). Hoover and Vasanthan (1994a) postulated that amylose chain mobility could increase on annealing, resulting in the formation of double helices arising from interactions between amylose–amylose and/or amylose–amylopectin chains.

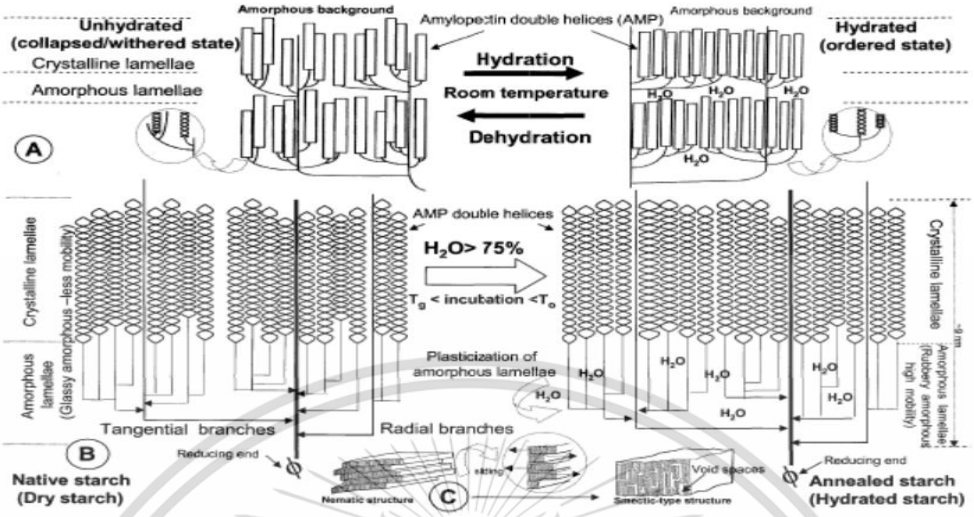


**Figure 2.12** Schematic representation of mechanism of annealing; hydration of starch at room temperature (A), crystalline perfection during annealing, movement of crystalline patterns during annealing (C).

**Source**: Adapted from Martuscelli and Pracella (1974) and Tester et al. (2000) with permission of The Royal Society of Chemistry Elsevier BV, and Elsevier

2.4.1.2.2 The impacts of annealing on starch attributes

The impacts of annealing on starch attribute including granule morphology, swelling power and solubility, pasting properties, crystallinity, as well as starch digestibility and glycemic index are described as follows:

1) Granule morphology

Annealing treatment did not change the size or the shape of starch. Several authors have found that no change in granule morphology of rice (Dias et al., 2010; Tsutsui et al., 2013), maize (Tester et al., 2000) , tube and root starch (Gomes et al., 2005), and barley (R. N. Waduge et al., 2006). However, annealing treatment could create fissure and pores on the granule surface of sago starch (Wang et al., 1997) and barley starch (R. N. Waduge et al., 2006).

2) Swelling power and solubility

Swelling power and solubility of starches (potato, cassava, wheat, bean, oat, and barley) were normally found to decrease as a result of annealing treatment (R. N. Waduge et al., 2006; Lan et al., 2008; Adebowale et al., 2009; Xu, Saleh, Liu, et al., 2018). The decrease in swelling and solubility of starch attributed to the interplay as following: (1) increased ordered double helical of amylopectin (crystalline perfect) (R. N. Waduge et al., 2006), (2) increased interaction between starch chains (amylose-amylose interaction and/or amylose-amylopectin interaction) (Jacobs & Delcour, 1998; Xu, Saleh, Liu, et al., 2018), (3) increased binding forces with in starch granules, and (4) increased amylose-lipid complex within the granules (Jayakody & Hoover, 2008). On the other hand, Dias et al. (2010) they observed that increase in the temperature of annealing treatment resulted in increased solubility of rice starch.

3) Pasting properties of starch

In general, pasting properties are changed after annealing treatment of starch compared to the native leading to increase the pasting temperature, improved shear stability, decreased peak viscosity, and final viscosity at the end of the cooling cycle (Jacobs & Delcour, 1998; Zavareze & Dias, 2011). These effects were shown in vary among annealed starches such as wheat, bean, oat, potato, barley, rice and sago (Waduge et al., 2006; Lan et al., 2008; Adebowale et al., 2009; Xu, Saleh, Liu, et al., 2018). The increase in pasting temperature of annealed starch attributed to interaction between double helices (in the crystalline perfect). The increase in pasting temperature of annealed starch is supported by (Lan et al., 2008; Dias et al., 2010; Xu, Saleh, Gong, et al., 2018). The decrease in peak viscosity and improve shear stability of annealed starch contributed to limit swelling of starch granule and amylose leaching, and increased interaction between starch chains during annealing treatment (Waduge et al., 2006; Jayakody & Hoover, 2008).

4) X-ray diffraction pattern and crystallinity

The effect of annealing treatment on X-ray diffraction pattern and crystallinity depends on botanical starch, and annealing conditions. Changes in the X-ray diffraction pattern is more pronounced in B-type (tube and root starches) than A-type starches

(Jayakody & Hoover, 2008; Zavareze & Dias, 2011). This change in X-ray pattern was reported by Gunaratne and Hoover (2002) reported that the change in X-ray pattern of annealed starch attributed to dehydration as well as to movement of a pair of double helices into the central channel. This movement during annealing treatment could changes the crystalline. The crystallinity of annealed starches is shown in vary starches. The increase in crystallinity of annealed starch reflects the interplay of the following factors: (1) amylopectin content (Waduge et al., 2006), (2) changes in orientation of the starch crystallites (Tester & Debon, 2000), (3) crystallite perfection (Jacobs & Delcour, 1998; Larsson & Eliasson, 1991; Lorenz et al., 1984; Muhrbeck & Svensson, 1996; Seow & Teo, 1993; Slade & Levine, 1987; Tester & Debon, 2000; Tester & Morrison, 1990), (4) enhanced ordering of the V-amylose–lipid complex (Lorenz et al., 1984) and (5) formation of amylose crystallites (Krueger et al., 1987a, 1987b).


**Figure 2.13** Model of the polymorphic transition from B-type to A-type starch in the solid state. The parallel double helices which form the duplex are labeled 0 and ½, indicating their relative translation along the c axis. Water molecules are shown as dots.

**Source**: Pérez et al. (2009)

5) Starch digestibility and glycemic index

Annealing treatment is known as hydrothermal method that was used to modify starch digestibility (Gomes et al., 2004; H.-J. Chung et al., 2009; Liu, Yu, et al., 2009). Annealing treatment of starch showed the decrease in starch digestibility since it was attributed to interplay of the factors following the crystalline perfection, interaction between amylose and amylose or amylopectin, amylose-lipid complex formation and the formation

of resistant starch (Lan et al., 2008; Chung et al., 2009; Xu, Saleh, Liu, et al., 2018). These results attributed to starch properties changed, including increased crystallinity, pasting temperature, gelatinization temperature, and enthalpy change of gelatinization. Li et al. (2018) found that the increase in the gelatinization temperature and pasting temperature effect by annealing treatment were related with resistant starch increased which resulting in the glycemic index decreased. Similar to the finding the result of Wang et al. (2017) concluded that increase in crystallinity, gelatinization temperature and enthalpy change of gelatinization temperature of annealed starch resulted in the decreased enzyme hydrolysis of starch as compared to the native starch. In contrast, some studies have indicated that annealed starches are more easily hydrolyzed by enzyme. Because annealing treatment promotes the formation of pores on the surface of starch granules with could alter the enzymatic hydrolysis of starch leading to glycemic index increased. However, the increase in enzyme hydrolysis of starch depends on the type of starch, conditions of annealing (Wang et al., 1997; Jayakody & Hoover, 2008).

The annealing treatment influences the physicochemical properties of starch granules to various extents, depending on the experimental conditions and the type of starch (Table 2.3).

**Table 2.3** Annealing conditions and impact on starches.

| Starch sources | Conditions | Impact of ANN on starch | References |
|---|---|---|---|
| • Potato, wheat | Starch to water ratio (1:5 w/w) at 30, 40, or 50°C for 24 h. | Decreased swelling and solubility | Wang et al.,(2017) |
| • Glutinous | Moisture content 50-55% for 4-6 h at 50°C | Pasting properties | Li et al., (2018) |
| • Potato, wheat | Starch to water ratio (1:5 w/w) at 30, 40, or 50°C for 24 h. | Increased Pasting temperature (PT) | Wang et al.,(2017) |
| | | Increased final viscosity (FV) | |
| | | Decreased peak viscosity (PV) | |
| • Rice | Starch to water ratio (1:9 w/w) at 45 – 55°C for 16 h. | Increased crystallinity | Dias et al., (2010) |
| • Corn | Starch to water ratio (1:10 w/w) at 30 or 50°C for 72 h. | Gelatinization properties | Liu et al., (2009) |
| | | Increased gelatinization temperatures | |
| | | - onset temperature (To) | |
| • Corn, pea, and lentil | Moisture content 70% and 10-15°C | - Conclusion temperature (Tc) | |
| • Potato, oat, and wheat | 50°C for 0.5 – 72 h. | Increased resistant starch and | Chung et al., (2009) |
| | | Decreased starch hydrolysis | Hoover & Zhou (2003) |

## 2.5 Ultrasound

Ultrasound is sound waves at a frequency above the normal human hearing rage (>20 KHz) (Jayasooriya et al., 2004; Jambrak et al., 2010; Pilli et al., 2011) as shown in Figure 2.14. The fundamental effect of ultrasound is to apply acoustic pressure to a medium in a sinusoidal manner. Ultrasound power is classified into two distinct of ultrasound, which can be broadly divided according to a large frequency range. The first type is low amplitude sound, commonly known as low power ultrasound. Amplitude is the oscillation displacement of the sound wave. Low power ultrasound, within the application in a rage of 2-10 MHz, is used for analytical purposes to measure the velocity and absorption coefficient of wave in a medium. It is often used in medical imaging, chemical analysis, medical diagnostics, and therapeutic medicine. The other classification of ultrasound is called high power ultrasound. It usually involves lower frequencies in a range of 20-100 kHz (rage base on this study). At this range, greater acoustic energy can be generated, inducing cavitation in liquids. It is used for cleaning, cell disruption, emulsification, and crystallization.

Moreover, the ultrasound technology has merits such as low energy consumption, shot processing time, and high reproducibility. The ultrasound technology was successfully used to foods processing such as homogenization, emulsification, extraction (release of plant material), crystallization (formation of smaller ice crystal in freezing), and separation (Azhar & Hamdy, 1979; Isono et al., 1994; Flores-Silva et al., 2017). Moreover, ultrasound is thought to be the most potentially novel technology in development starch properties (Zheng et al., 2013). Several the recent years, ultrasound technique has been also applied as a modification technique for modifying starch (Manchun et al., 2012; Zhu et al., 2012; Carmona‐García et al., 2016; Minakawa et al., 2019) and producing quick-cooked brown rice (Cui et al., 2010; Park & Han, 2016). Ultrasound technique can be generated with either piezoelectric or magnetostrictive transducers that created with high-energy vibrations which are amplified and transferred to a sonotrode or probe that is in direct contact with the fluid (Jambrak et al., 2010). The movement of the ultrasound energy in fluid medium initiates resulting in fast generation of small bubbles (cavities). As a result, the polymer chains near the collapsing microbubbles are caught in a high gradient shear field, which leads to break C-C bonds, and formation of long-chain radicals (Kang et al., 2016).

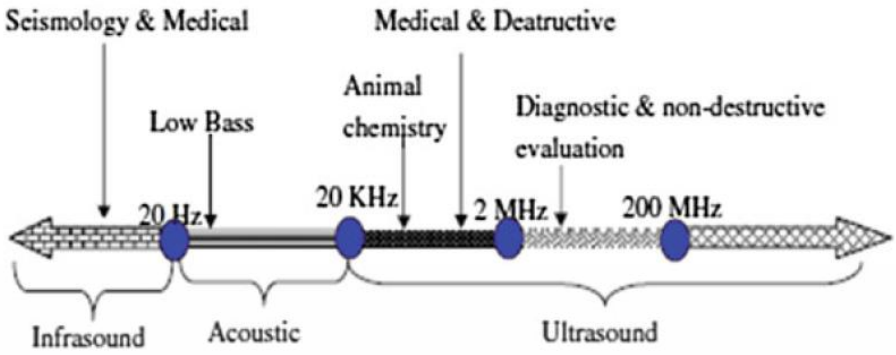


**Figure 2.14** Diagram of ultrasound range

**Source**: Pilli et al. (2011)

### 2.5.1 Cavitation

Cavitation is a phenomenon of bubble formation in liquid when negative pressure is applied (74,100). Cavitation may be divided into two categories, transient (inertial) and stable (non-interial). Transient cavitation bubbles are voids, vapor filled bubbles, believed to be produced using sound intensities in excess of 10 W/cm$^2$. Meanwhile, stable cavitation are non-linear oscillations which are produced in relatively lower intensities ranging from 1-3 W/cm$^2$. As the mechanical vibration of ultrasound propagate in liquid media, it compresses and stretches of liquid and generating pattern of compression and rarefaction (Figure 2.15). As the oscillation continues, it creates negative pressure within the liquid, breaks the liquid apart and eventually form voids within the media which is commonly called as microbubbles. These bubbles are said to initiate during the rarefaction cycle. The process by dissolved gas in the liquid is converted into free gas in the form of bubbles by the action of the sound field is called rectified diffusion. As the oscillation continues, the microbubbles will grow to unstable size and eventually collapse violently dissipating large amount of energy with localized temperature of 5000 K and pressures of 180 MPa.

Ultrasonic cavitation is said to occur in three steps: nucleation, growth, and collapse (Figure 15). Acoustic cavitation is affected by various factors such as viscosity, frequency, temperature, and vapor pressure. Cavitation is usually difficult in viscous liquids because it will have high resistance to shear. Similarly, when the liquid has high surface tension, there will be lesser dissolved gases, thus cavitation will also be difficult. It found that as ultrasonic frequency

increased, cavitation intensity decreased, as well as power dissipation. Mason et al. (1992) explained that at very high frequency, where the rate faction and compression cycles are very short, the finite time required for the rarefaction cycle is too small to permit a bubble to grow to a size sufficient to cause disruption of the liquid.

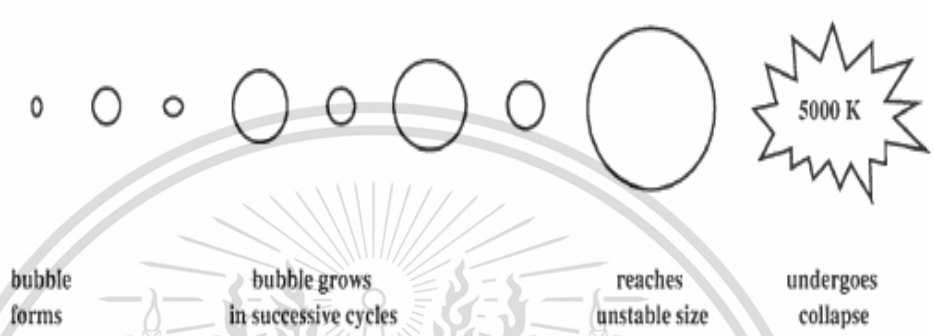


**Figure 2.15** Cavitation bubble formation, growth and collapse.

**Source**: Chowdhury and Viraraghavan (2009)

The ultrasound technique is used as physical method for modifying starch. Ultrasound treatment can affects the physicochemical properties of starch such as starch morphology, solubilities and swelling power, pasting properties, and gelatinization properties (Chemat & Hoarau, 2004; Zuo et al., 2009; Zhu et al., 2012; Sujka, 2017). However, the effect of ultrasound treatment on physicochemical properties depends on operation time, temperature, power, frequency, and botanical origin of starch (Park & Han, 2016).

### 2.5.2 Effects of ultrasound treatment on the starch

#### 2.5.2.1 Effects of ultrasound on the morphology of starch granules

Ultrasound treated starch led to the formation of crack, pores, and damage to the starch granules (Sujka & Jamroz, 2013; Flores-Silva et al., 2017). This effect was observed by scanning electron microscopy (SEM) (Figure 15). The effect of ultrasound treatment on the surface of starch granules depends on many factors such as ultrasound conditions (frequency, power, time operation, and temperature), concentration of the slurry (Huang et al., 2007; Luo et al., 2008; Jambrak et al., 2010; Sujka & Jamroz, 2013). This result as similar to the finding of Jambrak et al.

(2010) studied ultrasound treatment of maize starch for 15 min with a power of ultrasound with 2, 34, 55, and 77 W/cm$^2$ at a frequency 24 kHz showed that the increase in ultrasonication powers resulted in starch granules tendency to agglomerate and crack. Zuo et al. (2012) studied the ultrasound power in a range of 60-155 W (20 kHz) for 30 min treated potato starch; the damage on starch granules of this study presented more pores and cracking on the surface of potato starch granule. Flores-Silva et al. (2017) studied the characteristic of corn starch granules with the difference sonication time. Slurry of corn starch were suspended in distilled water with concentration of 30% w/v and treated with frequency at 24 kHz for 1, 2, 4, 8, and 16 min. Starch treated ultrasound with a longer time period developed fissures and cracks on the surface (shown in Figure 2.16).

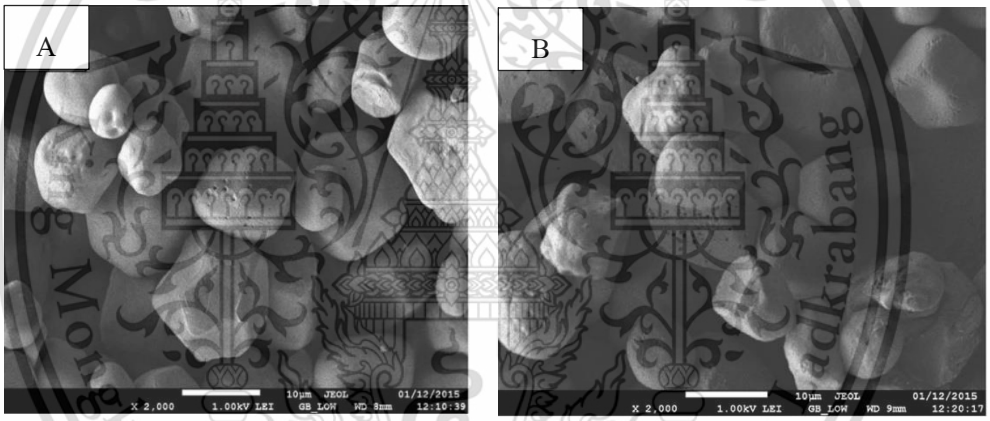


**Figure 2.16** SEM image of corn treated ultrasonic starch with frequency 24 kHz for 48 min (A) at 2000x magnification and 6500x magnification (B).

**Source**: Pamela et al. (2017)

#### 2.5.2.2 Effect of crystallinity of starch

Ultrasound treatment effects on the crystallinity of starch granules with several factors depended on ultrasound conditions and type of starch (Z.-Q. Huang et al., 2007; Luo & Lu, 2010). Ultrasound treatment had the effect on the polymorph type of A-type (maize starch), and B-type (tube starch) which observed by X-ray diffraction analysis. However, the crystallinity of starch might be increased or decreased depending on the conditions of ultrasound treatment and amylose content of starch. The increased crystallinity of starch treated ultrasound were reported by Pinto et

al. (2015) studied pinhão starch treated with ultrasound for 30 sec on and 5 sec off pulse at the amplitude frequency of 50% of 2 kHz. They reported this results that ultrasound treated pinhão starch had low crystallinity as compared to the native. Other studies are also reported that the crystallinity decreased after ultrasound treatment of cassava starch (Monroy et al., 2018), corn starch (Q. Huang et al., 2007), potato (Zhu et al., 2012). This effect attributed to cavitation process during ultrasound treatment which led to the destruction of crystalline arrays. Increased crystalline of starch treated ultrasound could be attributed to the disruption of amorphous region and/or rearrangement of starch chain (Zhu, 2015). This result presented in rice starch which agreed by the report of Cui et al. (2010) showed that crystalline increased after ultrasound treated brown rice. Park and Han (2016) also reported that rice starch treated ultrasound was observed by X-ray diffraction which was presented increase in crystallinity.

#### 2.5.2.3 Effect of pasting properties of starch

Ultrasound technique is used to modify the properties of starches in terms of physicochemical and their functional properties. The pasting properties was reported that ultrasound treatment reduced the viscosity during pasting. Many studies using different types of starch (corn, potato, and wheat) showed decrease in pasting viscosity (Huang et al., 2007; HerCeg et al., 2010; Majzoobi et al., 2015). The decrease in pasting viscosity of starch could be attributed to the disrupted granules with less swelling capacity, the damages on granules facilitating the penetration of water for hydration, and the broken starch chains as shown in the structure section. The decrease in pasting viscosity depends on ultrasound conditions, type of starch and amylose content. In contrast, ultrasound treatment showed increase in the pasting viscosity of starch.

#### 2.5.2.4 Effect of gelatinization properties of starch

Gelatinization of starch treated ultrasound was commonly analyzed by differential scanning calorimetry (DSC). The parameters of DSC for measuring include with gelatinization temperature (onset temperature ($T_o$), peak temperature ($T_p$), and conclusion temperature ($T_c$)) and enthalpy change of gelatinization ($\Delta H$). Several studied showed decreased the gelatinization temperature of maize starch (Q. Huang et al., 2007; Luo et al., 2008), cassava starch (Monroy et al., 2018), rice starch (Park & Han, 2016) and slightly change in that of wheat starch (Majzoobi et al., 2015). The decrease in gelatinization temperature attributed to the

destruction of crystal structure and the starch surface of ultrasound treated starch led to the requirement of the low temperature to gelatinization of starch. The enthalpy changes of gelatinization reflect the loss of molecular order of starch molecule (Hui Liu et al., 2006). Also decrease in enthalpy changes of gelatinization of starch affected by ultrasound treatment which was attributed to the disruption of amorphous region in the starch granule resulting in decrease in enthalpy change of gelatinization temperature (Park & Han, 2016). However, some studied showed increased the gelatinization temperature and enthalpy change of gelatinization which showed in maize starch (Jambrak et al., 2010), rice starch (Cui et al., 2010).

## 2.6 Fourier Transform Infrared Spectroscopy (FITR)

### 2.6.1 The Principle of FTIR spectroscopy

The total energy of a molecule consists of electronic energy, vibrational energy, rotational energy, and translation energy. According to its physical state, the energy due to different levels varies tremendously. Infrared radiation has adequate energy to result in transitions among vibrational, translational, and rotational energy levels of a molecule. The molecule can only absorb radiation from specific, narrow ranges of energies, raising its energy from the ground state to the excited state. Infrared spectroscopy is the study of transitions within vibrational and rotational energy levels resulting in from the absorption of infrared radiation (12800 – 10 $cm^{-1}$).

The FTIR spectroscopy in the mid-infrared region in a range of 4000 - 400 $cm^{-1}$. The FTIR instrument uses the interferometer system (Figure 2.17). The energy goes from the source to the beam splitter which divided the beam into two where one is transmitted onto a fixed mirror and the other to a moving mirror. The moving mirror moves back and forth at a constant velocity depending on the laser wavelength and both beams are reflected back into the beam splitter. The difference in beam distance from the moving versus fixed mirror produces and interferogram goes to the sample where some energy is transmitted and travels to the detector. Fourier Transform (FT) is a mathematical treatment which allows for the simultaneous collection of wavelengths though the detector.

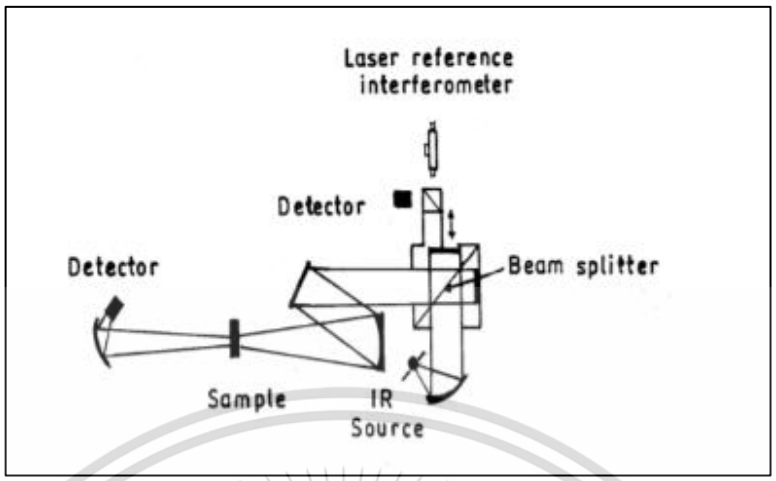


**Figure 2.17** Schematic diagram of the Michelson Interferometer FTIR spectrophotometer.

**Source**: Jaggi and Vij (2006)

The FTIR technique produces a fingerprint of each molecular structure which is a technique widely used for qualitative and quantitative characterization of the function groups of materials. It can provide important information on the structure, identity, environment of molecular materials. The infrared beam forms the FTIR unit passes through the sample and causes vibration, stretch, bending, and contraction of the chemical bonds. This occurs, excited chemical bonds absorb the infrared radiation at specific wavenumbers ($cm^{-1}$) (Table 2.4).

**Table 2.4** Frequencies of the major food components.

| Frequency ($cm^{-1}$) | Functional group | Mode of vibration | Food component |
|---|---|---|---|
| 3600-3200 | O-H | Stretch | Water, carbohydrates |
| 3300 | N-H (Amide A) | Stretch | Proteins |
| 3030 | C-H (*cis*) | Stretch | Unsaturated fats |
| 3000-2700 | C-H ($CH_2$, $CH_3$) | Stretch | Fats, Proteins, carbohydrates |
| 1745 | C=O (ester) | Stretch | Fats |
| 1725 | C=O (ester) | Stretch | Pectin |
| 1600-1700 | C=O (acidic) | Stretch | Fatty acid, acetic acid |

| Frequency ($cm^{-1}$) | Functional group | Mode of vibration | Food component |
|---|---|---|---|
| 1640 | O-H | Bend | Water |
| 1650 | C=O (Amide I) | Stretch | Proteins |
| | C-N (Amide I) | Stretch | Proteins |
| 1550 | N-H (Amide II) | Bend | Proteins |
| 1400-900 | C-O (acyl) | Stretch | Carbohydrates, fats |
| 1400-900 | C-H ($CH_2$) | Bend | Carbohydrates, fats |

**Source**: Modified from Hui and Sherkat (2005)

### 2.6.2 Application of FTIR in starch

The FTIR technique also applied in the starch to determine the functional groups which showed the information in the pattern of peak. It is sensitive to be changes the molecular structure. In addition, this technique can helps in the understanding of changes on pattern and information of the basis of chemical composition of starch sample (Flores-Morales et al., 2012). The FTIR spectra of starch typically presents bands at 2900-3000 $cm^{-1}$ (C-H stretching), 1100-1150 $cm^{-1}$ (C-O, C-C and C-O-H stretching) and 1100 - 900 $cm^{-1}$ (C-O-H bending) (Warren et al., 2016).

#### 2.6.2.1 Structure and composition of starch

The FTIR peaks of starch typically presents moisture, ash, carbohydrates and mixed with other compositions, including fat, and protein as presented in flour. In the spectrum of rice flour obtained by the FTIR represent the functional groups following; the wide band showed at 3300-3400 $cm^{-1}$ corresponding to O-H stretching. The intensity band at 2923 $cm^{-1}$, 1643 $cm^{-1}$ and 997 $cm^{-1}$ corresponding C-H stretching (CH2), C-O, C-O-H, and C-OC, respectively.

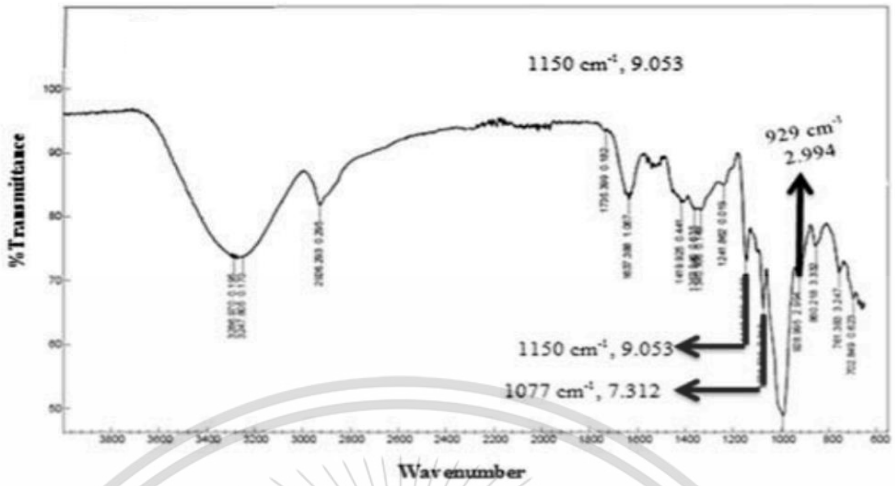


**Figure 2.18** FTIR spectra of rice flour

**Source**: Modified from Amin et al. (2017)

#### 2.6.2.2 The ratio of crystalline and amorphous of starch

The FTIR peaks of starches normally show sensitive to change in molecular structure level (short rage order), such as starch chain, helicity, crystallinity, and reorder of starch chains (O Sevenou et al., 2002). The wavenumber in a range from 1300-900 $cm^{-1}$ presented to be sensitive to change in starch structure. This wavenumber corresponds mainly C-O and C-C stretching vibration (Wang et al., 2015) (Figure 2.18). Particularly, this wavenumber region has been attributed to three main vibrational mode with maximum absorbances at 995, 1022 and 1047 $cm^{-1}$. There were widely studied in re-associated starches (retrograded starch) (van Soest & Vliegenthart, 1997), and enzyme hydrolyzed starched (O. Sevenou et al., 2002). From these studies reported that the band at 1022 $cm^{-1}$ is characterized increase in more amorphous region of starch, while the bands at 995 $cm^{-1}$ and 1047 $cm^{-1}$ are characterized in crystalline region of starch (Babu et al., 2019). The bands at 1047 and 1022 $cm^{-1}$ have been linked with order or crystallinity and amorphous regions in starch, respectively. Thus, the intensity ratio at 1047/1022 $cm^{-1}$ is associated with crystalline while, the ratio at 1022/995 $cm^{-1}$ is associated with amorphous region (Wang et al., 2015; Monroy et al., 2018). Moreover, the absorbance at the ratio of 1047/1022 $cm^{-1}$ and 1022/995 $cm^{-1}$ was applied in the research of ultrasound treated starches because this treatment could break starch chains (glycosidic linkages) by cavitation. This results led to decrease in the ratio of

1047/1022 $cm^{-1}$ while increase in 1022/995 $cm^{-1}$(Monroy et al., 2018; Babu et al., 2019). Similar to the finding of Monroy et al. (2018) found that the increase in the ratio of 1022/995 $cm^{-1}$ form 0.71 – 0.74 after sonication time increased (5-20 min) of cassava starch as compared to the native.

# CHAPTER 3

# METHODOLOGY

## 3.1 Materials

Three white rice cultivars: Glutinous rice (RD6), Khao Dawk Mali 105 (KDML105), were obtained from Ubon Ratchathani province, Thailand (15.2448° N, 104.8473° E), and Chai-Nat1 cultivar (CN1) was obtained from Chai-Nat province, Thailand (15.1852° N, 100.1251° E). Three rice cultivars were cropped in 2018 and milled into white rice. White rice grains of all cultivars were vacuum sealed in polyethylene film bags and storage at 4°C until used.

## 3.2 Reagents

3.2.1 Calcium chloride dihydrate ($CaCl_2.2H_2O$) (Merck, Germany)

3.2.2 Ethanol (95%) (AR grade, Merck, Germany)

3.2.3 Hydrochloric acid (Merck, Germany)

3.2.4 Iodine solution (0.2% I2 and 2.0% KI in distilled water) (Ajax Finechem, Australia)

3.2.5 Maleic acid (Ajax Finechem, Australia)

3.2.6 Potassium hydroxide (Ajax Finechem, Australia)

3.2.7 Potassium hydroxide (KOH) (Ajax Finechem, Australia)

3.2.8 Resistant starch kit (Resistant starch K-RSTAR 10.15, Megazyme, Iceland)

3.2.9 Sodium azide (Merck, Germany)

3.2.10 Sodium hydroxide (Carbo Erba Reagents, Italy)

3.2.11 Standard potato amylose (Merck, Germany)

## 3.3 Equipment

3.3.1 Centrifuge (Z-206A, Hermle, Germany)

3.3.2 Fourier transform infrared spectroscopy (FTIR) (Nicolet 6700, Thermo Scientific, Germany)

3.3.3 Grinding machine (SG-10HK, Cuisinart, USA)

3.3.4 Hot air oven (UNB 400, Memmert, Germany)

3.3.5 Magnetic stirrer (MS7-H550-Pro, Scilogex, USA)

3.3.6 Micro-pipettors and Tips (Mettler Toledo, Switzerland)

3.3.7 pH meter (SP-2100, Suntex, Taipei)

3.3.8 Pin mill (ZM 200, Retsch, Germany)

3.3.9 Rapid visco analyzer (RVA) (RVA-4, Newport scientific, Australia)

3.3.10 Screening machine (AS200, Retsch, Germany)

3.3.11 Shaker water bath (SV 1422, Memmert, Germany)

3.3.12 Tray dryer (Progress co. Ltd., Thailand) UV-Visible spectrophotometer (UV-1800, Shimadzu, Japan)

3.3.13 Vortex mixer (G560E, Scientific industries, USA)

3.3.14 Water bath (WNB 14, Memmert, Germany)

3.3.15 X-ray diffractometer (XRD) (model D8 discover, Bruker AXS, Germany)

## 3.4 Research methodology

### 3.4.1 Study the effects of ultrasound treatment and ultrasound-chilling treatment on physicochemical properties and *in vitro* glycemic index of rice grain

Three rice cultivars were used in this study including glutinous rice (RD6), Khao Dawk Mali 105 cultivar (KDML105), and Chai-Nat1 (CN1), respectively. All rice cultivars were treated with ultrasound treatment (U) and ultrasound and chilling treatment (UC), as following at below:

#### 3.4.1.1 Apparent amylose content

Apparent amylose content in each rice cultivars was examined by colorimetry method, according to Juliano (1982) as described in Appendix A1.

#### 3.4.1.2 Moisture content

The moisture content was analyzed for three rice cultivars, according to AACC 45-15A (2009) as described in Appendix A2.

#### 3.4.1.3 Ultrasound treatment (U)

Before ultrasound treatment (U), damaged rice grains were removed from rice samples. Ultrasound treatment (U) as following the method of Cui et al. (2010) was used with modifications. Ultrasound treatment, rice grains (500 g) were put in a wire basket ($19 \times 25 \times 9$ $cm^3$) and then immersed in 6 L of water at room temperature ($30 \pm 1^oC$). The rice sample was treated with ultrasound using ultrasonic bath (WUC-D10H, Wisd, Daihan scientific, Korea) for 15 and 30 min with amplitude at 40%, 70%, and 100% of ultrasonic power (665 W, 60 KHz). The increase of temperature range was recorded from 30 to $46^oC$ from all ultrasound treated rice samples. Ultrasound energy density at each condition was calculated following the equation of Giordano (2013), which showed as equation below. The calculated ultrasound energy density was showed in Table 3.1

$$\text{Ultrasound energy density } (kJ.L^{-1}) = \frac{\text{Power (W)} \times \text{Time (s)}}{\text{Volume (L)}} \quad (1)$$

**Table 3.1** Ultrasound power input and ultrasound intensity at each ultrasound conditions.

| Time (min) | Power (%) | Ultrasound power input (W) | Energy density ($kJ.L^{-1}$) |
|---|---|---|---|
| 15 | 40 | 162.80 | 24.42 |
| 15 | 70 | 284.90 | 42.74 |
| 15 | 100 | 407.00 | 61.05 |
| 30 | 40 | 162.80 | 48.84 |
| 30 | 70 | 284.90 | 85.47 |
| 30 | 100 | 407.00 | 122.10 |

After that, ultrasound treated rice samples (U) were dried at $40 \pm 5^oC$ in a tray dryer (progress co. Ltd., Thailand) to the moisture content of $11 \pm 1\%$. The dried U rice sample was kept in an aluminum foil - laminated bags until analysis. The controls of all rice cultivars were unmodified as “native”.

#### 3.4.1.4 Ultrasound and chilling treatment (UC)

The chilling treatment was treated rice grains after rice grains were treated ultrasound treatment to reorder starch chains for stronger structure of starch granules. The combinations of ultrasound and chilling treatment (UC), a half rice grains of ultrasound treated rice samples with various conditions (as outline in section 3.3.1.3) were put into polyethylene bags and then they were kept in the refrigerator at 4$^{o}$C for 24 hours. At the end of chilling period, all rice samples were dried at 40 ± 5$^{o}$C in a tray dryer to the moisture content of 11±1%. The dried UC rice samples were kept in an aluminum foil - laminated bags until analysis.

#### 3.4.1.5 Physicochemical properties analysis

The dried U rice and UC rice samples were ground into powder with a pin mill (ZM-200, Retsch, America) fitted with a 0.25 mm sieve. The rice powder was screened by 160 μm sieve for analysis of FTIR, XRD, pasting properties, and gelatinization properties.

3.3.1.5.1 Fourier transform infrared spectroscopy (FTIR)

This analysis was used to evaluate the crystallization degree of starch within the scope of short-range molecular order. Infrared spectra of all rice samples were recorded using a Nicolet 6700, Thermo Scientific (Madison, Germany). The rice powder was transferred into the FTIR system and each spectrum was scanned of 36 scans at 4 cm$^{-1}$ resolution in the wavenumber range at 4000 - 400 cm$^{-1}$. The ratio of absorbance at 1047 cm$^{-1}$ to 1022 cm$^{-1}$ was calculated (Babu et al., 2019). This ratio reflects the short-range crystallinity which related to double helix packing within the inner microstructure of starch granules.

3.3.1.5.2 X-ray diffraction (XRD)

X-ray diffraction (XRD) pattern of all rice samples was obtained using X-ray diffractometer (model D8 Discover, Buker AXS, Germany) operated at 40 kV and 40 mA. The rice powder was determined at scanning angle 2θ from 5 to 40$^{o}$ with a scan speed of 2$^{o}$ min$^{-1}$. Relative crystallinity was calculated the percent (%) using the equation of Rewthong et al. (2011), as below equation:

$$\text{Relative crystallinity (\%)} = (Ac/(Ac + Aa)) \times 100 \quad (2)$$

Where Ac is the crystalline area

Aa is the amorphous area.

3.3.1.5.3 Pasting properties

The pasting properties of U and UC rice sample of three rice cultivars were determined using a Rapid - Visco Analyzer (RVA) (model 4, Newport Scientific, Australia), according to Approved Method 61-02 (AACC, 2000). Each rice powder of three rice cultivars was weighed about 3.0 ± 0.05 g directly into 25 mL of distilled water in RVA canister. The sample was heated to 50°C and stirred at 160 rpm for 10 s for homogeneous dispersion. The slurry was held at 50°C for 1 min and then the temperature was linearly ramped up to 95°C and held at 95°C until 7.5 min, and finally cooled to 50°C and then held at 50°C until 12.5 min. The RVA parameter including the pasting temperature (PT), peak viscosity (PV), breakdown (BD), final viscosity (FV), and setback (SB) were recorded. The result was obtained by RVA amylograph and values for viscosity were reported in units termed centiPoint (cP).

3.3.1.5.4 Thermal properties

The thermal properties of three rice cultivars were determined using a differential scanning calorimetry (DSC 2 module, Mettler Toledo, Switzerland) and calibrated with indium before analysis. An empty pan was used as a reference. The rice powder (3.0±0.0005 mg.) and deionized water (9 µL) were added into an aluminum pan and immediately sealed. The pan was equilibrated for 24 hours at room temperature before heating in the DSC. After that, the pan was scanned over the range of 20 to 120$^{o}$C with a heating rate of 5$^{o}$C/min in a nitrogen atmosphere (20 mL/min). The DSC parameters including the onset temperature ($T_o$), peak temperature ($T_p$), conclusion temperature ($T_c$), and gelatinization enthalpy ($\Delta$H, J/g) were evaluated from DSC curve using the STARe Software.

3.3.1.5.5 *In vitro* glycemic index

The *In vitro* glycemic index or expected glycemic index (eGI) was analyzed by the AACC method 32-40.01 (AACC, 2000) with slightly modifications. All rice

samples of three rice cultivars were ground with a grinder (SG-10HK, Cuisinart, USA), then ground rice was sieved through 1.0 mm screen. The ground rice (100±5 mg) was added with 4.0 mL of pancreatic α-amylase into screw cap tube and incubated at 37°C in a shaking water bath for 30, 60, 90, 120, 150, and 180 min. After that, 8.0 mL of ethanol (99%v/v) was added and centrifuged at 1500xg for 10 min. The supernatant was decanted into a volumetric flask. The pellet was washed with 8 mL of ethanol (50%v/v). The supernatant was combined into the initial supernatant and adjusted the volume with sodium acetate buffer (pH 4.5) to 100 mL in a volumetric flask. Then, 0.1 ml of this solution was put into a test tube with 10 µl of dilute amyloglucosidase solution (300 U/ml) in 100 mM sodium maleate buffer (pH 6.0) and incubated for 20 min at 50°C. The glucose content was measured using glucose oxidase-peroxidase kit (GOPOD-kit).

Percentage of starch hydrolysis was calculated by the following equation of AACC (2000):

$$\text{Starch hydrolysis (\%)} = \Delta E \times (F/W) \times 90 \quad (3)$$

Where: ΔE = absorbance (reaction) read against the reagent blank.

F = conversion from absorbance to micrograms (the absorbance obtained for 100 µg of D-glucose in the GOPOD reaction is determined and F = 100 (µg of D-glucose) divided by the GOPOD absorbance for 100 µg of D-glucose.

W = dry weight of sample analyzed (mg.) as calculated following the equation:

$$\text{Dry weight of sample (mg.)} = \text{weight of sample} \times \frac{(100 - \text{moisture content})}{100} \quad (4)$$

The kinetic of starch hydrolysis of the glutinous rice was calculated by the model established of Goñi et al. (1997):

$$C = C_{\infty}(1 - e^{-kt}) \quad (5)$$

Where C, $C_\infty$, and k is the percentage of starch hydrolyzed at time t (min), the equilibrium percentage of starch hydrolyzed after 180 min, and the kinetic constant, respectively.

The hydrolysis curve area (AUC) was calculated by the following equation:

$$AUC = C_\infty (t_f - t_0) - (C_\infty / k)(1 - \exp^{(-k(tf - t0))}) \quad (6)$$

Where $t_f$ and $t_0$ were the final time (180 min) and the initial time (0 min), respectively. The hydrolysis index (HI) was calculated by dividing the area under the hydrolysis curve of sample by the area of a reference sample as white bread (President Bakery Public Company Limited, Thailand).

The eGI was calculated using the equation following Goñi et al. (1997):

$$eGI = 39.71+(0.549HI) \quad (7)$$

**3.4.1.6 Statistical analysis**

The experiment was conducted with Factorial Design in the Completely Randomized Design (CRD) within control (unmodified rice grains). Two factors of this study were examined including, (1) sonication times (15 and 30 min) and (2) power levels (40, 70, and 100% of ultrasound power). For the ultrasound treatments plus chilling treatment (UC) was conducted with CRD. Each physicochemical parameter and *in vitro* glycemic index were reported as the mean ± standard deviation at least triplicate measurements, with the exception of relative crystallinity was performed only one. Statistical analyses were performed with the software SPSS version 22.0 for windows (SPSS, Inc., Chicago, IL, USA). Analysis of variance (ANOVA) following by Duncan's multiple range test (DMRT) at $p<0.05$ was used for statistical analysis in this experiment.

The lowest GI rice sample of each rice cultivars was selected to further study on the combined physical modification methods of ultrasound-chilling-annealing treatments.

**3.4.2 Study the effects of ultrasound and annealing treatment on physicochemical properties and *in vitro* glycemic index of rice grains**

The rice grains sample of each rice cultivars was selected from the previous section to improve lowering the glycemic index using by annealing treatment (ANN). Rice grains sample of each rice cultivars was treated with ANN as the procedure described by Dias et al. (2010) with minor modifications. Ultrasound and chilling treated rice grains (UC) of each rice cultivars were further treated with ANN treatment. UC rice samples of each rice cultivars were placed in an aluminum tray (21 cm long x 30 cm wide), then covered with aluminum foil. After that, rice samples were incubated in an incubator (MIR-23, Sunyo, Japan) at 45, 50, or 55$^{o}$C for 16 h. At the end of incubation period, annealed rice samples were dried in a tray dryer at 40 ± 5$^{o}$C to moisture content of 11±1%.

**3.4.2.1 Physicochemical properties analysis**

The dried UC rice samples and annealed rice grains samples were ground into powder with a pin mill (ZM-200, Retsch, America) fitted with a 0.25 mm sieve. The rice powder was screened by 160 µm sieve for further analysis.

3.4.2.1.1 X-ray diffraction (XRD)

The analysis of XRD as described in the section 3.3.1.5.2

3.3.2.1.2 Pasting properties

The analysis of pasting properties as described in the section 3.3.1.5.3

3.4.2.1.2 Gelatinization properties

The analysis of pasting properties as described in the section 3.3.1.5.4

3.4.2.1.3 *In vitro* glycemic index

The analysis of glycemic index as described in the section 3.3.1.5.5

**3.4.2.2 Statistical analysis**

The experiment of this study was conducted in a completely randomized design (CRD) with three replications, except relative crystallinity was perform only one. Each

physicochemical parameter and expected glycemic index were reported as the mean ± standard deviation. Statistical analysis was performed with the software SPSS version 22.0 for windows (SPSS, Inc., Chicago, IL, USA). Analysis of variance (ANOVA) following by Duncan's multiple range test (DMRT) at $p<0.05$.

# CHAPTER 4

# RESULTS AND DISCUSSION

## 4.1 The effects of ultrasound treatments and ultrasound-chilling treatments on physicochemical properties and *in vitro* glycemic index of rice grains

This study was investigated sonication times and ultrasound power levels on the physicochemical properties and *in vitro* glycemic index of Thai rice grains. Three cultivars of Thai rice grains were used including, RD6, KDML105, and CN1 rice cultivars. The experiment of this part was conducted with factorial design in CRD. These had two factors, (1) sonication times for 15 and 30 min, and (2) power levels at 40%, 70% and 100% of ultrasound power. Moreover, this part was studied the effect of ultrasound plus chilling treatments on physicochemical properties and glycemic index of rice grains. The experiment was performed in CRD.

### 4.1.1 The moisture content and apparent amylose content of three rice cultivars

The moisture content and apparent amylose content of three rice cultivar are shown in Table 4.1. The moisture content of rice samples is about 11%wb. Three rice cultivars were significantly different in amylose contents ($p$<0.05). Amylose content of three rice cultivars was low amylose content (7.04 g/100g) for RD6, low amylose content (16.91 g/100g) for KDML105, and high amylose (29.35 g/100) for CN1 rice. The CN1 rice has a higher amylose content in comparison to RD6 and KDML105 rice. Apparent amylose content is the major constituent of rice, which usually used to classify following amylose content into five groups including, high (25-32%), medium (20-25%), low (10-20%), very low (2-10%) and waxy (0-2%) (Juliano, 1985).

**Table 4.1** Moisture content and amylose content of three rice cultivars

| Rice cultivars | Moisture content (% wb) $^{ns}$ | Apparent amylose content g/100g | Classification of amylose content |
|---|---|---|---|
| RD6 | 11.32±0.04 | 7.04±0.02$^{c}$ | Very low |
| KDML105 | 11.28±0.17 | 16.91±0.40$^{b}$ | Low |
| CN1 | 11.02±0.32 | 29.35±0.82$^{a}$ | High |

**4.1.2 The effect of ultrasound treatments on physicochemical properties and *in vitro* digestibility of rice grains**

This part was studied the conditions of ultrasound treatment; times, and power levels, for three rice cultivars: RD6, KDML105, and CN1 rice. The experimental of this part was performed in factorial design in CRD. This has two factors: processing time has two levels (15 and 30 min) and ultrasound power levels has three levels (40, 70 and 100% of ultrasound power). From analysis of variances of the physicochemical properties and glycemic index of ultrasound treated rice samples are presented in Table 4.2 for RD6, Table 4.3 for KDML105, and Table 4.4 for CN1 cultivar as follows:

The variance analysis of RD6 rice showed that sonication time and power levels had significant interaction ($p<0.05$) in pasting viscosity, breakdown, final viscosity, enthalpy change, kinetic rate (k-value), hydrolysis index (HI), and expected glycemic index (eGI). While FTIR (1047/1022cm$^{-1}$), pasting temperature, setback, onset temperature, peak temperature, and conclusion temperature were not significantly interaction between that factors ($p\geq0.05$) as shown in Table 4.2.

The variance analysis of KDML105 rice showed that sonication time and power levels had significant interaction ($p<0.05$) in pasting viscosity, breakdown, final viscosity, setback, onset temperature, conclusion temperature, enthalpy change, kinetic rate (k-value), hydrolysis index (HI), and expected glycemic index (eGI). While pasting temperature, and peak temperature were not significantly interaction between that factors ($p\geq0.05$) as shown in Table 4.3.

The variance analysis of CN1 rice showed that sonication time and power levels had significant interaction ($p<0.05$) in pasting viscosity, breakdown, final viscosity, setback, kinetic rate k-value, hydrolysis index (HI), and expected glycemic index (eGI). While pasting temperature, onset temperature, peak temperature, conclusion temperature, and enthalpy change were not significantly interaction between them ($p\geq0.05$) as shown in Table 4.4.

The detail of these interaction will be discussed in further section as follows.

**Table 4.2** Analysis of variance of sonication times and percentage of ultrasound power on physicochemical properties of RD6 cultivar.

| Physiochemical properties | Sonication times | Percentage of ultrasound power | Sonication time × percentage of ultrasound power |
|---|---|---|---|
| FTIR (1047/1022 $cm^{-1}$) | * | ns | ns |
| Pasting temperature (PT) | ns | * | ns |
| Pasting viscosity (PV) | * | ns | * |
| Breakdown (BD) | * | * | * |
| Final viscosity (FV) | ns | ns | * |
| Set back (SB) | * | * | ns |
| Onset temperature (To) | * | ns | ns |
| Peak temperature (Tp) | ns | ns | ns |
| Conclusion temperature (Tc) | ns | ns | ns |
| Enthalpy change ($\Delta$H) | * | * | * |
| Kinetic rate (k-value) | * | ns | * |
| Hydrolysis Index (HI) | * | * | * |
| Expected glycemic index (eGI) | * | * | * |

* : Significant interaction at $p<0.05$.

ns : Non-significant interaction at $p\geq0.05$.

**Table 4.3** Analysis of variance of sonication times and percentage of ultrasound power on physicochemical properties of KDML105 cultivar.

| Physiochemical properties | Sonication times | Percentage of ultrasound power | Sonication time × percentage of ultrasound power |
|---|---|---|---|
| FTIR (1047/1022 $cm^{-1}$) | * | ns | ns |
| Pasting temperature (PT) | * | ns | * |
| Pasting viscosity (PV) | * | * | * |
| Breakdown (BD) | ns | ns | * |
| Final viscosity (FV) | * | * | * |
| Set back (SB) | * | ns | * |
| Onset temperature (To) | * | ns | ns |
| Peak temperature (Tp) | ns | * | ns |
| Conclusion temperature (Tc) | * | ns | ns |
| Enthalpy change ($\Delta$H) | * | * | * |
| Kinetic rate (k-value) | ns | * | * |
| Hydrolysis Index (HI) | ns | * | * |
| Expected glycemic index (eGI) | ns | * | * |

* : Significant interaction at $p<0.05$.

ns : Non-significant interaction at $p\geq0.05$.

**Table 4.4** Analysis of variance of sonication times and percentage of ultrasound power on physicochemical properties of CN1 cultivar.

| Physiochemical properties | Sonication times | Percentage of ultrasound power | Sonication time × percentage of ultrasound power |
|---|---|---|---|
| FTIR (1047/1022 $cm^{-1}$) | * | ns | ns |
| Pasting temperature (PT) | ns | ns | ns |
| Pasting viscosity (PV) | * | * | * |
| Breakdown (BD) | ns | ns | * |
| Final viscosity (FV) | * | * | * |
| Set back (SB) | * | ns | * |
| Onset temperature (To) | * | ns | ns |
| Peak temperature (Tp) | * | ns | ns |
| Conclusion temperature (Tc) | * | ns | ns |
| Enthalpy change (H) | ns | * | ns |
| Kinetic rate (k-value) | * | * | * |
| Hydrolysis Index (HI) | ns | * | * |
| Expected glycemic index (eGI) | * | * | * |

* : Significant interaction at $p<0.05$.

ns : Non-significant interaction at $p\geq0.05$.

#### 4.1.2.1 The effects of ultrasound treatments and ultrasound-chilling treatments on Fourier Transform Infrared (FTIR) spectrum and crystallinity of rice grains

The FTIR spectra pattern presented band that associated to stretching, flexion, and deformation correspond to functional groups of samples (Flores-Morales et al., 2012). The FTIR patterns for natives and treated rice grains of three rice cultivars; RD6, KDML105, and CN1 rice, are presented in Figure 4.1. The FTIR spectra associated with the main functional groups characteristic of rice samples (Monroy et al., 2018). The FTIR spectra of ultrasound treated rice grains (U) of three rice cultivars showed no obvious changes after ultrasound treatments. Even though increased sonication times and ultrasound power levels did not change FTIR spectra. The reason might be because ultrasound waves could not change the functional groups of starch molecules (Zheng et al., 2013). Therefore, the structure of starch molecules treated ultrasound was similar to its native of three rice cultivars. Also, the FTIR patterns of ultrasound plus chilling treated rice grains (UC) were not changed (data showed in appendix B1). According to Figure 4.1, the wide band presented in a range from 3300 to 3400 $cm^{-1}$ corresponded to vibration of O-H group (Flores-Silva et al., 2017). The intensity band at 2923 $cm^{-1}$ attributed to C-H vibration, absorption band of fat and the band at ~1532 $cm^{-1}$ corresponded to amide II. The bands as followed at: 1643 $cm^{-1}$ to the stretching vibration of C-O bond, 1344 $cm^{-1}$ to C-O-H, and 997 $cm^{-1}$ to C-O-C groups. The band in range from 900 to 1300 $cm^{-1}$ corresponds mainly to C-O and C-C stretching vibration (Warren et al., 2016; Monroy et al., 2018). In addition, the band at 1047 $cm^{-1}$ represented the crystalline regions, and that at 1022 $cm^{-1}$ represented amorphous regions. Thus, the absorbance ratio of 1047 and 1022 $cm^{-1}$ is normally measure the short-range crystallinity (Flores-Silva et al., 2017), which related to the double helices packing within starch granules. The results of that ratio are presented in Table 4.5 for RD6, Table 4.6 for KDML105, and Table 4.7 for CN1 cultivars, respectively. Ultrasound-chilled rice (UC) samples are also presented in the same table of their rice cultivars.

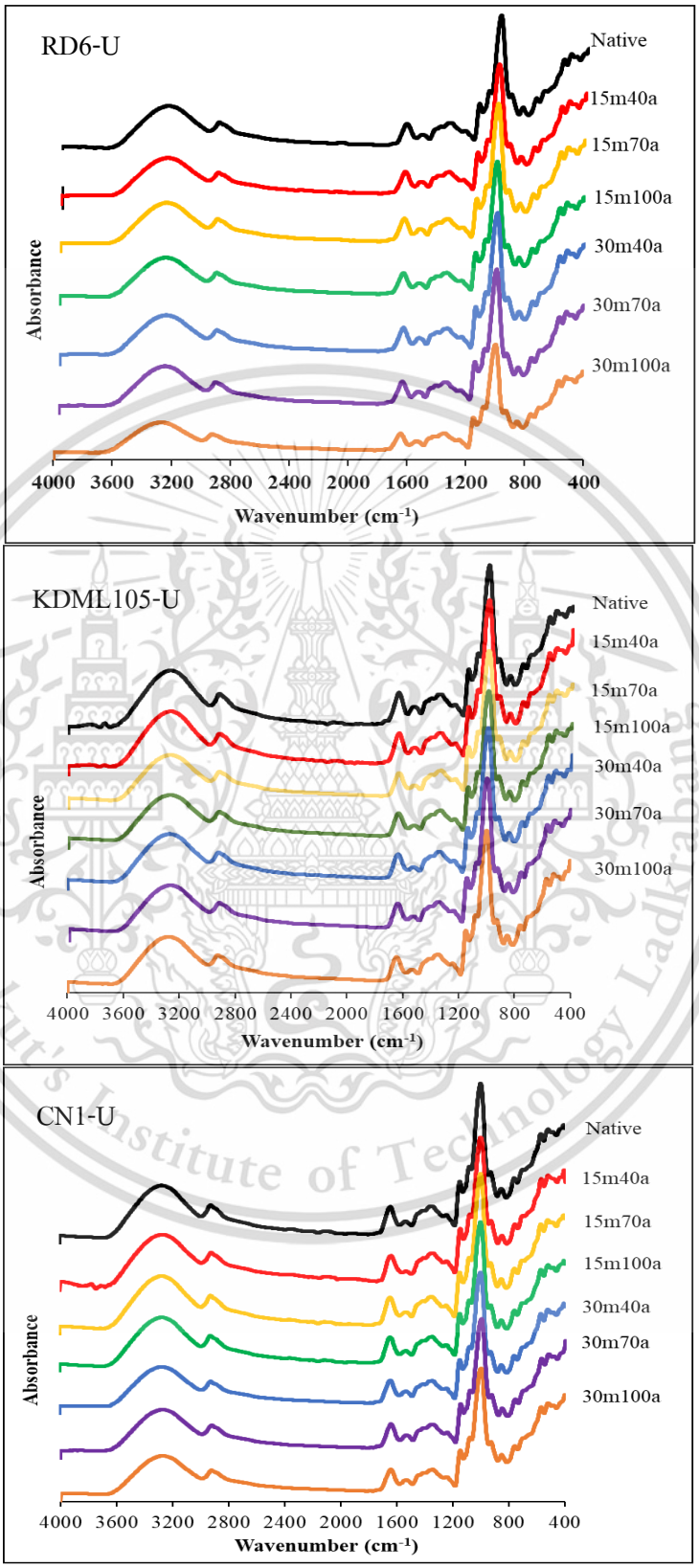


**Figure 4.1** FITR spectra of the natives and ultrasound treated rice samples of three rice cultivars.

According to Table 4.2 - 4.4 are presented variance analysis of the absorbance at 1047/1022 $cm^{-1}$ of rice grans treated ultrasound (U). The ratio at absorbance at 1047/1022 $cm^{-1}$ of ultrasound treatment and ultrasound - chilling treatments (UC) for RD6, KDML105 and CN1 rice are presented in Table 4.5, 4.6 and 4.7, respectively, as follows:

The ratio of absorbance at 1047/1022 $cm^{-1}$ was no significant interaction ($p \geq 0.05$) between sonication times and ultrasound power levels for RD6, KDML105, and CN1 rice cultivars as shown in Table 4.2 – 4.4. Ultrasound treated rice with increased sonication times and ultrasound power levels demonstrated decrease in proportion of crystalline to amorphous. The ratio of 1047/1022 $cm^{-1}$ tended to decrease in a range between 0.779 and 0.662 (15.02%) for RD6, 0.707 and 0.673 (4.81%) for KDML105, and 0.682 and 0.670 (1.76%) for CN1 rice, as compared to its natives. These indicated that the crystallinity regions disrupted by ultrasound treatment (Flores-Silva et al., 2017). This result agreed with the finding of Monroy et al. (2018). The changes in the ratio of 1047/1022 $cm^{-1}$ of three rice cultivars appear not only dependent on ultrasound conditions, but also on type and composition of the starch. For example, the sonication with 15 min at 40% power level decreased the crystallinity of RD6 more than that KDML105 and CN1 rice. This suggests that high amylose content had resistant susceptibility in destroying crystalline regions to ultrasound treatments (Luo et al., 2008; Zhu, 2015). However, the factors of ultrasound time and amplitude did not apparently affect the ratio at 1047/1022 $cm^{-1}$ of ultrasound treated rice, which implied to the crystalline and amorphous region of rice flour molecule treated by ultrasound.

In addition, the ultrasound treated rice followed chilling treatments (UC) of three rice cultivars. The ratio of 1047/1022 $cm^{-1}$ of UC samples tended to slightly increase. Kang et al. (2016) noted that linear starch chains are exposed by debranching of amylopectin molecules or/and fragmentation of amylose molecules as affected by ultrasound, which could be more re-arranged resulting in increased crystallinity.

**Table 4.5** The absorbance ratio at 1047/1022 $cm^{-1}$ of native, ultrasound treatment, and ultrasound-chilling treatment for RD6 rice.

| Rice cultivar | Sonication time | Ultrasound power | 1047/1022 ($cm^{-1}$) | |
|---|---|---|---|---|
| | (min.) | (%) | U [ns] | UC |
| RD6 | Native | - | 0.779±0.001 | 0.779±0.001[a] |
| | 15 | 40 | 0.671±0.002 | 0.672±0.001[a] |
| | 15 | 70 | 0.662±0.001 | 0.662±0.192[a] |
| | 15 | 100 | 0.664±0.001 | 0.667±0.005[a] |
| | 30 | 40 | 0.680±0.001 | 0.682±0.011[a] |
| | 30 | 70 | 0.665±0.001 | 0.666±0.001[a] |
| | 30 | 100 | 0.665±0.001 | 0.661±0.001[a] |

The data referred to the mean ± standard deviation (n=3). Values followed by the lowercase letters in the same column were significantly different at $p<0.05$.

Native: rice without modification, U: ultrasound treatment, UC: ultrasound and chilling treatments.

**Table 4.6** The absorbance ratio at 1047/1022 $cm^{-1}$ of native, ultrasound treatment, and ultrasound-chilling treatment for KDML105 rice.

| Rice cultivar | Sonication time | Ultrasound power | 1047/1022 ($cm^{-1}$) | |
|---|---|---|---|---|
| | (min.) | (%) | U [ns] | UC |
| KDML105 | Native | | 0.707±0.007 | 0.707±0.007[a] |
| | 15 | 40 | 0.684±0.011 | 0.708±0.001[a] |
| | 15 | 70 | 0.679±0.001 | 0.701±0.001[b] |
| | 15 | 100 | 0.679±0.001 | 0.685±0.001[c] |
| | 30 | 40 | 0.675±0.001 | 0.700±0.001[b] |
| | 30 | 70 | 0.676±0.001 | 0.692±0.002[c] |
| | 30 | 100 | 0.673±0.001 | 0.693±0.002[c] |

The data referred to the mean ± standard deviation (n=3). Values followed by the lowercase letters in the same column were significantly different at $p<0.05$.

Native: rice without modification, U: ultrasound treatment, UC: ultrasound and chilling treatments.

**Table 4.7** The absorbance ratio at 1047/1022 $cm^{-}$ of native, ultrasound treatment, and ultrasound-chilling treatment for CN1 rice.

| Rice cultivar | Sonication time (min.) | Ultrasound power (%) | 1047/1022 ($cm^{-1}$) U [ns] | 1047/1022 ($cm^{-1}$) UC |
|---|---|---|---|---|
| CN1 | Native | - | 0.682±0.00 | 0.682±0.00[c] |
| | 15 | 40 | 0.682±0.00 | 0.693±0.01[ab] |
| | 15 | 70 | 0.686±0.00 | 0.687±0.00[b] |
| | 15 | 100 | 0.670±0.00 | 0.671±0.01[c] |
| | 30 | 40 | 0.670±0.00 | 0.699±0.00[a] |
| | 30 | 70 | 0.680±0.00 | 0.697±0.00[a] |
| | 30 | 100 | 0.676±0.00 | 0.670±0.00[c] |

The data referred to the mean ± standard deviation (n=3). Values followed by different superscripts within a column were significantly different at $p<0.05$.

Native: rice without modification, U: ultrasound treatment, UC: ultrasound and chilling treatments.

#### 4.1.2.2 The effects of ultrasound treatments and ultrasound-chilling treatments on X-ray diffraction pattern and relative crystallinity of rice grains

X-ray diffractograms of three rice cultivars are presented in Figure 4.2. In general, the branch chains and structure of the amylopectin side chains are usually represented A, B, and C types, that depending on source of starches (Thirumdas et al., 2016). The X-ray pattern of rice normally presents an A-type. This type shows strong diffractions at single peak at $15^{o}$ and 23, followed by double peak at $17^{o}$ and $18^{o}$ ($2\theta$), and a small peak at $20^{o}$ ($2\theta$) represented a bound of amylose-lipid complex, which presented V-type (Guo et al., 2015). Thus, samples of three rice cultivars were also presented in A+V type. Ultrasound treatments (U), grains of three rice cultivars treated with longer sonication times and higher power levels were still similar pattern as compared to their native. This result was supported in maize starch (Babu et al., 2019), casava (Monroy et al., 2018), brown rice (Park & Han, 2016), and potato (Zhu et al., 2012); their pattern unchanged after ultrasound treatments. Chilling after ultrasound treatments (UC), the X-ray patterns for three rice cultivars were similar to their native, indicating that chilling did not cause change in the crystalline structure. These results related to our previous report of FTIR spectra (Figure 4.1).

Relative crystallinity of three rice cultivars are presented in Table 4.8. The crystallinity of natives for RD6, KDML105, and CN1 was 31.99%, 22.94%, and 25.88%, respectively. Normally, the relative crystallinity is significantly positive correlation with amylopectin side chains and negative correlation with amylose content (Wani et al., 2012; Zhang et al., 2019). Glutinous rice (RD6 cultivar) showed a higher relative crystallinity values than normal rice (KDML105 and CN1 cultivars), which related to their amylose content as presented in Table 4.1. The relative crystallinity of ultrasound treatments from RD6 and KDML105 cultivars was decreased from 31.99% to 27.20% and 22.94% to 16.59%, respectively, when those rice samples were treated with longer sonication times and at higher power levels of ultrasound treatment. This could attributed to debranching of amylopectin molecules or/and fragmentation of amylose molecules caused by the effect of ultrasound waves in C-O-C linkages, resulting in crystallinity decreased (Flores-Silva et al., 2017). However, at 70 and 100% of ultrasound power treated RD6 and KDML105 rice samples showed that crystallinity slightly decreased. While longer sonication times of ultrasound treatments and at the same level of ultrasound power, i.e. ultrasound treatments

at 15m70a and 30m70a, showed distinctly decreased crystallinity. These results suggested that sonication time had higher impact than ultrasound power on crystallinity. Similar the result was reported by Monroy et al. (2018) found that ultrasound treated casava starch with difference times (5, 10, 20 min) at power of 750 w; the crystallinity was fell to 20.9% to 17.40% by increasing sonication times.

In contrast to the relative crystallinity of CN1 rice showed slightly increased from 25.88% to 28.21% after ultrasound treatment for 15 min, but it tended to decrease thereafter (27.14% to 26.14%), especially at higher power levels as showed in Table 4.8. Bai et al. (2017) found that decreased crystallinity was exhibited after ultrasound treatment with increased ultrasound power from 30 to 120 W. The initial increased crystallinity after ultrasound treatment for 15 min could be attributed to the disruption of amorphous regions, and after that ultrasound may induce the destruction of crystalline regions, resulting in crystallinity increased (Zhu, 2015). Moreover, some study noted that different types of rice samples might be expected different packing of the crystalline and amorphous parts in the granules gives rise to their different susceptibility to the ultrasound treatment (Zhu, 2015; Kang et al., 2016).

For ultrasound-chilling treatments (UC), remarkable results of RD6 and KDML105 rice cultivars showed increased relative crystallinity, after ultrasound followed by chilling treatment as compared to its ultrasound treated rice (shown in Table 4.8). Flores-Silva et al. (2017) reported that the higher crystallinity indicated that more packed re-arrangement of the double-helices structure. However, relative crystallinity of UC for CN1 rice was slightly changed. Wang et al. (2015) suggested that starch re-arrangement and association of starch chains depend on size chains of amylose or amylopectin.

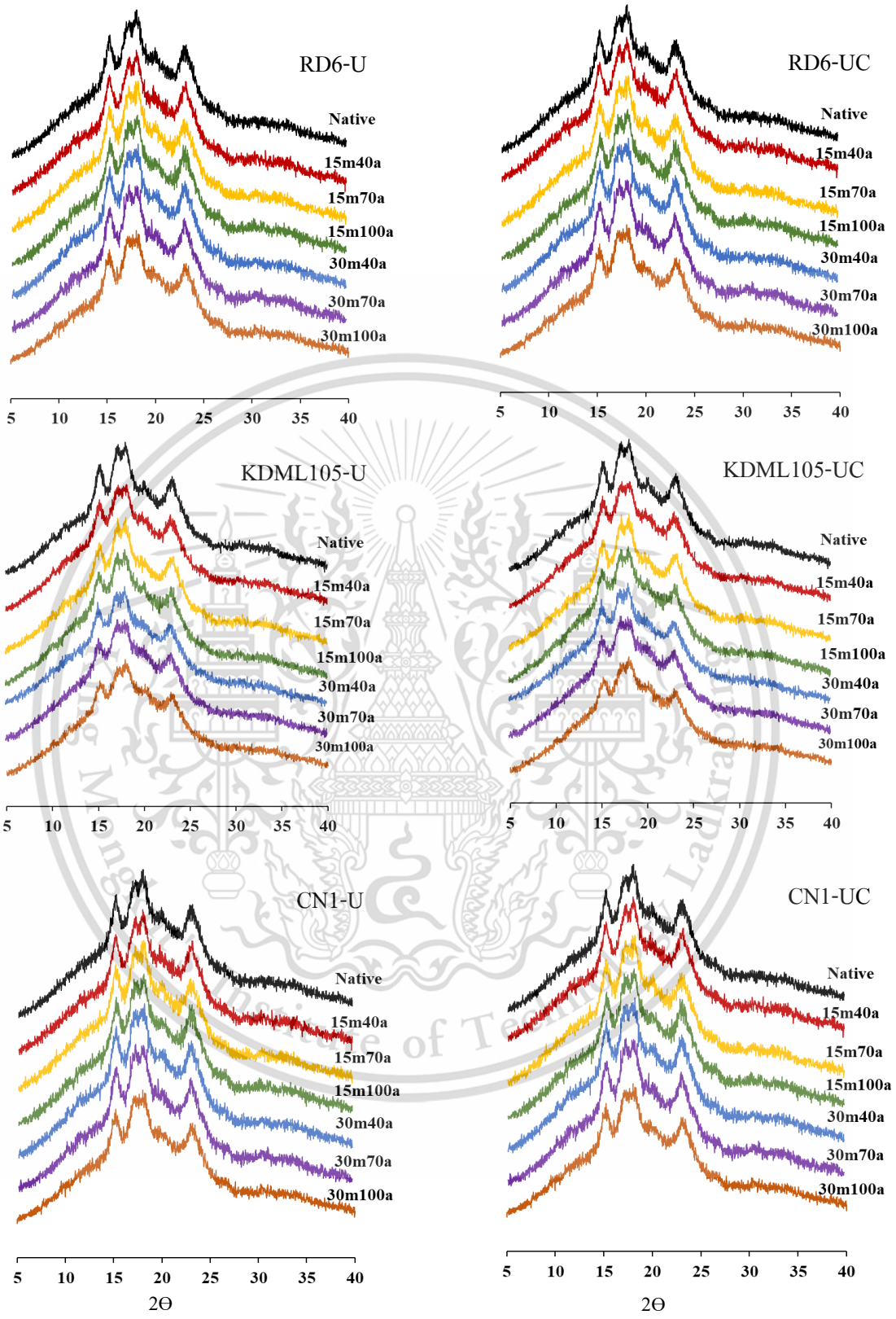


**Figure 4.2** XRD patterns of three rice cultivars.

U: ultrasound treatments, UC: ultrasound-chilling treatments. 15 and 30m: sonication times. 40, 70, and 100: percentage of ultrasound power

**Table 4.8** The percentage of crystallinity and diffraction pattern of natives, ultrasound treatment, and ultrasound-chilling treatments for three rice cultivars.

| Cultivars | Time | Ultrasound power | Crystallinity (%) | | Diffraction pattern |
|---|---|---|---|---|---|
| | (min.) | (%) | U | UC | |
| RD6 | Native | | 31.99 | 31.99 | A+V type |
| | 15 | 40 | 30.87 | 32.16 | A+V type |
| | 15 | 70 | 28.71 | 32.21 | A+V type |
| | 15 | 100 | 28.74 | 30.60 | A+V type |
| | 30 | 40 | 29.53 | 30.84 | A+V type |
| | 30 | 70 | 27.87 | 32.22 | A+V type |
| | 30 | 100 | 27.20 | 32.15 | A+V type |
| KDML105 | Native | | 22.94 | 22.94 | A+V type |
| | 15 | 40 | 20.70 | 22.54 | A+V type |
| | 15 | 70 | 19.36 | 25.80 | A+V type |
| | 15 | 100 | 18.71 | 20.89 | A+V type |
| | 30 | 40 | 17.58 | 23.70 | A+V type |
| | 30 | 70 | 16.59 | 21.79 | A+V type |
| | 30 | 100 | 16.59 | 22.72 | A+V type |
| CN1 | Native | | 25.88 | 25.88 | A+V type |
| | 15 | 40 | 26.97 | 27.42 | A+V type |
| | 15 | 70 | 26.87 | 28.20 | A+V type |
| | 15 | 100 | 28.21 | 26.44 | A+V type |
| | 30 | 40 | 27.14 | 27.85 | A+V type |
| | 30 | 70 | 26.25 | 27.65 | A+V type |
| | 30 | 100 | 26.14 | 27.18 | A+V type |

U: ultrasound treatment, UC: ultrasound-chilling treatments.

Native: rice without modification.

#### 4.1.2.3 The effects of ultrasound treatments and ultrasound-chilling treatments on pasting properties of rice grains

Pasting parameters of rice samples; pasting time (PT), pasting viscosity (PV), breakdown (BD), and final viscosity (FV), were tested for three rice cultivars. The results of pasting properties of ultrasound treatment and ultrasound-chilling treatments for each rice cultivars are as follow:

Variance analyses of pasting properties of pasting properties for RD6 rice are presented in Table 4.2. Ultrasound treated rice samples with sonication times (15 and 30 min) and ultrasound power levels (40, 70, and 100% of ultrasound power) showed significance interaction ($p$<0.05) in pasting viscosity, break down, final viscosity, but pasting temperature and setback values were no significant interaction ($p$≥0.05) between sonication times and ultrasound power. Although pasting temperature was no interaction, but it was decreased (66.48 to 64.65$^{o}$C) when treated for longer times with higher power levels; i.e sonication time for 30 min at 40 - 100% of ultrasound power. The increased sonication times and power levels led to change in pasting viscosity (3346.67 – 3838.67 cP), final viscosity (2562 – 2922 cP), breakdown (124.67 – 1416.67 cP), and setback values (417 - 563 cP), nevertheless these changed depending on ultrasound conditions. Particularly, longer sonication times led to the greater damaged starch structures and the surface of rice grains than ultrasound power levels (Ulloa et al., 2015). These results be due to some destruction of the shell and grain fragmentations (as shown in appendix B-2.) causing attributed to a possible damage of amylopectin or/and amylose chains within starch granules leading to decrease in peak viscosity (Pinto et al., 2015). As comparison with native, ultrasound treatments showed higher breakdown values than native, causing the destruction of starch granules resulted in starch granules have less resistance during heating and stirring starch paste (Zhu et al., 2020). Furthermore, final viscosity and setback showed higher than native could be due to a linear starch chains fragment or breaking the C-O-C of and/or α-1,6 glycosidic linkage of amylose and amylopectin chains by ultrasound (Kang et al., 2016) in to outside prone to re-associate during cooling of starch pate. Bernardo et al. (2018) reported that higher amplitude of ultrasound processing resulted in destroyed starch granules.

Additionally, ultrasound treated RD6 rice samples were then chilling treatment (UC). Chilling after ultrasound treated rice samples exhibited the increased pasting temperature (75.40 - 78.73$^{o}$C). The increased pasting temperature could be because of re-association between starch molecules by chilling treatment attributed to strong interaction inner starch molecules (Klein et al., 2013; Pinto et al., 2015). These data agree with increased relative crystallinity (Table 4.8). Ultrasound – chilled rice samples lead to be decreased pasting viscosity (2922.67 – 3244.00 cP), breakdown (1188.33 – 917.00 cP), setback (465.00 – 570.33 cP), and final viscosity (2481.00 – 2612.33 cP). Remarkable decreased pasting viscosity, breakdown, setback, and final viscosity of UC treatments compared to its ultrasound condition. Pinto et al. (2015) reported that storage starch after ultrasound treatment at 4$^{o}$C might be improve more packing of double-helixes within starch granules leading to stronger structures, that require less water-absorbing resulting in lower pasting viscosity.

Statistic result of variance for KDML105 rice showed that sonication times and ultrasound power levels had significant interaction ($p<0.05$) in pasting temperature, pasting viscosity, breakdown, final viscosity, and set back as shown in Table 4.3. Ultrasound treatment with longer sonication times and higher power levels gave a significant reduction in pasting temperature in a range between 75.28 and 70.12$^{o}$C and pasting viscosity in a range between 3740.67 and 3200.67 cP. The reduction of pasting temperature is associated to damaging starch molecules, resulting in starch granules are easier melting at low temperature (Ulbrich et al., 2020). The decreased pasting viscosity is related with breaking of amylopectin chains or reduction of molecular order leading to limited binding of water molecules to the free hydroxyl groups of amylopectin by hydrogen bonds (Jambrak et al., 2010). Kang et al. (2016) suggested that decreased viscosity was affected by the ultrasound destroyed starch chains, which occurs in amylopectin more easily than amylose. Some researchers also reported that reduced gelatinization temperature, and viscosity after ultrasound treatment (Zuo et al., 2009; Zhu et al., 2012). Reduced data related to our result of relative crystallinity (Table 4.8). Increased breakdown value was showed in rice treated ultrasound with increased sonication times and power levels. Ultrasound treatments induced the matrix of rice starch fragment, resulting in decreased resistant shear during heating (Park & Han, 2016). Since setback is related to re-association of linear amylose chains. The increase in setback value of increased sonication times and power levels of ultrasound treatments showed increased at initial

period and then tended to limiting change significant difference ($p \geq 0.05$) in a range from 865.00 cp to 946.67 cp. As compared to its native, the result found that decreased pasting temperature, pasting viscosity, setback, while increased breakdown and setback. These could be related to breakage of glycosidic linkage and weakening the network between starch chains (Kang et al., 2016). Huang et al. (2007) supported that decreased pasting temperature and viscosity after sonication.

Additionally, pasting properties were tested in ultrasound-chilling treatments (UC). Ultrasound – chilled rice samples showed tended to increased pasting temperature (75.40 - 78.73$^{o}$C) ,while decrease in pasting viscosity (2970.67 – 2615.33 cP), breakdown (564.67 – 698.00 cP), setback (552.30 – 634.33 cP), and final viscosity (4034.33 - 3351.67 cP). Increased pasting temperature and pasting viscosity were found in all UC treatments as compared to their ultrasound condition, indicating that chilling treatment after ultrasound may improve more impacts of double-helixes of starch structures leading to strong impact into starch molecules that require higher temperature to break up bounds to gelatinize. Since chilling improved stronger interactions between the starch chains leading to lower pasting viscosity in which much less water-absorbing (Klein et al., 2013; Pinto et al., 2015). Even though, more impact within starch molecules after UC treatment, their molecules are easily breaking resulting in increased breakdown value, which we suggest is effect of starch molecules breaking by ultrasound treatment. Increased final viscosity values were affected by chilling after ultrasound treatment. Chilling treatment displayed re-organization of starch chains led to the formation of longer double helices within starch granules resulting in stronger gel during cooling system (Vamadevan & Bertoft, 2018).

Statistic results of variance for CN1 cultivar showed that sonication times and ultrasound power levels had significant interaction ($p<0.05$) as affected on pasting viscosity, breakdown, final viscosity, and set back, excepted pasting temperature was not significantly interaction ($p \geq 0.05$) as shown in Table 4.4. Pasting temperature of ultrasound treat rice samples presented in a range between 81.10 and 80.13$^{o}$C. However, ultrasound treated rice for longer sonication times and at higher power levels demonstrated pasting viscosity tend to decrease from 2126.67 to 1919.00 cp. This might be suggested that amylopectin chains were destroyed with longer period and higher sonic energy input (Monroy et al., 2018). The increased breakdown values could be attributed to disrupted grains and starch granules less shear resistance. Huang et al. (2007) studied

the effect of sonication times (3-15 min, 500 W) on pasting properties of corn starch. His result showed that the decreased pasting viscosity and increased breakdown values when starch was treated with increased sonication time. Zheng et al. (2013) reported that more ultrasound energy input led to increase degradation of starch granules. The setback value of ultrasound treatments showed significantly decreased ($p$<0.05) from 1566.67 to 1299.00 cp. As comparison with native, ultrasound treatments were no significant different ($p$≥0.05) in pasting temperature, while pasting viscosity, breakdown, and final viscosity, setback values showed increased significant difference ($p$<0.05). The increased pasting viscosity and breakdown values after ultrasound treatments because of damage starch granules; weakening of the linkages between amylose-amylose, amylose-amylopectin and/or amylopectin-amylopectin contributed to facilitating water absorption, and enhanced viscosity and breakdown increase (Barrera et al., 2013; Monroy et al., 2018). Moreover, the starch pastes during cooling system presented setback values decreased indicating that amorphous regions destruction (Huang, Q. et al., 2007).

Chilling after ultrasound treatments (UC) of CN1 rice showed similar results of KDML105 rice. Pasting properties presented increase in pasting temperature (between 83.68 and 85.05$^{o}$C), breakdown (between 214.33 and 298.33 cP), and setback (between 1691.00 and 1894.33 cp ) but decrease in pasting viscosity (between 2004.67 and 1665.67 cP ) and final viscosity (2678.33 and 2471.33 cP) (Table 4.11) as compared to its ultrasound condition. This could be confirmed that stored ultrasound treated rice at 4$^{o}$C leading to change viscosity properties of rice samples by inducing starch chains rearrange to more compact and strong starch structures (Huang, Q. et al., 2007; Barrera et al., 2013; Monroy et al., 2018) as discussed in the XRD section.

Furthermore, in all parts of pasting properties for three rice cultivars (native) were different pasting profiles (Figure 4.3) and pasting properties (Table 4.5 – 4.7). During heating in water, starch granules swell, and amylose leaches out. This is generally exhibited that the increase in viscosity, which observed by Visco-Analyzer (J. l. Jane et al., 1999).The pasting viscosity decreases with high amylose content and is positively correlation to amount of amylopectin content. Moreover, higher amylose content increased pasting temperature and setback (Han & Hamaker, 2001; Srichuwong et al., 2005; Chung et al., 2011). In this result, the pasting properties of three rice cultivars showed different in pasting temperature, peak viscosity, breakdown, final viscosity, and setback. CN1 cultivar showed higher pasting temperature than KDML105 and RD6, respectively (CN1>KDML105>RD6). This due to its amylose content showed positive correlation

with pasting temperature analyzed either by DSC as shown in Table 4.12-4.13. In other words, amylopectin can take up water easier and faster than amylose, therefore pasting system with high amylopectin content have low pasting temperature. The highest peak viscosity was showed in RD6 and next was KDML105 and CN1 cultivars, respectively (RD6>KDML105>CN1), because high amylopectin provided high viscosity (Juhász & Salgó, 2008). Breakdown value is related to the thermal stability of swollen starch granules during heating and shearing, i.e. higher breakdown indicates that less resistance to shear force (J. Jane et al., 1999; Keeratiburana et al., 2020). CN1 cultivar provided lower breakdown value than KDML105 and RD6 (CN1>KDML105>RD6), respectively. Final viscosity and setback values are represented to re-association during cooling of the main amylose that released following. The highest final viscosity and setback were showed in CN1 rice cultivar (CN1>KDML105>RD6), might be due to their amylose lead out after heating. During cooling phase, amylose leased outside the starch granules can re-associated between amylose, resulting in high viscosity and setback.

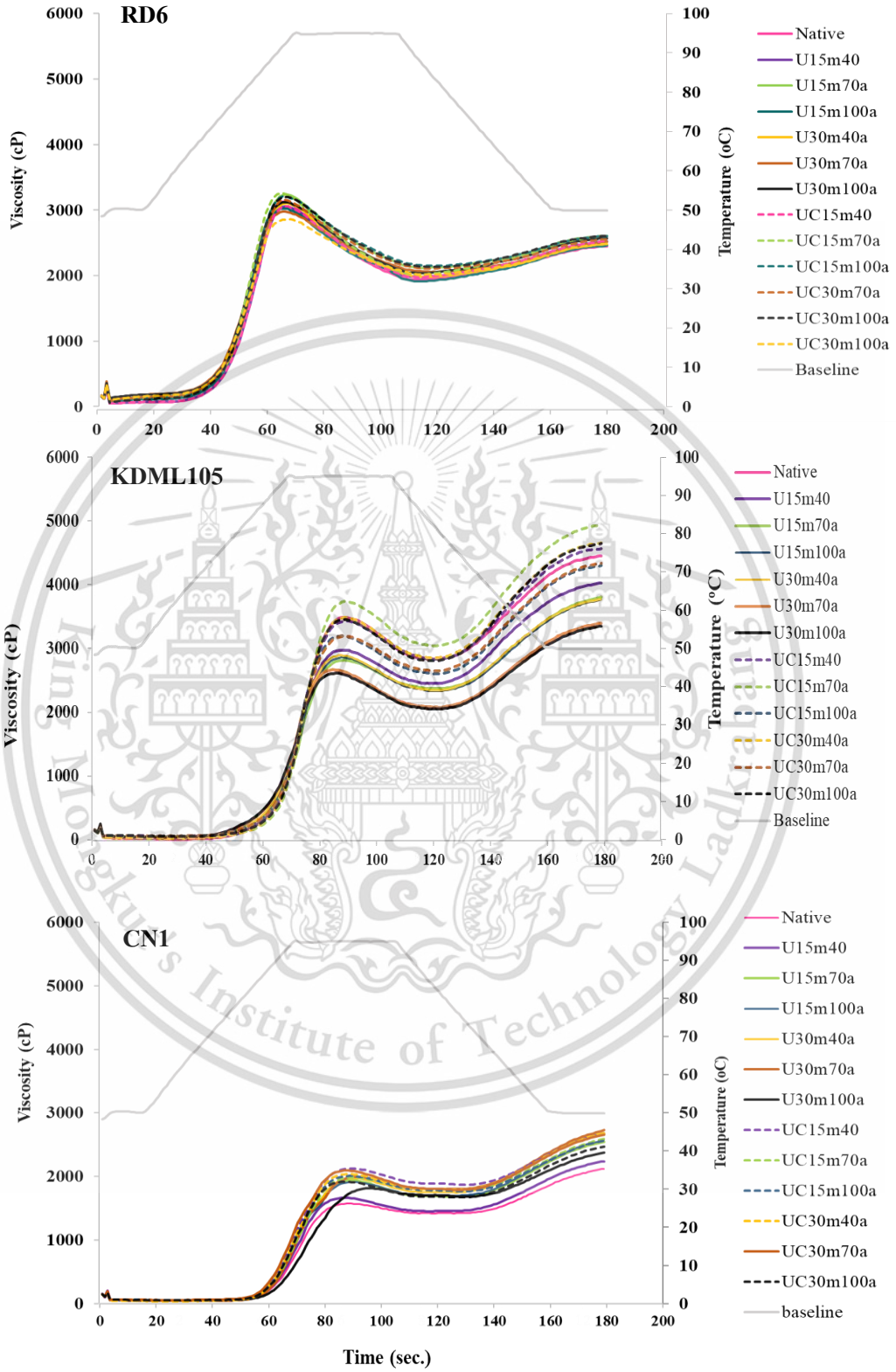


**Figure 4.3** Pasting profiles of native, ultrasound treatment, and ultrasound-chilling treatments for three rice cultivars.

**Table 4.9** Pasting properties of native, ultrasound treatment, and ultrasound-chilling treatments for RD6 cultivar.

| Pasting properties | Treatments | Native | Ultrasound conditions | | | | | |
|---|---|---|---|---|---|---|---|---|
| | | | 15m40a | 15m70a | 15m100a | 30m40a | 30m70a | 30m100a |
| PT ($^{o}$C) | U $^{ns}$ | 65.95±0.91 | 66.48±0.10 | 66.52±0.78 | 66.22±0.93 | 65.92±0.83 | 64.65±1.21 | 65.40±0.43 |
| | UC | 65.95±0.91$^{d}$ | 67.77±1.16$^{c}$ | 69.35±0.43$^{a}$ | 67.60±0.87$^{c}$ | 67.87±0.49$^{c}$ | 67.28±0.80$^{c}$ | 68.03±1.33$^{b}$ |
| PV (cP) | U | 3079.00±87.469$^{d}$ | 3894.33±9.27$^{a}$ | 3532.33±10.97$^{b}$ | 3493.00±59.56$^{c}$ | 3838.67±47.65$^{a}$ | 3419.00±20.95 | 3346.67±41.88$^{c}$ |
| | UC | 3079.00±87.469$^{c}$ | 3177.67±132.27$^{a}$ | 3244.00±44.58$^{a}$ | 3061.67±79.03$^{c}$ | 3156.00±50.69$^{b}$ | 3133.67±14.47$^{b}$ | 2922.67±59.81$^{d}$ |
| BD (cP) | U | 1186.33±42.193$^{d}$ | 1240.67±21.57$^{c}$ | 1307.67±56.50$^{b}$ | 1419.67±35.81$^{a}$ | 1226.00±50.47$^{c}$ | 1253.33±60.62$^{c}$ | 1387.00±26.00$^{b}$ |
| | UC | 1186.33±42.193$^{a}$ | 1069.67±88.75$^{a}$ | 1117.67±41.88$^{a}$ | 1188.33±65.77$^{a}$ | 1077.00±38.97$^{b}$ | 917.00±72.55$^{b}$ | 1048.00±39.28$^{b}$ |
| FV (cP) | U | 2407.33±57.29$^{f}$ | 2745.00±23.30$^{e}$ | 2891.67±3.79$^{b}$ | 2787.67±60.54$^{bc}$ | 2638.00±19.70$^{d}$ | 2562.00±44.19$^{e}$ | 2922.67±30.53$^{a}$ |
| | UC | 2407.33±57.29$^{b}$ | 2559.67±87.18$^{a}$ | 2612.33±7.51$^{a}$ | 2489.00±38.97$^{b}$ | 2544.00±63.59$^{a}$ | 2583.00±13.45$^{a}$ | 2481.00±37.99$^{b}$ |
| SB (cP) | U $^{ns}$ | 514.66±10.96$^{a}$ | 492.67±57.18$^{b}$ | 417.00±25.24$^{b}$ | 563.00±12.77$^{a}$ | 445.00±42.29$^{b}$ | 472.67±68.13$^{b}$ | 471.00±35.04$^{b}$ |
| | UC | 514.66±10.96 | 497.00±55.32 | 486.00±9.85 | 570.33±21.55 | 465.00±26.15 | 475.33±17.62 | 497.33±37.69 |

The data referred to the mean ± standard deviation (n=3). Values followed by different superscripts within the same row were significantly different at $p \leq 0.05$.

Native: rice without modification, U: ultrasound treatment, UC: ultrasound and chilling treatments. 15 and 30m: sonication times. 40, 70, and 100: percentage of ultrasound power.

PT: pasting temperature, PV: peak viscosity, BD: breakdown, and FV: final viscosity.

**Table 4.10** Pasting properties of native, ultrasound treatment, and ultrasound-chilling treatments for KDML105 cultivar.

| Pasting properties | Treatments | Native | Ultrasound conditions | | | | | |
|---|---|---|---|---|---|---|---|---|
| | | | 15m40a | 15m70a | 15m100a | 30m40a | 30m70a | 30m100a |
| PT ($^{o}$C) | U | 76.65±0.80$^{a}$ | 75.28±0.28$^{a}$ | 73.95±0.70$^{b}$ | 74.20±1.49$^{b}$ | 73.35±1.69$^{b}$ | 70.42±0.76$^{c}$ | 70.12±1.65$^{c}$ |
| | UC | 76.65±0.80$^{a}$ | 76.67±1.26$^{ab}$ | 76.97±1.96$^{ab}$ | 76.47±0.37$^{ab}$ | 76.36±0.39$^{ab}$ | 75.40±0.45$^{b}$ | 78.73±2.01$^{a}$ |
| PV (cP) | U | 4147.33±18.45$^{a}$ | 3434.00±11.27$^{d}$ | 3740.67±18.77$^{b}$ | 3200.67±29.14$^{e}$ | 3489.33±49.81$^{c}$ | 3217.33±36.12$^{e}$ | 3462.00±29.60$^{cd}$ |
| | UC | 4147.33±18.45$^{a}$ | 2817.67±29.57$^{d}$ | 2970.67±19.50$^{b}$ | 2860.67±27.93$^{c}$ | 2894.67±10.69$^{c}$ | 2668.33±16.04$^{e}$ | 2615.33±24.42$^{f}$ |
| BD (cP) | U | 912.00±37.32$^{a}$ | 449.67±45.28$^{c}$ | 521.67±33.23$^{b}$ | 529.67±33.38$^{b}$ | 550.67±46.46$^{b}$ | 590.67±35.80$^{b}$ | 562.7±33.01$^{b}$ |
| | UC | 912.00±37.32$^{a}$ | 602.67±3.06$^{cd}$ | 698.00±27.06$^{b}$ | 597.67±33.01$^{cd}$ | 641.67±45.94$^{bc}$ | 564.67±34.44$^{d}$ | 652.33±11.50$^{bc}$ |
| FV (cP) | U | 4867.00±25.53$^{a}$ | 3803.33±43.88$^{c}$ | 4034.33±34.43$^{b}$ | 3763.67±9.45$^{c}$ | 3773.00±19.50$^{c}$ | 3397.67±19.50$^{d}$ | 3351.67±4.92$^{d}$ |
| | UC | 4867.00±25.53$^{a}$ | 4564.67±12.10$^{d}$ | 4937.00±15.39$^{a}$ | 4302.00±26.88$^{e}$ | 4657.67±55.58$^{c}$ | 4343.67±18.01$^{e}$ | 4640.67±29.26$^{c}$ |
| SB (cP) | U | 723.00±21.66$^{c}$ | 790.67±28.01$^{bc}$ | 871.33±34.02$^{a}$ | 877.33±47.59$^{a}$ | 946.67±21.39$^{a}$ | 884.66±80.87$^{a}$ | 865.00±43.59$^{ab}$ |
| | UC | 723.00±21.66$^{c}$ | 551.67±20.23$^{d}$ | 599.00±19.08$^{bc}$ | 584.67±49.70$^{cd}$ | 634.33±10.21$^{b}$ | 561.33±14.98$^{cd}$ | 552.33±4.73$^{d}$ |

The data referred to the mean ± standard deviation (n=3). Values followed by different superscripts within the same row were significantly different at $p \leq 0.05$.

Native: rice without modification, U: ultrasound treatment, UC: ultrasound and chilling treatments. 15 and 30m: sonication times. 40, 70, and 100: percentage of ultrasound power.

PT: pasting temperature, PV: peak viscosity, BD: breakdown, and FV: final viscosity.

**Table 4.11** Pasting properties of native, ultrasound treatment, and ultrasound-chilling treatments for CN1 cultivar.

| Pasting properties | Treatments | Native | Ultrasound conditions | | | | | |
|---|---|---|---|---|---|---|---|---|
| | | | 15m40a | 15m70a | 15m100a | 30m40a | 30m70a | 30m100a |
| PT ($^{o}$C) | U$^{ns}$ | 82.33±0.49 | 81.10±1.23 | 80.28±1.85 | 80.13±1.62 | 80.83±0.87 | 80.32±1.88 | 80.57±1.42 |
| | UC | | 83.68±0.03$^{c}$ | 85.05±0.48$^{a}$ | 84.33±0.51$^{abc}$ | 84.82±0.46$^{ab}$ | 84.25±0.40$^{bc}$ | 84.55±0.09$^{ab}$ |
| PV (cP) | U | 1573.33±20.01$^{f}$ | 2126.67±4.62$^{a}$ | 1989.67±17.04$^{c}$ | 2006.67±21.08$^{c}$ | 2041.33±19.01$^{c}$ | 2089.00±15.72$^{bc}$ | 1919.00±14.00$^{d}$ |
| | UC | | 1665.67±18.88$^{e}$ | 1942.66±23.03$^{b}$ | 1912.66±10.60$^{c}$ | 1982.00±9.17$^{a}$ | 2004.67±4.04$^{a}$ | 1845.33±9.45$^{d}$ |
| BD (cP) | U | 161.33±11.37$^{d}$ | 216.67±13. 28$^{bc}$ | 266.00±17.09$^{a}$ | 217.00±18.36$^{bc}$ | 227.67±6.11$^{b}$ | 188.67±22.37$^{cd}$ | 238.00±33.40$^{ab}$ |
| | UC | | 258.67±6.03$^{b}$ | 214.33±13.05$^{c}$ | 241.33±10.07$^{b}$ | 248.33±6.66$^{b}$ | 298.33±13.05$^{a}$ | 249.33±9.24$^{b}$ |
| FV (cP) | U | 2119.67±37.63$^{e}$ | 2239.67±20.60$^{d}$ | 2548.00±15.59$^{bc}$ | 2573.00±37.03$^{b}$ | 2693.00±10.39$^{a}$ | 2700.67±57.07$^{a}$ | 2485.00±59.73$^{c}$ |
| | UC | | 2678.33±18.15$^{a}$ | 2588.67±26.35$^{b}$ | 2591.33±38.76$^{b}$ | 2675.67±10.02$^{a}$ | 2650.33±17.21$^{a}$ | 2471.33±10.97$^{c}$ |
| SB (cP) | U | 1631.67±15.37$^{a}$ | 1435.33±7.02$^{c}$ | 1566.67±11.59$^{b}$ | 1432.67±13.32$^{c}$ | 1429.00±5.00$^{c}$ | 1320.00±12.77$^{d}$ | 1299.00±7.00$^{e}$ |
| | UC | | 1733.33±23.69$^{c}$ | 1894.33±7.24$^{a}$ | 1699.00±14.93$^{c}$ | 1810.00±15.13$^{b}$ | 1691.00±3.61$^{d}$ | 1831.00±6.25$^{b}$ |

The data referred to the mean ± standard deviation (n=3). Values followed by different superscripts within the same row were significantly different at $p \leq 0.05$.

Native: rice without modification, U: ultrasound treatment, UC: ultrasound and chilling treatments. 15 and 30m: sonication times. 40, 70, and 100: percentage of ultrasound power.

PT: pasting temperature, PV: peak viscosity, BD: breakdown, and FV: final viscosity.

#### 4.1.2.4 The effects of ultrasound treatments and ultrasound-chilling treatments on thermal properties of rice grains

Thermal properties of three rice cultivars are shown in Table 4.12 for RD6, Table 4.13 for KDML105, and Table 4.14 for CN1 cultivars, respectively. Thermal properties were tested, including onset temperature (To), peak temperature (Tp), conclusion temperature (Tc), and enthalpy change ($\Delta$H). The results of rice grains treated with ultrasound and ultrasound-chilling treatments for each rice cultivars are as follow:

Following statistical variance of thermal properties for RD6 cultivar is shown in Table 4.3. The interaction between sonication times and ultrasound power levels was significantly different ($p$<0.05) in enthalpy change ($\Delta$H), but onset temperature (To), peak temperature (Tp) and conclusion temperature (Tc) were no significant interaction between that factors ($p$≥0.05). The endothermic transition of ultrasound treated rice samples as related to gelatinization which presented in a range from 58.10 to 74.67°C (Table 4.12). The onset temperature or the initial temperature of gelatinization of starch is melting temperature of amylopectin and/or to disruption of double helices formed by H-bonds within amylopectin side chains (Elgadir et al., 2009). Although, sonication times and ultrasound power levels were no interaction. The increase in sonication times showed significantly difference decrease in onset temperature ($p$<0.05). While increase in ultrasound power levels were not significant different ($p$≥0.05). onset temperature of ultrasound treated rice samples presented in a range between 60.42 and 58.10°C. The decreased $\Delta$H values (1.43 and 0.70 J/g) were found in ultrasound treatments with longer sonication times and higher ultrasound power levels. This might be due to starch granules fragmentation causing by increased energy input which create the cavitation forces. The sudden collapse of cavitation bubbles induces high pressure gradients and high local velocities of liquid layers which causes shearing force with capabilities of destroying the starch granules. This phenomenon results in the breaking or destroying the chains of amylopectin and/or amylose chains (Zheng et al., 2013). These indicated that ultrasound treatment causes a structural disturbance in the crystalline regions of the granules more than the amorphous regions. These data agree with the XRD finding, particularly with the reduction of its relative crystallinity. As compared to the native, To, Tp, Tc and $\Delta$H of all ultrasound treatments were lower than its native. Similar the finding of

Carmona-García et al. (2016) reported that ultrasound power decreased the gelatinization temperature and enthalpy of non-waxy rice starch. Jambrak et al. (2010) found that ultrasound treated led to decreased gelatinization temperature of corn starch.

Additionally, thermal properties were tested in ultrasound-chilling treatments (UC). Ultrasound – chilled rice samples showed tended to increase in To, Tc and $\Delta$H a range between 58.54 – 62.03$^{o}$C, 74.12 – 75.35 $^{o}$C, and 1.00 – 1.99 J/g, respectively. While unchanged Tp (68.51–68.88 $^{o}$C). Increased To, Tc, and $\Delta$H indicated that chilling treatment improved more impacts of double-helixes of starch structures leading to strong impact into starch molecules, which require higher temperature to gelatinize (Vamadevan & Bertoft, 2018) as discussed in the pasting section.

Statistical variances of thermal properties of KDML 105 cultivar are shown in Table 4.3. The interactions between sonication times and ultrasound power levels were significantly different ($p$<0.05) in the conclusion temperature (Tc), and enthalpy change ($\Delta$H). But the onset temperature (To), and peak temperature (Tp) were not significant interaction($p$≥0.05). According to Table 4.3, although To and Tp of ultrasound treated rice samples were no interaction between increasing sonication times and ultrasound power levels. There were slightly decreased ($p$≥0.05) in a range between 74.71 and 73.45$^{o}$C after ultrasound treatments (Table 4.13). These reflected reducing formation of perfect crystallites of starch granules, particularly ultrasound treatment for 30 min at higher power levels. Additionally, reduction of $\Delta$H was found in ultrasound treatment with increased treatment times and power levels, which it decreased a range between 0.91 and 0.74 J/g, because of grain destruction, and starch chains fragmentation, mainly amylopectin chains present in the branched crystalline regions (Pinto et al., 2015). As comparison of native and ultrasound treatments showed significantly decreased in To, Tp, Tc, and $\Delta$H ($p$<0.05). These results could be caused by the destruction within starch molecules (Cui et al., 2010).

Furthermore, chilling after ultrasound treatments (UC) exhibited increase in To, Tc and $\Delta$H a range between 59.12– 62.69$^{o}$C, 68.27 – 68.57 $^{o}$C, 73.37 – 75.10 $^{o}$C, and 1.10 – 1.40 J/g, respectively. While unchanged Tp (68.51–68.88 $^{o}$C). Increased To, Tc, and $\Delta$H attributed to chilling treatment improved strong packing starch molecules, which require higher temperature to gelatinize (Vamadevan & Bertoft, 2018).

Statistical variance of thermal properties of CN1 cultivar is shown in Table 4.4. The interactions between sonication times and ultrasound power levels were not significantly different ($p \geq 0.05$) in onset temperature (To), peak temperature (Tp), conclusion temperature (Tc), and enthalpy change ($\Delta$H). The ultrasound treatments exhibited gelatinization in a range temperature from 70.94 to 81.66°C. Gelatinization parameters, To (71.27 – 70.94°C), Tp (76.45 – 75.80°C ), Tc (81.66 – 80.55 °C), and $\Delta$H (1.14 – 1.05 J/g) were slightly changed after ultrasound treatments, especially ultrasound treatment for 30 min at 70% and 100% of ultrasound power (Table 4.14). Zhu (2015) reported that changing gelatinization temperature of starch as affected by ultrasound treatments could be attributed to the conditions of ultrasound employed (power, frequency, and time), and ratio of amylose/amylopectin. Sine, starch granule disintegration caused by cavitation force. This phenomenon results in mostly breaking the chains of amylopectin by disrupting covalent bonds, which causes the decrease in gelatinization temperature (Zheng et al., 2013). In this case, we suggested that CN1 rice has high amylose content, which might be resistant to ultrasound treatment. For the ultrasound – chilling treatment (UC), gelatinization temperature (To, Tp, and Tc) and enthalpy values were not changed as shown in Table 4.14. However, some gelatinization parameters (To, and Tc) were slightly increased when rice samples were chilled after ultrasound treatments for 30 min at 70% of ultrasound power.

In addition, the natives of three rice cultivars presented different in these properties due to their amylose content. The gelatinization temperatures of three rice cultivars were a range between 62.32 and 75.53°C for RD6, 61.62 and 77.70°C for KDML105, and 77.62 and 81.86 °C for CN1 cultivars. The gelatinization temperature increased with increase in amylose content. This related to previous finding in the pasting temperature (PT). The enthalpy change ($\Delta$H) was presented as corresponding to the amount of crystal order or double-helical structure in starch suspensions that disrupted at heating scan (Hongsheng Liu et al., 2006). Values of the enthalpy change of all native rice were 1.81 J/g for RD6, 1.34 J/g for KDML105, and 1.12 J/g for CN1. This suggested that this parameter is related to the process of amylopectin gelatinization: RD6 > KDML105 > CN1. Cooke and Gidley (1992) reported that the value of $\Delta$H mostly reflect the loss of double helical order.

**Table 4.12** Thermal properties of the native, ultrasound treatments, and ultrasound-chilling treatments of RD6 cultivar.

| Parameters | Treatments | Native | Ultrasound conditions | | | | | |
|---|---|---|---|---|---|---|---|---|
| | | | 15m40a | 15m70a | 15m100a | 30m40a | 30m70a | 30m100a |
| To ($^{o}$C) | U | 62.38±1.54$^{a}$ | 60.42±0.40$^{b}$ | 60.18±0.04$^{b}$ | 60.42±0.40$^{b}$ | 58.10±0.27$^{b}$ | 58.76±0.37$^{b}$ | 58.10±0.27$^{b}$ |
| | UC | 62.38±1.54$^{a}$ | 60.10±0.47$^{b}$ | 62.03±0.98$^{a}$ | 62.02±0.18$^{a}$ | 60.37±0.11$^{b}$ | 58.71±0.33$^{c}$ | 58.54±0.49$^{c}$ |
| Tp ($^{o}$C) | U $^{ns}$ | 69.03±0.19 | 68.06±0.25 | 68.73±0.48 | 68.21±0.00 | 68.06±0.25 | 68.73±0.48 | 68.56±0.12 |
| | UC | 69.03±0.19$^{a}$ | 68.88±0.01$^{b}$ | 68.82±0.01$^{b}$ | 68.60±0.18$^{b}$ | 68.51±0.08$^{b}$ | 68.55±0.00$^{b}$ | 68.55±0.00$^{b}$ |
| Tc ($^{o}$C) | U $^{ns}$ | 75.53±0.32 | 74.59±0.25 | 74.67±0.44 | 74.57±0.02 | 74.59±0.25 | 74.67±0.49 | 74.26±0.95 |
| | UC | 75.53±0.32$^{a}$ | 74.85±0.32$^{b}$ | 74.85±0.32$^{b}$ | 75.34±0.03$^{a}$ | 75.35±0.00$^{a}$ | 75.00±0.05$^{a}$ | 74.12±0.11 |
| $\Delta$H (J/g) | U | 1.81±0.19$^{a}$ | 1.43±0.08$^{b}$ | 1.04±0.04$^{c}$ | 0.96±0.01$^{d}$ | 0.86±0.04$^{d}$ | 0.74±0.01$^{e}$ | 0.70±0.30$^{e}$ |
| | UC | 1.81±0.19$^{b}$ | 1.16±0.47$^{c}$ | 1.84±0.02$^{b}$ | 1.99±0.01$^{a}$ | 1.93±0.01$^{a}$ | 1.80±0.12$^{b}$ | 1.00±0.01$^{d}$ |

Data values are mean ± standard deviation followed by different letters with the same row denote significant differences ($p$<0.05).

Native: rice without modification, U: ultrasound treatment, UC: ultrasound and chilling treatments. 15 and 30m: sonication times. 40, 70, and 100: percentage of ultrasound power.

To: onset temperature, Tp: peak temperature, Tc: conclusion temperature, Tc-To: transition temperature range, and $\Delta$H: enthalpy change.

**Table 4.13** Thermal properties of the native, ultrasound treatments, and ultrasound-chilling treatments of KDML105 cultivar.

| Parameters | Treatments | Native | Ultrasound conditions | | | | | |
|---|---|---|---|---|---|---|---|---|
| | | | 15m40a | 15m70a | 15m100a | 30m40a | 30m70a | 30m100a |
| To ($^{o}$C) | U | 61.62 ±0.27$^{a}$ | 58.28 ±0.57$^{b}$ | 58.85 ±0.14$^{b}$ | 58.30 ±0.95$^{b}$ | 58.27 ±1.12$^{b}$ | 59.35 ±0.42$^{b}$ | 59.52 ±0.52$^{b}$ |
| | UC | 61.62±0.27$^{b}$ | 61.46±0.21$^{b}$ | 62.69±0.45$^{a}$ | 62.02±0.18$^{ab}$ | 62.69±0.45$^{a}$ | 59.35±0.07$^{c}$ | 59.12±0.36$^{c}$ |
| Tp ($^{o}$C) | U | 68.84±0.18$^{a}$ | 68.55±0.00$^{a}$ | 68.34±0.18$^{ab}$ | 67.88±0.24$^{bc}$ | 67.89±0.24$^{bc}$ | 67.78±0.06$^{bc}$ | 67.51±0.42$^{c}$ |
| | UC | 68.84±0.18$^{a}$ | 68.27±0.18$^{b}$ | 68.57±0.01$^{a}$ | 68.57±0.00$^{a}$ | 68.27±0.18$^{b}$ | 68.14±0.01$^{b}$ | 68.55±0.00$^{a}$ |
| Tc ($^{o}$C) | U | 77.70±0.30$^{a}$ | 74.34±0.11$^{bc}$ | 74.71±0.52$^{bc}$ | 74.12±0.11$^{bc}$ | 74.16±0.24$^{bc}$ | 74.18±0.16$^{bc}$ | 73.45±0.76$^{c}$ |
| | UC | 77.70±0.30$^{a}$ | 73.37±0.01$^{c}$ | 75.10±0.07$^{b}$ | 74.94±0.28$^{b}$ | 73.37±0.01$^{c}$ | 74.39±0.12$^{c}$ | 74.12±0.11$^{c}$ |
| $\Delta$H (J/g) | U | 1.34±0.22$^{a}$ | 0.91±0.11b | 0.79±0.02$^{b}$ | 0.88±0.01$^{b}$ | 0.83±0.0$^{b}$ | 0.79±0.02$^{b}$ | 0.74±0.01$^{b}$ |
| | UC | 1.34±0.22$^{ab}$ | 1.24±0.04ab | 1.40±0.07$^{a}$ | 1.23±0.06$^{ab}$ | 1.29±0.02$^{ab}$ | 1.19±0.11$^{ab}$ | 1.10±0.13$^{b}$ |

Data values are mean ± standard deviation followed by different letters with the same row denote significant differences ($p$<0.05).

Native: rice without modification, U: ultrasound treatment, UC: ultrasound and chilling treatments. 15 and 30m: sonication times. 40, 70, and 100: percentage of ultrasound power.

To: onset temperature, Tp: peak temperature, Tc: conclusion temperature, Tc-To: transition temperature range, and $\Delta$H: enthalpy change.

**Table 4.14** Thermal properties of the native, ultrasound treatments, and ultrasound-chilling treatments of CN1 cultivar.

| Parameters | Treatments | Native | Ultrasound conditions | | | | | |
|---|---|---|---|---|---|---|---|---|
| | | | 15m40a | 15m70a | 15m100a | 30m40a | 30m70a | 30m100a |
| To ($^{o}$C) | U | 71.62±0.27$^{a}$ | 71.27±0.00$^{a}$ | 71.07±0.09$^{ab}$ | 70.87±0.25$^{b}$ | 70.96±0.66$^{b}$ | 70.82±0.08$^{b}$ | 70.94±0.13$^{b}$ |
| | UC | 71.62±0.27$^{ab}$ | 70.16±0.23$^{d}$ | 70.43±0.10$^{d}$ | 70.44±0.21$^{d}$ | 72.05±0.03$^{a}$ | 71.12±0.10$^{c}$ | 71.33±0.19$^{bc}$ |
| Tp ($^{o}$C) | U | 76.59±0.12$^{a}$ | 76.45±0.18$^{ab}$ | 76.17±0.18$^{abc}$ | 76.05±0.24$^{abc}$ | 75.87±0.11$^{bc}$ | 75.97±0.00$^{bc}$ | 75.80±0.59$^{c}$ |
| | UC | 76.59±0.12 | 76.10±0.19 | 76.00±0.06 | 76.30±0.71 | 76.38±0.00 | 75.67±0.76 | 76.22±0.47 |
| Tc ($^{o}$C) | U | 81.86±0.23$^{a}$ | 81.27±0.57$^{abc}$ | 81.66±0.01$^{ab}$ | 81.66±0.02$^{ab}$ | 80.58±0.85$^{c}$ | 80.96±0.36$^{bc}$ | 80.92±0.32$^{bc}$ |
| | UC | 81.86±0.23$^{a}$ | 81.53±0.16$^{ab}$ | 81.36±0.37$^{b}$ | 80.43±0.06$^{c}$ | 80.38±0.15$^{c}$ | 80.47±0.23$^{c}$ | 81.04±0.06$^{b}$ |
| $\Delta$H (J/g) | U | 1.12±0.01$^{ab}$ | 1.14±0.01$^{a}$ | 1.22±0.07$^{ab}$ | 1.22±0.06$^{ab}$ | 1.13±0.02$^{a}$ | 1.14±0.04$^{ab}$ | 1.05±0.02$^{b}$ |
| | UC | 1.12±0.01$^{b}$ | 1.29±0.01$^{a}$ | 1.31±0.04$^{a}$ | 1.20±0.05$^{ab}$ | 1.17±0.01$^{b}$ | 1.15±0.08$^{b}$ | 1.07±0.06$^{b}$ |

Data values are mean ± standard deviation followed by different letters with the same row denote significant differences ($p$<0.05).

Native: rice without modification, U: ultrasound treatment, UC: ultrasound and chilling treatments. 15 and 30m: sonication times. 40, 70, and 100: percentage of ultrasound power.

To: onset temperature, Tp: peak temperature, Tc: conclusion temperature, Tc-To: transition temperature range, and $\Delta$H: enthalpy change.

#### 4.1.2.5 The effects of ultrasound treatments and ultrasound-chilling treatments on *in vitro* glycemic index

The interaction between sonication times and ultrasound power levels for the digestion rate constant (k-value), hydrolysis index (HI), and expected glycemic index (eGI) of the native, ultrasound treated rice, and ultrasound-chilling samples for RD6, KDML105, and CN1 cultivars are shown in Table 4.3, Table 4.3, and Table 4.5, respectively. Starch hydrolysis percentage curves ($C_\infty$) of three rice cultivars are shown in Figure 4.4. The results for three rice cultivars were treated ultrasound and ultrasound-chilling are showed as follows:

Variance analysis of *in vitro* digestibility of ultrasound treatments (sonication times and power levels) for RD6 rice was showed in Table 4.3. The sonication times and ultrasound power levels were significant interaction ($p<0.05$) as presented in digestion rate constant (k-value), hydrolysis index (HI), and expected glycemic index (eGI). The increased sonication times and ultrasound power levels showed significantly increased k-value ($p<0.05$) in range between 15.77 to 20.60 $(min^{-1}) \times 10^{-3}$. Rice samples were longer treated in ultrasound bath leading to more receptive to attract by ultrasound action, which exhibited cracking of grain-shell, and destroying of starch granules (Wang et al., 2020). Also, the increased power levels exhibited increased energy density causing disruption of starch granules by cavitation making them more susceptible to enzymatic activity (Wang et al., 2020). Moreover, ultrasound treatments contributed to increase in HI from 73.09 to 77. 38, and eGI from 80.64 to 83.64, especially ultrasound treated rice for 30 min with 100% of ultrasound power displayed the highest eGI value (83.64). This indicated that the fragmentation of starch granules especially the crystalline regions to be weaker resulting in higher access of α-amylase and amyloglucosidase starch hydrolysis leading to increased hydrolysis index and glycemic index (Liu et al., 2005; Ding et al., 2016). Furthermore, the ultrasound treated RD6 rice samples showed higher *in vitro* digestibility parameters for all ultrasound treatments as compared to its native (81.08). Flores-Silva et al. (2018) also reported that ultrasound treatment could promote increase in enzyme susceptibility. Furthermore, these data were supported with our finding in decreased pasting temperature, crystallinity, and enthalpy.

For ultrasound-chilled RD6 rice samples presented lower HI and eGI as compared to their ultrasound treatments. These results were supported by increasing relative

crystallinity and $\Delta H$. Since ultrasound treatment damaged crystalline regions, its molecule rearranged to compact structure after being treated by chilling, which led to the stronger structure Flores-Silva et al. (2017); reported that the higher crystallinity an enthalpy value indicated that more packed re-arrangement of the double-helices structures, resulting in less enzymatic susceptible attack on starch granules. Therefore, chilling after ultrasound treatment could reduce glycemic index of rice grains. The lowest eGI of RD6 rice was ultrasound treated rice for 15 min with 100% of ultrasound power following chilling treatment, which was 75.34.

The results of KDML105 cultivar presented significant interaction ($p$<0.05) between sonication times and ultrasound power levels in k-value, HI and eGI (shown in Table 4.4). Rice grains were treated by combinations of sonication time and ultrasound power levels showed that the increase in both factors led to significant increase in k-values ($p$<0.05) in range between 12.15 and 17.20 ($min^{-1}$) x $10^{-3}$ especially, ultrasound treated rice at 100% of ultrasound power for both times has high k-value. The increased HI and eGI were found in ultrasound treatments with increased sonication times and ultrasound power levels which increased in range between 51.88 and 63.69, 68.19 and 76.72 for HI, and eGI, respectively. Moreover, the ultrasound treatments exhibited higher k-value, HI, and eGI than the native, excepted ultrasound treatment for 15 min at 40% of ultrasound power (15m40a). These results are therefore decreased enzyme resistance, since the crystalline regions are destroyed by ultrasound treatment leading to easy hydrolysis in starch granules by the enzymes. These results were related to decreased To, relative crystallinity, and $\Delta H$.

Besides, KDML105 rice samples showed significantly decreased range between 13.95 and 11.70 ($min^{-1}$)×$10^{-3}$ for k-value, 50.16 and 49.89 for HI, and 67.25 and 64. 08 for eGI after chilling after ultrasound treatments as compared to its ultrasound condition. Moreover, those parameters were lower than its native (k-value (13.85 $min^{-1}$×$10^{-3}$), HI (52.47), and eGI (68.52)) (Table 4.16). These results could be due to ultrasound treatment reduced the amounts of order structures, then re-arranged the molecular chains to form ordered structures that increased resistance of starch granules to enzymatic hydrolysis (Ding et al., 2019). This increased in vitro digestibility related to increased relative crystallinity, enthalpy. The lowest eGI was showed in chilling after ultrasound treatments for 15 and 30 min at 70% of ultrasound power (64.08 and 63.76,

respectively), but those treatments were not significantly difference ($p \geq 0.05$). Wang et al. (2015) reported that starch re-arrangement and association of starch chains depend on size chains of amylose or amylopectin, with the optimum size range being DP between about 14 and 24, time, or conditions.

The variance analyses of *in vitro* digestibility for CN rice are shown in Table 4.5. The results showed that parameters, k-value, HI, and eGI, significant interaction between sonication times and ultrasound power levels ($p<0.05$). Ultrasound treated rice with longer time and higher ultrasound power levels exhibited increased k-value range between 10.55 and 14.75 $(min^{-1})\times10^{-3}$, 37.46 and 40.39 for HI and 59.53 and 61.88 for eGI, especially sonication time for 30 min with increasing ultrasound power levels from 70% to 100%. This indicated that more available starches for hydrolysis (Ding et al., 2016). However, HI and eGI of ultrasound treated rice samples were slightly decreased as compared to its native (45.08 and 64.46 respectively). These results were attributed to increase in ordered structures leading to the increase in relative crystallinity (Figure 4.8), and enthalpy value (Table 4.14). Hoover and Vasanthan (1994) reported that crystalline region is resistant to the enzyme because of its tight packing arrangement.

In addition, the *in vitro* digestibility parameters of three rice cultivars were difference in k-value, HI, and eGI. These showed that k-value of native samples for RD6, KDML105 and CN1 cultivar was 16.38, 13.85, and 10.70 $(min^{-1})\times10^{-3}$, respectively. Hydrolysis index was 75.58, 52.47, and 45.08. respectively and eGI was 81.08, 68.52, 64.46, respectively. These results showed that different rice cultivars gave various values of those parameter because of different amylose content. However, CN1 rice presented the lowest of all *in vitro* parameters. In general, high amylose rice is reported to be more resistant than amylopectin to starch hydrolysis because of its impact liner structure (Dhital et al., 2015). Rice with high amylose content is reported less breakdown by $\alpha$-amylase than rice with high amylopectin because amylose is harder to breakdown (U Lehmann & F Robin, 2007; Zhu et al., 2011).

Figure. 4.4 shows the starch hydrolysis curves for rice samples. The hydrolysis of ultrasound treated rice samples for three rice cultivars exhibited higher starch hydrolysis as compared to their native, demonstrating that the higher enzyme susceptibility to hydrolyze starch molecule. This result could be attributed to destroyed structure of starch molecules. Furthermore,

chilling after ultrasound treatment promoted treatments showed the reduction of hydrolysis percentage. These results could be attributed to increased crystallinity, resulting in stronger structure within starch granule. This was supported by increased pasting temperature, crystallinity, enthalpy value as discussed above. Moreover, the difference curves exhibited significantly different kinetic of starch hydrolysis between cultivars.RD6 rice showed a sharp increase in starch hydrolysis after 30 min as compared to KDML105 and CN1 rice. However, CN1 rice showed lowest starch hydrolysis. These results might be because their amylose content. Amylose content had an obvious impact on starch degradation and thus on the predicted glycemic index. This was related to their glycemic index.

Considering rice samples to further study were selected from the lowest glycemic index of each rice cultivars. This study found that chilling after ultrasound treated rice could reduce the glycemic index of three rice cultivars. Thus, conditions of ultrasound treatment for three rice cultivars were chosen as follows: 15 min at 100% of ultrasound power for RD6, and 15 min at 70% of ultrasound power for KDML105, and CN1 cultivars followed chilling treatment.

**Table 4.15** The hydrolysis index, rate of digestion and expected glycemic index of RD6 cultivar.

| Parameters | Treatments | Native | Ultrasound conditions | | | | | |
|---|---|---|---|---|---|---|---|---|
| | | | 15m40a | 15m70a | 15m100a | 30m40a | 30m70a | 30m100a |
| k ($min^{-1}$) × $10^{-3}$ | U | 16.38±0.19$^{e}$ | 15.77±0.06$^{e}$ | 17.29±0.18$^{d}$ | 18.04±0.06$^{c}$ | 18.28±0.17$^{c}$ | 19.56±0.15$^{b}$ | 20.60±0.01$^{a}$ |
| | UC | 16.38±0.19$^{c}$ | 16.25±0.78$^{c}$ | 16.45±0.64$^{c}$ | 15.30±0.28$^{d}$ | 15.65±1.06$^{d}$ | 18.45±0.50$^{b}$ | 19.00±0.14$^{a}$ |
| HI | U | 75.58±0.38$^{ab}$ | 73.09±1.33$^{bc}$ | 73.56±1.72$^{bc}$ | 77.38±1.46$^{a}$ | 74.26±0.58$^{cd}$ | 75.58±0.38$^{ab}$ | 76.10±0.15$^{ab}$ |
| | UC | 75.58±0.38$^{ab}$ | 69.33±0.24$^{de}$ | 70.76±0.56$^{cd}$ | 64.89±0.81$^{f}$ | 67.83±0.75$^{ef}$ | 65.42±1.92$^{f}$ | 65.27±0.41$^{f}$ |
| eGI | U | 81.08±0.14$^{bc}$ | 80.64±0.76$^{bc}$ | 79.84±0.73$^{cd}$ | 82.19±0.80$^{ab}$ | 82.20±0.80$^{ab}$ | 81.92±0.80$^{ab}$ | 83.64±1.80$^{a}$ |
| | UC | 81.08±0.14$^{a}$ | 77.77±0.1$^{c}$ | 78.56±0.31$^{b}$ | 75.34±0.44$^{e}$ | 76.94±0.41$^{de}$ | 75.62±1.05$^{e}$ | 75.54±0.23$^{e}$ |

Data values are mean ± standard deviation followed by different letters with the same row denote significant differences ($p$<0.05).

k: Rate of digestion (digestion rate constant)HI: Expected glycemic index.

Native: rice without modification, U: ultrasound treatment, UC: ultrasound and chilling treatments. 15 and 30m: sonication times. 40, 70, and 100: percentage of ultrasound power.

**Table 4.16** The hydrolysis index, rate of digestion and expected glycemic index of KDML105 cultivar.

| Parameters | Treatments | Native | Ultrasound conditions | | | | | |
|---|---|---|---|---|---|---|---|---|
| | | | 15m40a | 15m70a | 15m100a | 30m40a | 30m70a | 30m100a |
| k ($min^{-1}$) × $10^{-3}$ | U | 13.85±0.00$^{d}$ | 12.15±0.00$^{e}$ | 13.25±0.00$^{d}$ | 15.20±0.00$^{c}$ | 12.30±0.00$^{e}$ | 16.95±0.00$^{b}$ | 17.20±0.00$^{a}$ |
| | UC | 13.85±0.00$^{a}$ | 12.35±0.00$^{b}$ | 13.10±0.00$^{a}$ | 12.45±0.00$^{b}$ | 11.70±0.00$^{c}$ | 13.00±0.00$^{a}$ | 13.95±0.00$^{a}$ |
| HI | U | 52.47±0.14$^{b}$ | 51.88±0.13$^{b}$ | 53.77±1.48$^{b}$ | 63.41±1.68$^{a}$ | 50.99±0.72$^{b}$ | 64.12±1.09$^{a}$ | 63.69±0.91$^{a}$ |
| | UC | 52.47±0.14$^{a}$ | 49.89±0.34$^{bc}$ | 47.63±0.61$^{cd}$ | 47.06±1.79$^{d}$ | 44.39±1.84$^{e}$ | 43.80±0.52$^{e}$ | 50.16±0.20$^{ab}$ |
| eGI | U | 68.52±0.08$^{b}$ | 68.19±0.07$^{b}$ | 69.29±1.19$^{b}$ | 76.72±2.57$^{a}$ | 67.70±0.40$^{b}$ | 74.91±0.60$^{a}$ | 74.68±0.50$^{a}$ |
| | UC | 68.52±0.08$^{a}$ | 67.10±0.19$^{bc}$ | 64.08±1.01$^{cd}$ | 65.55±0.98$^{e}$ | 65.86±0.33$^{e}$ | 63.76±0.28$^{cd}$ | 67.25±0.11$^{a}$ |

Data values are mean ± standard deviation followed by different letters with the same row denote significant differences ($p$<0.05).

k: Rate of digestion (digestion rate constant)HI: Expected glycemic index.

Native: rice without modification, U: ultrasound treatment, UC: ultrasound and chilling treatments. 15 and 30m: sonication times. 40, 70, and 100: percentage of ultrasound power.

**Table 4.17** The hydrolysis index, rate of digestion and expected glycemic index of CN1 cultivar.

| Parameters | Treatments | Native | Ultrasound conditions | | | | | |
|---|---|---|---|---|---|---|---|---|
| | | | 15m40a | 15m70a | 15m100a | 30m40a | 30m70a | 30m100a |
| K ($min^{-1}$) × $10^{-3}$ | U | 10.70±0.00$^{d}$ | 10.55 ±0.00$^{d}$ | 11.55±0.00$^{c}$ | 10.45±0.00$^{d}$ | 11.95±0.00$^{c}$ | 12.70±0.00$^{b}$ | 14.75±0.00$^{a}$ |
| | UC | 10.70±0.00$^{c}$ | 10. 95±0.00$^{c}$ | 9.75±0.00$^{d}$ | 10.20±0.00$^{c}$ | 9.20±0.00$^{d}$ | 12.25±0.00$^{b}$ | 14.45±0.00$^{a}$ |
| HI | U | 45.08±0.34$^{a}$ | 37.46±0.14$^{d}$ | 36.46±0.29$^{e}$ | 38.73±0.73$^{c}$ | 34.45±0.82$^{f}$ | 36.08±0.07$^{e}$ | 40.39±0.85$^{b}$ |
| | UC | 45.08±0.34$^{a}$ | 38.93±0.15$^{c}$ | 31.76±0.92$^{f}$ | 36.36±33.24$^{d}$ | 34.64±5.77$^{e}$ | 36.86±0.14$^{d}$ | 40.39±0.80$^{b}$ |
| eGI | U | 64.46±0.19$^{a}$ | 60.28±0.07$^{c}$ | 59.73±0.16$^{d}$ | 59.67±0.18$^{d}$ | 59.95±0.07$^{c}$ | 59.53±0.04$^{d}$ | 61.88±0.47$^{b}$ |
| | UC | 64.46±0.19$^{a}$ | 61.08±0.08$^{b}$ | 57.15±0.51$^{d}$ | 60.73±0.34$^{c}$ | 58.62±0.45$^{d}$ | 57.47±0.14$^{b}$ | 60.97±0.40$^{c}$ |

Data values are mean ± standard deviation followed by different letters with the same row denote significant differences ($p$<0.05).

k: Rate of digestion (digestion rate constant)HI: Expected glycemic index.

Native: rice without modification, U: ultrasound treatment, UC: ultrasound and chilling treatments. 15 and 30m: sonication times. 40, 70, and 100: percentage of ultrasound power.

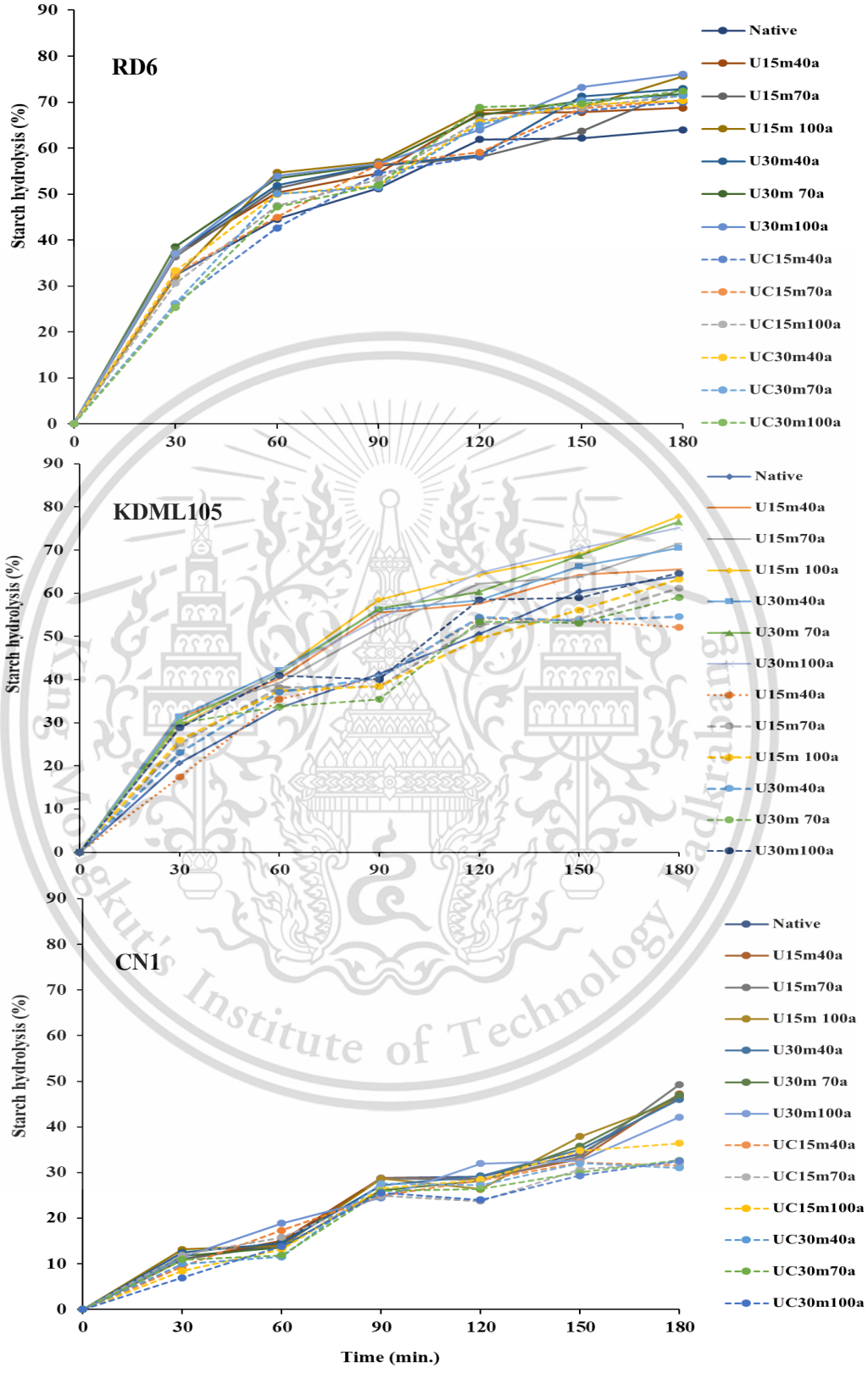


**Figure 4.4** The percentage of starch hydrolysis of natives, ultrasound treatment (U), and ultrasound-chilling treatment (UC) for three rice cultivars

## 4.2 The effects of combined ultrasound-chilled followed by annealing treatments on physicochemical properties and *in vitro* glycemic index of rice grains

The present study was determined annealing treatment after combined ultrasound plus chilling treatment to reduce the glycemic index of rice grains. From a previous study, the ultrasound treatments (15min at 100% for RD6, 15min at 70% for KDML105 and CN1 rice) plus chilling treated rice samples with the lowest glycemic index of each rice cultivars were selected to further modify by annealing treatments at 45°C (UC+ANN45), 50°C (UC+ANN50), or 55°C (UC+ANN55) for 16 h. After that, rice samples were analyzed physicochemical properties, including, x-ray diffraction, pasting properties, thermal properties, and *in vitro* glycemic index. The results are presented as follows:

### 4.2.1 The effect of annealing treatment after ultrasound-chilling treatments on X-ray diffraction pattern and crystallinity for rice grains

The X-ray diffraction pattens of native, ultrasound-chilling (UC), and ultrasound-chilled followed by annealing treatments (UC+ANN) for RD6, KDML105 and CN1 rice cultivars are shown in Figure 4.5. All rice cultivars were similarly exhibited XRD patterns with strong diffractions single peak at 15° and 23, followed by double peak at 17° and 18° (2θ), which displayed a typical A-type crystalline structure, and a small peak at 20° (2θ) represented a bound between amylose-lipid complex which presented $V_h$-type (Guo et al., 2015). Moreover, the XRD pattern of three rice cultivars was not change when rice samples were treated UC+ANN. The increased annealing temperatures were also not changed the crystalline type of rice samples (Xu, Saleh, Gong, et al., 2018). These results were in good agreement with previous studies on yam (Adebowale et al., 2009), potato (Shin et al., 2005), and maize starch (Tester et al., 2000); XRD pattern was still similar to its native after annealing. However, the grains crystallinity of three rice cultivars was changed after annealing treatments as presented in Table 4.18.

The relative crystallinity of RD6 rice is presented in Table 4.18. The relative crystallinity of native was 31.99%. Ultrasound-chilling rice (UC) attributed to relative crystallinity slight up to 32.59% as compared to native. This confirmed that the effect of chilling at 4°C after

ultrasound treatment led to re-association of starch chains by packing of double helices within crystalline region (Flores-Silva et al., 2018). Additionally, annealing treated RD6 rice after ultrasound (UC+ANN) was not change in relative crystallinity.

For KDML105 rice, the relative crystallinity of native was 23.08% after that it increased to 26.30%, when UC treated rice grains due to re-association of starch chains within crystalline region by chilling treatment (Flores-Silva et al., 2018). The relative crystallinity of UC+ANN treatment was increased up to 29.30%, 29.46%, and 29.53% by increased temperatures of annealing treatment at 45, 50, and 55$^{o}$C, respectively, but they were no significant difference ($p$>0.05). The increased relative crystallinity of UC+ANN could be effects of rearrangement of starch chains within amorphous and crystalline region of starch granules, which promoted more crystalline structures (Zavareze & Dias, 2011; Pinto et al., 2015). This data was supported by Zhong et al. (2020) reported that the relative crystallinity was increased by microwave treatment subjected ANN of rice starch and rice flour.

The relative crystallinity of CN1 rice cultivar is also presented in Table 4.18. The relative crystallinity was slightly changed after UC treatment to 27.82% as compared to its native (26.07%). CN1 rice was treated with ANN after UC treatments showed increased crystallinity. Despite the relative crystallinity increased in UC+ANN treatments, but the relative crystallinity unchanged when rice grains treated annealing with higher temperature, which presented in a range of 29.63 to 29.98% might be due to the relative crystallinity is hardly to change in starch depending on various factors; temperature, type of starch, and size chains of amylose and amylopectin (Bian & Chung, 2016; Zhong et al., 2020). Zavareze and Dias (2011) denoted that the increased crystallinity followed the order: normal>waxy>high amylose.

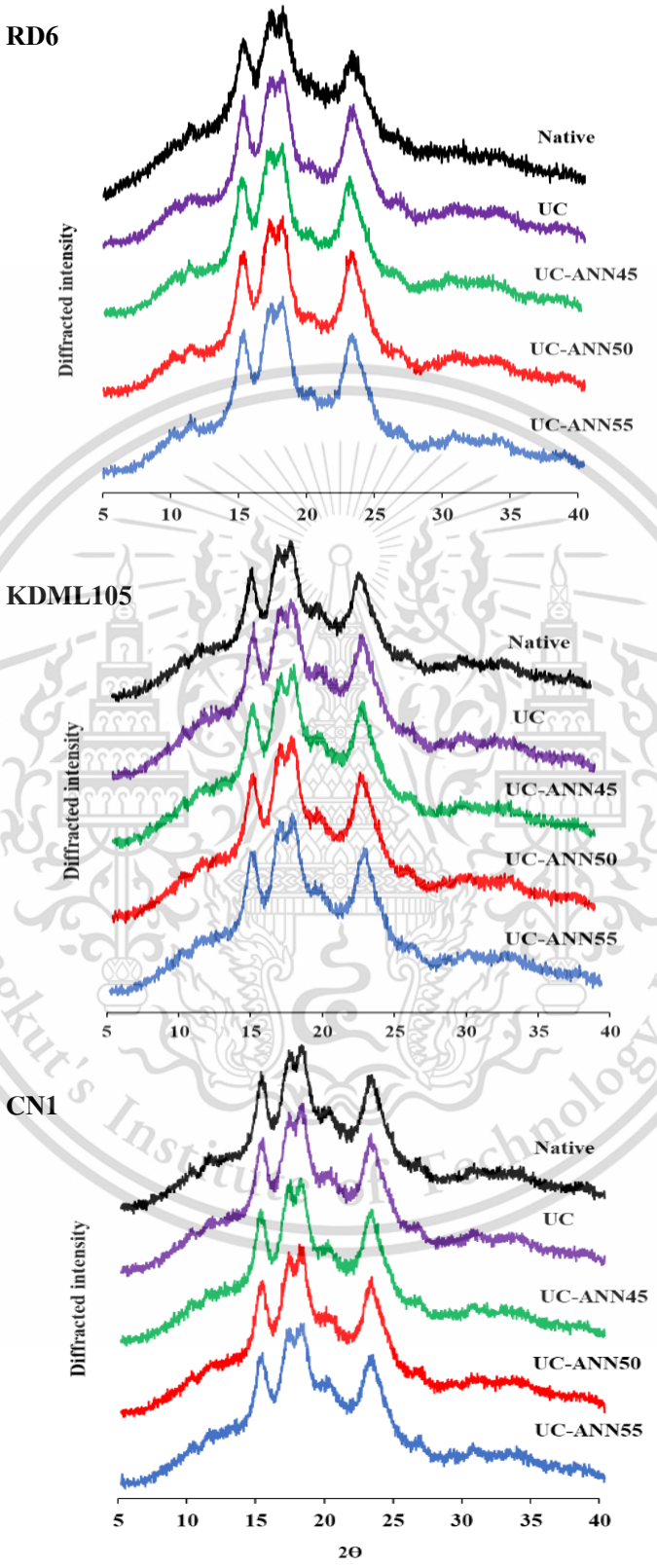


**Figure 4.5** X-ray diffraction patterns and crystallinity of natives, ultrasound-chilling treatments (UC), and ultrasound-chilled rice followed annealing treatments (UC+ANN) for three rice cultivars

**Table 4.18** The percentage of crystallinity and type of crystalline structure of native, ultrasound-chilling treatment (UC), and ultrasound-chilled rice followed annealing treatments (UC+ANN) for three rice cultivars.

| Rice cultivars | Samples | Crystallinity (%) | Diffraction pattern |
|---|---|---|---|
| RD6 | Native | 31.99 | A+V type |
| | UC | 32.55 | A+V type |
| | UC+ANN45 | 31.98 | A+V type |
| | UC+ANN50 | 32.11 | A+V type |
| | UC+ANN55 | 31.87 | A+V type |
| KDML105 | Native | 23.08 | A+V type |
| | UC | 26.30 | A+V type |
| | UC+ANN45 | 29.30 | A+V type |
| | UC+ANN50 | 29.46 | A+V type |
| | UC+ANN55 | 29.53 | A+V type |
| CN1 | Native | 26.07 | A+V type |
| | UC | 27.82 | A+V type |
| | UC+ANN45 | 29.98 | A+V type |
| | UC+ANN50 | 29.71 | A+V type |
| | UC+ANN55 | 29.63 | A+V type |

UC: ultrasound plus chilling treatment. UC+ANN: combined ultrasound-chilling and annealing treatments. 45, 50 and 55: incubation temperatures of annealing treatment ($^{o}$C).

### 4.2.2 The effect of annealing treatment after ultrasound-chilling treatments on pasting properties for rice grains

The pasting profile and pasting properties of three rice cultivars were tested after rice was treated by ultrasound-chilling followed by annealing treatments at 40, 50, or 55°C. Also, their native and UC treatment were tested that properties. Pasting profiles of three rice cultivars are presented in Figure 4.6. The pasting properties are shown in Table 4.19 for RD6, Table 4.20 for KDML105, and Table 4.21 for CN1 cultivars, respectively. The results of three rice cultivars are described as follows:

The pasting profiles and pasting properties of the native, UC, and UC+ANN of RD6 rice are presented in Figure 4.6 and Table 4.19, respectively. The pasting properties of UC and UC+ANN presented significantly higher ($p$<0.05) in all pasting profiles testing, pasting temperature, pasting viscosity, breakdown, final viscosity, and setback than its native. The increased pasting values of UC treatment due to rice grains was stored at 4°C since it has been shown in a previous study. Starch chains can associate by amylose-amylose, amylose-amylopectin, or amylose-lipid. These effects lead to strong interaction within starch granules. Ultrasound is also affected on surface cracking of grains and/or cracking of starch granules resulting in starch granules could absorbed more water leading to increased pasting viscosity, breakdown, and final viscosity. In addition, UC treated rice was treated temperature at 45, 50 or 55°C. This effect of temperatures could explain by annealing treatment (ANN). The higher annealing temperature contributed to increased pasting temperature from 65.63 to 75.72°C. This was showed significant in UC+ANN50 and UC+ANN55, but it was not significant different ($p$≥0.05) in UC+ANN45 sample. It could be explained that annealing treatment promoted stronger bond within starch granules, resulting in required a higher temperature to starch gelatinization (Samarakoon et al., 2020).

The pasting profile and the pasting properties of KDML105 samples are showed in Figure 4.9 and Table 4.20, respectively. The pasting temperatures of the native, UC and UC+ANN treatments were not significantly different ($p$≥0.05), which presented in a rage from 83.82 to 84.45°C. The UC treatment decreased peak viscosity, final viscosity, and setback, while increased breakdown as compared to its native. The decrease in peak viscosity is supposedly contributed to the stronger interaction between starch molecules as affected by chilling after ultrasound treatment

increased rearrangement of ordered structures that facilitated penetrate of water in the starch granules. These data supported with the increase in relative crystallinity (Figure 4.8). The UC+ANN treatments significantly increased peak viscosity compared to the UC treatment. In addition, the peak viscosity values were increased from 3891.50 to 4072.33 cP when increased annealing temperatures, but there was no difference between combined ultrasound plus chilling followed annealing treatment at 50°C and 55°C (UC+ANN50 and UC+ANN55). The breakdown value is related to the thermal stability of swollen starch granules in the starch paste during heating and shearing. The decrease in breakdown indicates that more stable structure of starch granules to shear force (Pinto et al., 2015; Keeratiburana et al., 2020). The decreased breakdown value of UC treated rice grains might be due to re-association of starch molecules to form more ordered structure (Ding et al., 2019). This was supported by the increasing in relative crystallinity. However, the breakdown values of UC+ANN samples were significantly increased from 995.25 to 616.00 cP, when ultrasound-chilled rice grains treated higher annealing temperatures from 45 to 55°C. The decrease in breakdown value of the UC+ANN samples might be due to increased binding force within starch granules by increasing interaction between starch chains, amylose-amylose interaction and/or amylose-amylopectin interaction, leading to breakdown values decreased (Jayakody & Hoover, 2008; Xu, Saleh, Liu, et al., 2018). Final viscosity and setback are represented to rearrangement of amylose during cooling. The increased final viscosity and setback were similar result of Hormdok and Noomhorm (2007) reported that annealing rice starch increased its retrogradation.

For CN1 cultivar, the pasting profile and pasting properties are presented in Figure 4.6 and Table 4.21. The effect of UC+ANN at 45, 50 and 55°C on pasting properties showed increased pasting temperature from 85.00 to 89.35°C, indicating that the higher temperature of annealing promoted a strengthening of the bonds between amylose-amylose, amylose-amylopectin or amylopectin-amylopectin molecules lead to starch requires higher heat to gelatinize starch granules (Gomes et al., 2004). Moreover, the peak viscosity, breakdown, final viscosity, and setback values were decreased by increased annealing temperatures. The decreased peak viscosity is influenced by the interplay between the extent of crystalline perfection and amylose-amylose and/or amylose-amylopectin interactions. Both crystalline perfection and those interactions decrease the hydration of amorphous regions of starch (Zavareze & Dias, 2011). Thus, decreasing granular swelling could

prevented leaching out of amylose molecules, resulting in decreased pasting viscosity. The reduction of final viscosity and setback of UC+ANN treated rice samples indicated that the strengthening of intragranular boned forces in starch granules require higher temperature to structural disintegration and past formation occurs which promote the reduction in final viscosity and setback.

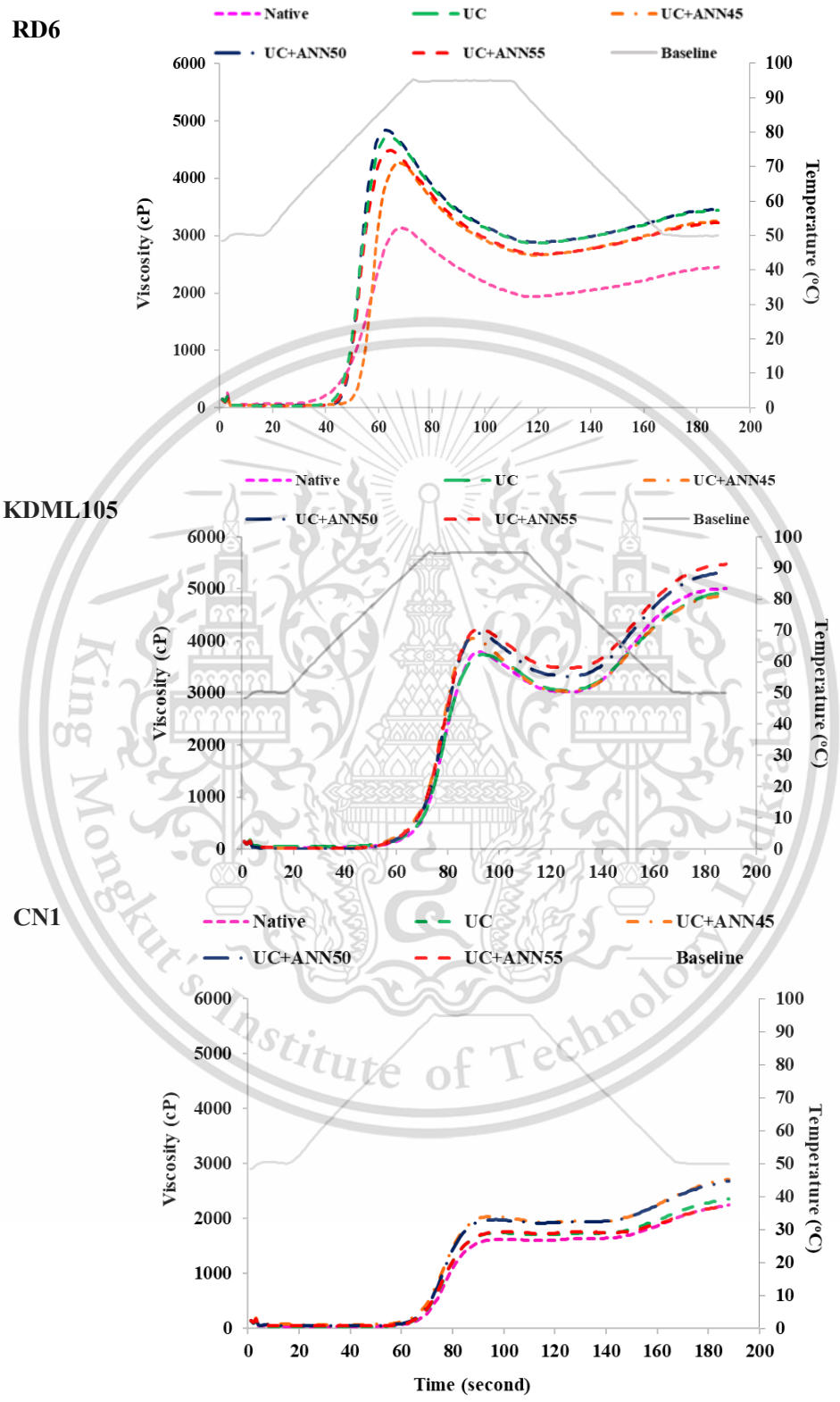


**Figure 4.6.** Rapid viscosity profiles of natives, ultrasound-chilling treatment (UC), and ultrasound-chilled rice followed annealing treatments (UC+ANN) for three rice cultivars

**Table 4.19** The pasting properties of native, ultrasound-chilling treatment (UC) and ultrasound-chilled rice followed annealing treatments (UC+ANN) for RD6 rice cultivar.

| Samples | Pasting temperature (°C) | Peak viscosity (cP) | Breakdown (cP) | Final viscosity (cP) | Setback (cP) |
|---|---|---|---|---|---|
| RD6-Native | 65.63±0.78$^{e}$ | 3152.33±39.55$^{e}$ | 1277.33±37.02e | 2459.33±34.67e | 523.00±10.58c |
| UC | 69.07±0.03$^{d}$ | 5120.67±25.42$^{a}$ | 2092.00±59.03a | 3625.33±9.29a | 596.67±49.72ab |
| UC+ANN45 | 72.83±0.06$^{c}$ | 4506.67±17.50$^{d}$ | 1809.33±36.91d | 3249.33±11.93d | 552.00±29.46bc |
| UC+ANN50 | 74.15±0.48$^{b}$ | 4780.00±37.03$^{c}$ | 1932.33±3.78c | 3497.33±27.83c | 649.67±31.56a |
| UC+ANN55 | 75.72±0.41$^{a}$ | 4958.33±16.74$^{b}$ | 2011.33±14.47b | 3552.67±21.83b | 605.67±15.63ab |

The data referred to the mean ± standard deviation (n=3). Values followed by different superscripts within a column were significantly different at $p<0.05$.

UC: ultrasound plus chilling treatment.

UC+ANN: combined ultrasound-chilling and annealing treatment.

45, 50 and 55: incubation temperatures of annealing treatment (°C).

**Table 4.20** The pasting properties of native, ultrasound-chilling treatment (UC) and ultrasound-chilled rice followed annealing treatments (UC+ANN) for KDML105 rice cultivar.

| Samples | Pasting temperature [ns] (°C) | Peak viscosity (cP) | Breakdown (cP) | Final viscosity (cP) | Setback (cP) |
|---|---|---|---|---|---|
| KDML105-Native | 83.82±0.67 | 3792.00±21.79[c] | 769.00±5.57[b] | 5000.33±21.13[c] | 1208.33±11.02[b] |
| UC | 84.02±0.46 | 3725.33±13.05[d] | 919.33±19.55[a] | 4666.67±12.10[e] | 941.33±17.04[d] |
| UC+ANN45 | 84.28±0.43 | 3891.50±26.08[b] | 955.25±17.86[a] | 4754.25±28.45[d] | 862.75±25.86[e] |
| UC+ANN50 | 84.33±0.51 | 4064.00±5.00[a] | 793.67±43.41[b] | 5223.67±29.67[b] | 1159.67±33.62[c] |
| UC+ANN55 | 84.45±0.75 | 4072.33±9.07[a] | 616.00±24.52[c] | 5420.33±13.50[a] | 1348.00±8.89[a] |

The data referred to the mean ± standard deviation (n=3). Values followed by different superscripts within a column were significantly different at $p<0.05$.

UC: ultrasound plus chilling treatment, UC+ANN: combined ultrasound-chilling and annealing treatment.

45, 50 and 55: incubation temperatures of annealing treatment (°C).

**Table 4.21** The pasting properties of native, ultrasound-chilling treatment (UC), and ultrasound-chilled rice followed annealing treatments (UC+ANN) for CN1 rice cultivar.

| Samples | Pasting temperature (°C) | Peak viscosity (cP) | Breakdown (cP) | Final viscosity (cP) | Setback (cP) |
|---|---|---|---|---|---|
| CN1-Native | 85.00±0.09$^{d}$ | 1573.33±20.01$^{e}$ | 161.33±11.37$^{e}$ | 2119.67±37.63$^{c}$ | 616.67±30.50$^{b}$ |
| UC | 88.22±0.49$^{bc}$ | 1812.00±43.97$^{c}$ | 589.67±11.85$^{b}$ | 2465.33±68.09$^{b}$ | 621.50±39.04$^{b}$ |
| UC+ANN45 | 87.47±0.40$^{c}$ | 2042.00±8.19$^{a}$ | 673.33±19.86$^{a}$ | 2715.33±27.57$^{a}$ | 801.17±140.74$^{a}$ |
| UC+ANN50 | 88.77±0.42$^{ab}$ | 1978.33±5.51$^{b}$ | 546.00±19.47$^{c}$ | 2673.00±6.25$^{a}$ | 759.67±76.05$^{a}$ |
| UC+ANN55 | 89.35±0.70$^{a}$ | 1759.33±12.66$^{c}$ | 478.33±15.70$^{d}$ | 2442.33±18.04$^{b}$ | 512.17±40.29$^{b}$ |

The data referred to the mean ± standard deviation (n=3). Values followed by different superscripts within a column were significantly different at $p<0.05$.

UC: ultrasound plus chilling treatment, UC+ANN: combined ultrasound-chilling and annealing treatment.

45, 50 and 55: incubation temperatures of annealing treatment (°C).

### 4.2.3 The effect of annealing treatment after ultrasound-chilling treatments on thermal properties for rice grains

The thermal properties of rice samples were evaluated from the parameters, including onset temperature (To), peak temperature (Tp), conclusion temperature (Tc), and enthalpy change ($\Delta$H) as measured by DSC are presented in Table 4.22 for RD6, Table 4.23 for KDML105 and Table 4.24 for CN1 rice, respectively. These results were explained as follows:

**Table 4.22** The thermal properties of ultrasound-chilling treatment (UC), and ultrasound-chilled rice followed annealing treatments (UC+ANN) for RD6 rice.

| Samples | To ($^{o}$C) | Tp ($^{o}$C) | Tc ($^{o}$C) | $\Delta$H (J/g) |
|---|---|---|---|---|
| RD6-Native | 58.76±0.37$^{c}$ | 69.03±0.19$^{d}$ | 74.32±0.13$^{b}$ | 1.87±0.06$^{a}$ |
| UC | 62.21±1.30$^{b}$ | 68.13±0.51$^{cd}$ | 74.48±0.29$^{b}$ | 1.92±0.06$^{a}$ |
| UC+ANN45 | 62.79±0.12$^{b}$ | 68.74±0.18$^{c}$ | 75.53±0.32$^{a}$ | 1.82±0.06$^{a}$ |
| UC+ANN50 | 63.03±0.40$^{ab}$ | 70.00±0.16$^{b}$ | 75.36±0.12$^{a}$ | 2.35±0.07$^{b}$ |
| UC+ANN55 | 64.14±0.63$^{a}$ | 71.65±0.54$^{a}$ | 76.46±0.04$^{a}$ | 2.30±0.05$^{b}$ |

Data values are mean ± standard deviation followed by different letters with the same column denote significant differences ($p$<0.05). UC: ultrasound plus chilling treatment. UC+ANN: combined ultrasound-chilling and annealing treatment. 45, 50 and 55: incubation temperatures of annealing treatment ($^{o}$C).
To: onset temperature, Tp: peak temperature, Tc: conclusion temperature, and $\Delta$H: enthalpy change.

According to Table 4.22, the native, UC and UC+ANN treated RD6 rice samples were observed thermal properties. The UC treated RD6 rice showed higher onset temperature (To) than that its native. This indicated that starch molecules were packed into the order of the double helices within granules during storage at 4$^{o}$C. However, peak temperature (Tp), conclusion temperature (Tc) and $\Delta$H showed no significant difference ($p$≥0.05). The U+ANN treated rice samples showed increased in To, Tp, and $\Delta$H compared to native and UC treatment. However, To, Tp, and $\Delta$H of UC+ANN45 sample were not significant different (p≥0.05). In addition, the increase in annealing temperatures from 45 to 55$^{o}$C contributed to increases in To, Tp, and $\Delta$H. The increased in

gelatinization temperature is associated with a decrease in swelling power, which provide decreased viscosity of starch granules (Zavareze & Dias, 2011). This indicated that some granular structures are stronger that reflected in the higher onset temperature for starch melting. The highest To and $\Delta$H were found in UC+ANN at 50 or 55$^{o}$C (UC+ANN50 and U+ANN55, respectively). This was supported by Kohyama and Sasaki (2006) found that the higher temperature required to gelatinize starch after annealing treatment at 50$^{o}$C as compared to 20$^{o}$C.

**Table 4.23** The thermal properties of ultrasound-chilling treatment (UC), and ultrasound-chilled rice followed annealing treatments (UC+ANN) for KDML105 rice.

| Samples | To ($^{o}$C) | Tp ($^{o}$C) | Tc ($^{o}$C) | $\Delta$H (J/g) |
|---|---|---|---|---|
| KDML105-Native | 61.81±0.38$^{c}$ | 68.71±0.25$^{b}$ | 77.69±0.21$^{a}$ | 1.63±0.13$^{c}$ |
| UC | 61.97±0.67$^{c}$ | 68.68±0.13$^{b}$ | 74.02±0.49$^{c}$ | 1.77±0.05$^{ab}$ |
| UC+ANN45 | 62.90±0.22$^{b}$ | 68.91±0.10$^{b}$ | 73.76±0.13$^{c}$ | 1.59±0.01$^{bc}$ |
| UC+ANN50 | 63.46±0.14$^{b}$ | 69.01±0.16$^{b}$ | 73.68±0.23$^{c}$ | 1.90±0.09$^{a}$ |
| UC+ANN55 | 65.81±0.67$^{a}$ | 70.85±0.57$^{a}$ | 75.45±0.56$^{b}$ | 1.90±0.10$^{a}$ |

Data values are mean ± standard deviation followed by different letters with the same column denote significant differences ($p$<0.05). UC: ultrasound plus chilling treatment. UC+ANN: combined ultrasound-chilling and annealing treatment. 45, 50 and 55: incubation temperatures of annealing treatment ($^{o}$C).
To: onset temperature, Tp: peak temperature, Tc: conclusion temperature, and $\Delta$H: enthalpy change.

Thermal properties of KDML105 rice samples are shown in Table 4.23. The gelatinization temperatures of native presented in the temperature range from 61.81 to 77.69$^{o}$C and enthalpy change ($\Delta$H) was 1.63 J/g. The UC treatment did not change To, and Tp as compared to native. In fact, a previous our study, rice grain samples were treated by ultrasound treatment resulting in the gelatinization temperatures decreased (Table 4.13), while combined ultrasound and chilling (UC) increased To, Tp, and Tc. This result confirmed that chilling after ultrasound treated rice samples promoted crystalline structure by arrangement of starch chains resulting higher temperature to melting starch. The UC treatment samples showed significantly increased $\Delta$H as compared to its native. The increased $\Delta$H might be due to reorganization of starch chains during

chilling treatment attributing to increase crystalline stability. For all UC+ANN samples, the increased gelatinization temperatures (To, Tp, and Tc) through annealing treatment taking after UC treatment. These results agreed with increase in pasting temperature and relative crystallinity. The increased To, Tp, and Tc of UC+ANN samples attributed to starch structure change within starch granules by involving amylose-amylose, amylose-amylopectin and/or amylose-lipid interaction. These results recognized that ANN followed UC treatment promoted the gelatinization temperatures increased and narrows temperature range decreased as a result of perfection of crystalline. ANN treatment increases the mobility of amylopectin chains which causes reorientation of amylopectin to form more ordered (R. Waduge et al., 2006; da Rosa Zavareze & Dias, 2011). Kohyama and Sasaki (2006) reported that annealing treatment changed the perfection of crystalline structure leading to the formation of new double helices. The $\Delta$H of UC+ANN treatment of KDML105 rice, UC+ANN with higher temperatures showed increase in $\Delta$H. This is related with increased relative crystallinity. The gelatinization parameters are correction with the degree of crystalline since a higher crystallinity in starch structure require more thermal energy for melting the crystalline, thus higher temperature to starch gelatinization (Samarakoon et al., 2020). This result similar to the studies of R. Waduge et al. (2006) reported that annealing effect resulting in increased To, Tp, and Tc.

**Table 4.24** The thermal properties of ultrasound-chilling treatment (UC), and ultrasound-chilled rice followed annealing treatments (UC+ANN) for CN1 rice.

| Samples | To ($^{o}$C) | Tp ($^{o}$C) | Tc ($^{o}$C) | $\Delta$H (J/g) |
|---|---|---|---|---|
| CN1-Native | 71.62±0.27$^{d}$ | 76.59±0.12$^{b}$ | 81.86±0.23$^{a}$ | 1.12±0.01$^{c}$ |
| UC | 72.29±0.07$^{b}$ | 77.81±0.05$^{b}$ | 81.99±0.12$^{a}$ | 2.02±0.05$^{b}$ |
| UC+ANN45 | 72.02±0.20$^{bc}$ | 76.01±0.21$^{c}$ | 79.67±0.20$^{b}$ | 2.84±0.02$^{a}$ |
| UC+ANN50 | 71.96±0.01$^{c}$ | 75.84±0.05$^{c}$ | 79.42±0.06$^{b}$ | 2.83±0.14$^{a}$ |
| UC+ANN55 | 73.83±0.07$^{a}$ | 77.77±0.18$^{a}$ | 82.12±0.28$^{a}$ | 2.68±0.73$^{a}$ |

Data values are mean ± standard deviation followed by different letters with the same column denote significant differences ($p$<0.05). To: onset temperature, Tp: peak temperature, Tc: conclusion temperature, and $\Delta$H: enthalpy change.

According to Table 4.24 is presented thermal properties of CN1 rice. Thermal properties of this rice showed slightly different in RD6 and KDML105 rice. It was noted that the difference in the gelatinization temperatures and enthalpy change of those rice cultivars correlated with their amylose content which was explained by Varavinit et al. (2003). CN1 rice showed not significantly difference $T_o$ after ANN treatment at 45, and 50$^oC$ but it was slightly increased after annealing treatment at 55$^oC$. The increase in gelatinization temperature is associated with a decrease in swelling, provided that starch structures is retained. This is reflected in a higher temperature for the onset temperature (Tester et al., 2000). Annealing treatments exhibited increase in $\Delta H$ from 1.12 to 2.84 J/g. Annealing caused increased the enthalpy value of rice samples. These results suggested that ordered structures of CN1 rice were affected after annealing treatment, consistent with the results of XRD. These results agreed with the finding of Liu, Yu, et al. (2009) reported that annealing treatment lead to the contribution of ordering and incorporation of amylose into amylopectin crystallite that could affected increased gelatinization temperature and enthalpy.

### 4.2.4 The effect of annealing treatment after ultrasound-chilling treatments on *In vitro* glycemic index for rice grains

The results of *in vitro* glycemic index for three rice cultivars are shown in Table 4.25, including hydrolysis index (HI), rate of digestion (k), and expected glycemic index (eGI). Starch hydrolysis percentage curves ($C_\infty$) of three rice cultivars are shown in Figure 4.7.

The digestion rate constant (k-value) was not significantly changed ($p \geq 0.05$) when rice samples were treated with UC treatment, found in RD6, KML105 and CN1 rice. However, when ANN treatments plus after UC treatment of three rice cultivars were significantly decreased kinetic constant by decreased from 21.20 to 14.85 for RD6, 17.13 to 13.73 for KDML105 cultivar and 12.93 to 9.37 for CN1 cultivar. These results showed that annealing treatment promotes reorganization of starch granules attributing to an increase in granular stability. This effect could be led to the formation of resistant starch (Gomes et al., 2005; H. J. Chung et al., 2009). reported that decreased in enzyme susceptibility has been attributed to perfection of crystallites after annealing treatment. This supported by increased relative crystallinity. Therefore, UC+ANN treatments are more resistant to the digestive enzyme.

The hydrolysis index (HI) is used for estimating the glycemic index of carbohydrate foods (Annor et al., 2015). The HI of native samples, the CN1 rice showed lower HI than the KDML105 and RD6 cultivar, respectively (CN1<KDML105<RD6), because high amylose content is more suitable for producing resistant starch (Li et al., 2018). Moreover, high amylose content presents lower hydrolysis by α-amylase attributing to the major component of amylose is crystalline which reflects compact structure of starch granules (R. J. C. Hsu et al., 2015; Kale et al., 2015). In addition, UC treatment in this study showed in significant ($p$<0.05) decrease in HI of three rice cultivars. It was observed that the ANN treatments were subjected after ultrasound-chilled rice grains, which showed more decreased HI. Thus, the addition of ANN treatment after UC treatment of three rice cultivars markedly decreased the HI value. Specifically, the UC+ANN treated rice at highest temperature (UC+ANN55) of both rice cultivars resulted in the lowest HI as compared to ANN subjected with lower temperatures (UC+ANN45 and UC+ANN50).

The expected glycemic index (eGI) of natives, UC, and UC+ANN treated rice sample for both rice cultivars are presented in Table 3. The eGI of natives for RD6, KDML105 and CN1 rice was 84.14, 67.99 and 60.59, respectively. This data confirmed that high amylose rice leading to lower starch hydrolyzed that promoted lower eGI. The decreased eGI could be more effects of annealing treatment subjected UC treatment. The annealing effect on decreased eGI due to a more ordered structure of rearrangement of double helices that can increase the formation of granular stability (Jayakody & Hoover, 2008; Keeratiburana et al., 2020). This result related to the increased crystallinity of rice treated UC+ANN samples.

Figure. 4.7 showed starch hydrolysis for three rice cultivars. Rice samples exhibited digestion of total starch hydrolyzed from 0 to 180 min. The hydrolysis of treated rice samples (UC and UC+ANN) for three rice cultivars exhibited lower starch hydrolysis as compared to their native, demonstrating that the lower enzyme susceptibility to hydrolyze starch molecule. This result could be attributed to stronger structure of starch molecule which promoted by UC treatment and UC+ANN treatment. The UC+ANN treatments showed the reduction of hydrolysis percentage, especially UC+ANN at 55$^{o}$C of both rice cultivars had lowest starch hydrolysis. Particularly, CN1 rice showed lowest slope of a curve in all samples as compared to RD6 and KDML105 rice. This was related to its k-value and glycemic index.

**Table 4.25** The hydrolysis index, rate of digestion and expected glycemic index of ultrasound-chilling treatment (UC), and ultrasound-chilled rice followed annealing treatments (UC+ANN) for three rice cultivars.

| Rice cultivars | k ($min^{-1}$) × $10^{-3}$ | HI | eGI |
|---|---|---|---|
| **RD6** | | | |
| Native | 21.20±0.01[a] | 81.48±0.50[a] | 84.14±0.80[a] |
| UC | 20.00±0.01[a] | 79.83±0.15[a] | 80.71±0.77[b] |
| UC+ANN45 | 17.60±0.01[b] | 71.77±0.02[b] | 76.78±1.63[c] |
| UC+ANN50 | 17.75±0.01[b] | 68.01±0.60[c] | 77.15±1.39[c] |
| UC+ANN55 | 14.85±0.01[c] | 66.76±0.83[c] | 77.62±1.02[c] |
| **KDML105** | | | |
| Native | 17.13±1.15[a] | 63.31±0.37[a] | 67.99±0.33[a] |
| UC | 16.87±0.76[a] | 57.90±0.51[b] | 66.15±0.48[b] |
| UC+ANN45 | 14.63±0.98[b] | 57.57±0.10[b] | 65.59±0.25[b] |
| UC+ANN50 | 14.57±0.29[b] | 53.94±0.74[c] | 63.48±0.12[c] |
| UC+ANN55 | 13.73±0.65[b] | 50.76±0.55[d] | 63.18±0.48[c] |
| **CN1** | | | |
| Native | 12.93±2.19[a] | 42.07±1.59[a] | 60.59±1.99[a] |
| UC | 12.67±2.32[a] | 30.88±1.69[b] | 56.09±1.22[b] |
| UC+ANN45 | 9.50±0.04[b] | 30.17±1.70[b] | 56.849±1.38[b] |
| UC+ANN50 | 9.73±0.31[b] | 30.26±0.86[b] | 56.619±0.70[b] |
| UC+ANN55 | 9.37±0.09[b] | 26.46±0.56[c] | 54.03±0.50[c] |

Data values are mean ± standard deviation followed by different letters with the same row denote significant differences ($p$<0.05).

k: Rate of digestion (digestion rate constant)HI: Expected glycemic index.

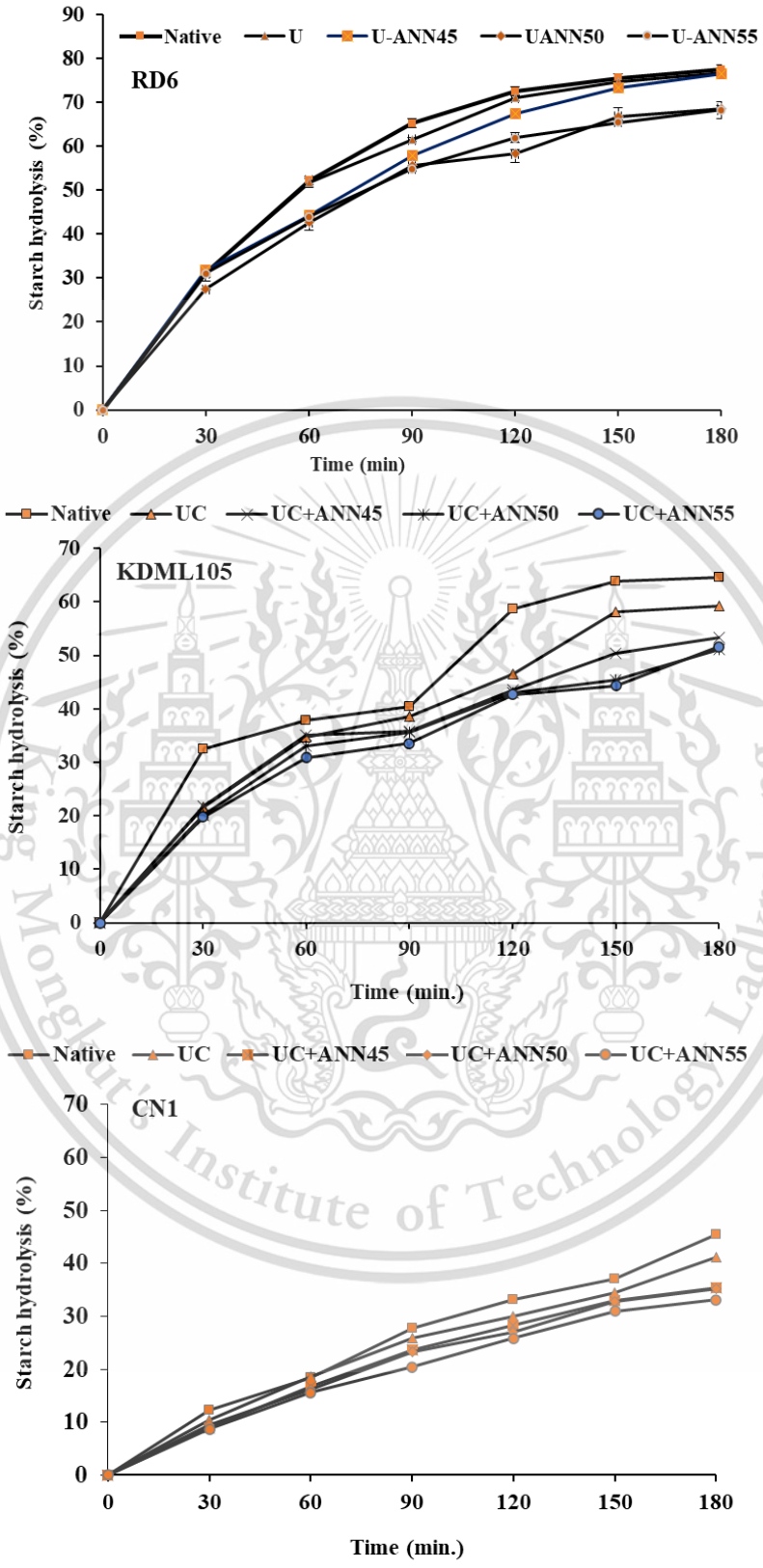


**Figure 4.7** The percentage of starch hydrolysis of natives, ultrasound-chilling treatment (UC) and ultrasound-chilled rice followed annealing treatments (UC+ANN) for three rice cultivars.

# CHAPTER 5

# CONCLUSION

## 5.1 Conclusions

The objective of the study was to study the effects of the combination of ultrasound and chilling treatment and ultrasound-chilling followed by annealing treatments on physicochemical properties and *in vitro* glycemic index of Thai rice with differing amylose content. These are concluded as follows:

5.1.1 The increased sonication times and ultrasound power levels of ultrasound treatments were studied for Thai rice grains with differing amylose content (RD6 (7.04% g/100), KDML105 (16.91% g/100) and CN1 (29.35 g/100) ). The effects of ultrasound treatments were tested, with or without subsequent chilling treatment, on the crystallinity, thermal properties, pasting properties and *in vitro* glycemic index of three rice cultivars. Ultrasound treatment in three cultivars resulted in no change in functional groups and structural patterns found using Fourier transform infrared spectroscopy (FTIR) and X-ray diffraction pattern. However, ultrasound treatment induced disruption of double helix complexes and changes of their relative crystallinity resulting in higher glycemic index in RD6 and KDML105, and CN1 rice. Ultrasound treatment in three rice cultivars had different relative crystallinity, pasting temperature, gelatinization temperatures, $\Delta$H, and their eGI, which were affected by their amylose content. Moreover, the increase in sonication times and ultrasound power levels produced disruption of starch granules as shown by the decrease of viscosity, To and $\Delta$H. While CN1 showed slightly affected on those properties. However, CN1 showed decrease in relative crystallinity, pasting temperature, gelatinization temperatures, $\Delta$H, and their GI. Additionally, chilling after ultrasound treatment of three rice cultivars contributed to the increase in PT and PV of pasting properties, relative crystallinity, and $\Delta$H, while decrease in k-value, HI, and eGI. Particularly, ultrasound treatments for 15 min at 100% of ultrasound power for RD6, or 15 min at 70% of ultrasound power for KDML105 and CN1 followed by chilling treatment displayed the lowest glycemic index. These results demonstrated that ultrasound treatment followed

by chilling successfully lowered glycemic index compared to the natives of three cultivars tested and the extent of these changes depended on the sonication time and power level of the ultrasound, cultivar and their amylose content. However, ultrasound and chilling treatment of rice grains could help slightly reduce their glycemic index.

5.1.2 The pasting properties, thermal properties, relative crystallinity, and *in vitro* glycemic index were significantly changed by ultrasound-chilling treatments, and ultrasound-chilled followed by annealing treatment (UC+ANN) treatments. Especially, UC+ANN of three rice cultivars exhibited a large change in pasting temperature, gelatinization temperatures, and *in vitro* glycemic index of three rice cultivars. Annealing treatment promotes the reorganization of starch chains to perfect crystalline attributing to stronger granular structures. The higher temperatures of annealing treatment could help the arrangement of amorphous region within starch granules leading to lower glycemic index. However, difference types of rice presented difference annealing conditions to exhibit lowest eGI. RD6 rice, KDML105 and CN1 were treated annealing temperature at 45, 50, and 55$^{o}$C, respectively. Thus, combination of UC+ANN could be expected to be a technology for modifying rice grains to improve resistant enzymatic hydrolyses.

## 5.2 Recommendations

The following recommendations are made for further study:

5.2.1 The effect of ultrasound treatment for further study should investigated chain length distribution of amylose or amylopectin.

5.2.2 Cooking condition of rice grains on glycemic index should be further investigated.

5.2.3 Modified rice grains should be tested *in vivo* glycemic index.

5.2.4 The lowest glycemic index rice application to product such as bakery, diabetic food, and other products should be investigated.

# REFFERENCES


American Association of Cereal Chemists (AACC). (2000). Approved methods of analysis (11th ed). St. Paul, MN: The Association. Aproved method 32-40.01.

American Association of Cereal Chemists (AACC). (2009). Approved methods of analysis (11th ed). St. Paul, MN: The Association. Aproved method 44-15.02.

Adebowale, K. O., Henle, T., Schwarzenbolz, U., and Doert, T. (2009). Modification and properties of African yam bean (Sphenostylis stenocarpa Hochst. Ex A. Rich.) Harms starch I: Heat moisture treatments and annealing. ***Food Hydrocolloids***, *23*(7), 1947-1957.

Adedayo, B. C., Adebayo, A. A., Nwanna, E. E., and Oboh, G. (2018). Effect of cooking on glycemic index, antioxidant activities, α-amylase, and α-glucosidase inhibitory properties of two rice varieties. ***Food Science & Nutrition***, *6*(8), 2301-2307.

Afolabi, T. A., Opara, A. O., Kareem, S. O., and Oladoyinbo, F. O. (2018). In vitro digestibility of hydrothermally modified Bambara groundnut (Vigna subterranean L.) starch and flour. ***Food Science & Nutrition***, *6*(1), 36-46.

Aibara, S., Ismail, I. A., Yamashita, H., Ohta, H., Sekiyama, F., and Morita, Y. (1986). Changes in rice bran lipids and free amino acids during storage. ***Agricultural and Biological Chemistry***, *50*(3), 665-673.

Amin, T., Naik, H., Hussain, S. Z., Rather, A., Murtaza, I., and Dar, B. (2017). Structural properties of high-protein, low glycaemic index (GI) rice flour. ***International journal of food properties***, *20*(11), 2793-2804.

Anjum, F., Pasha, I., Bugti, M. A., and Butt, M. (2007). Mineral composition of different rice varieties and their milling fractions. ***Pak. J. Agri. Sci***, *44*(2), 332-336.

Annor, G. A., Marcone, M., Corredig, M., Bertoft, E., and Seetharaman, K. (2015). Effects of the amount and type of fatty acids present in millets on their in vitro starch digestibility and expected glycemic index (eGI). ***Journal of Cereal Science***, *64*, 76-81.

Arns, B., Bartz, J., Radunz, M., Evangelho, J. A. d., Pinto, V. Z., Zavareze, E. d. R., and Dias, A. R. G. (2015). Impact of heat-moisture treatment on rice starch, applied directly in grain paddy rice or in isolated starch. ***LWT - Food Science and Technology***, *60*(2), 708-713.

Azhar, A., and Hamdy, M. (1979). Sonication effect on potato starch and sweet potato powder. ***Journal of food science**, 44*(3), 801-804.

Babu, A. S., Mohan, R. J., and Parimalavalli, R. (2019). Effect of single and dual-modifications on stability and structural characteristics of foxtail millet starch. ***Food Chemistry**, 271*, 457-465.

Bai, W., Hebraud, P., Ashokkumar, M., and Hemar, Y. (2017). Investigation on the pitting of potato starch granules during high frequency ultrasound treatment. ***Ultrason Sonochem**, 35*(Pt B), 547-555.

Baik, M.-Y., Kim, K.-J., Cheon, K.-C., Ha, Y.-C., and Kim, W.-S. (1997). Recrystallization kinetics and glass transition of rice starch gel system. ***Journal of agricultural and food chemistry**, 45*(11), 4242-4248.

Bernardo, C. O., Ascheri, J. L. R., Chávez, D. W. H., and Carvalho, C. W. P. (2018). Ultrasound Assisted Extraction of Yam (Dioscorea bulbífera) Starch: Effect on Morphology and Functional Properties. ***Starch‐Stärke**, 70*(5-6), 1700185

Bertoft, E. (2017). Understanding starch structure: Recent progress. ***Agronomy**, 7*(3), 56.

Bian, L., and Chung, H.-J. (2016). Molecular structure and physicochemical properties of starch isolated from hydrothermally treated brown rice flour. ***Food Hydrocolloids**, 60*, 345-352.

Biliaderis, C., Maurice, T., and Vose, J. (1980). Starch gelatinization phenomena studied by differential scanning calorimetry. ***Journal of food science**, 45*(6), 1669-1674.

Biliaderis, C. G., Page, C. M., Maurice, T. J., and Juliano, B. O. (1986). Thermal characterization of rice starches: A polymeric approach to phase transitions of granular starch. ***Journal of agricultural and food chemistry**, 34*(1), 6-14.

Blakeney, A. (1984). Rice grain quality. ***Rice Growing in New South Wales***, 1-5.

Brand-Miller, J., McMillan-Price, J., Steinbeck, K., and Caterson, I. (2009). Dietary Glycemic Index: Health Implications. ***Journal of the American College of Nutrition**, 28*(4), 446-449.

Brouns, F., Bjorck, I., Frayn, K., Gibbs, A., Lang, V., Slama, G., and Wolever, T. (2005). Glycaemic index methodology. ***Nutrition research reviews**, 18*(1), 145-171.

Campos, A., Sena Neto, A. R., Rodrigues, V. B., Luchesi, B. R., Moreira, F. K. V., Correa, A. C., Mattoso, L. H. C., and Marconcini, J. M. (2017). Bionanocomposites produced from cassava starch and oil palm mesocarp cellulose nanowhiskers. ***Carbohydr Polym**, 175*, 330-336.

Carmona‐García, R., Bello‐Pérez, L., Aguirre‐Cruz, A., Aparicio‐Saguilán, A., Hernández‐Torres, J., and Alvarez‐Ramirez, J. (2016). Effect of ultrasonic treatment on the morphological, physicochemical, functional, and rheological properties of starches with different granule size. ***Starch‐Stärke**, 68*(9-10), 972-979.

Chairote, E.-o. (2009). *Preparation and study on red yeast rice prepared from glutinous rice using Monascus purpureus Isolated from Chinese Traditional red yeast rice.* (Ph.D), Chiang Mai: Graduate School, Chiang Mai University, 2009.

Champagne, E. T., Bett‐Garber, K. L., Thompson, J., Mutters, R., Grimm, C. C., and McClung, A. M. (2005). Effects of drain and harvest dates on rice sensory and physicochemical properties. ***Cereal Chemistry**, 82*(4), 369-374.

Champagne, E. T., Wood, D. F., Juliano, B. O., and Bechtel, D. B. (2004). The rice grain and its gross composition. ***Rice chemistry and technology**, 3*, 77-107.

Chan, H., Brand-Miller, J., Holt, S., and Wilson, D. (2001). The glycaemic index values of Vietnamese foods. ***European Journal of Clinical Nutrition**, 55*(12), 1076.

Chemat, F., and Hoarau, N. (2004). Hazard analysis and critical control point (HACCP) for an ultrasound food processing operation. ***Ultrason Sonochem**, 11*(3-4), 257-260.

Chiu, Y. T., and Stewart, M. L. (2013). Effect of variety and cooking method on resistant starch content of white rice and subsequent postprandial glucose response and appetite in humans. ***Asia Pac J Clin Nutr**, 22*(3), 372-379.

Chowdhury, P., and Viraraghavan, T. (2009). Sonochemical degradation of chlorinated organic compounds, phenolic compounds and organic dyes–a review. ***Science of the total environment**, 407*(8), 2474-2492.

Chung, H.-J., Liu, Q., and Hoover, R. (2009). Impact of annealing and heat-moisture treatment on rapidly digestible, slowly digestible and resistant starch levels in native and gelatinized corn, pea and lentil starches. ***Carbohydrate Polymers**, 75*(3), 436-447.

Chung, H.-J., Liu, Q., Lee, L., and Wei, D. (2011). Relationship between the structure, physicochemical properties and in vitro digestibility of rice starches with different amylose contents. ***Food Hydrocolloids**, 25*(5), 968-975.

Chung, H. J., Hoover, R., and Liu, Q. (2009). The impact of single and dual hydrothermal modifications on the molecular structure and physicochemical properties of normal corn starch. ***Int J Biol Macromol**, 44*(2), 203-210.

Chusak, C., Ying, J. A. Y., Zhien, J. L., Pasukamonset, P., Henry, C. J., Ngamukote, S., and Adisakwattana, S. (2019). Impact of Clitoria ternatea (butterfly pea) flower on in vitro starch digestibility, texture and sensory attributes of cooked rice using domestic cooking methods. ***Food Chemistry**, 295*, 646-652.

Cooke, D., and Gidley, M. J. (1992). Loss of crystalline and molecular order during starch gelatinisation: origin of the enthalpic transition. ***Carbohydrate Research**, 227*, 103-112.

Cui, L., Pan, Z., Yue, T., Atungulu, G. G., and Berrios, J. (2010). Effect of Ultrasonic Treatment of Brown Rice at Different Temperatures on Cooking Properties and Quality. ***Cereal Chemistry Journal**, 87*(5), 403-408.

Curá, J. A., Jansson, P. E., and Krisman, C. R. (1995). Amylose is not strictly linear. ***Starch=Stärke**, 47*(6), 207-209.

da Rosa Zavareze, E., and Dias, A. R. G. (2011). Impact of heat-moisture treatment and annealing in starches: A review. ***Carbohydrate Polymers**, 83*(2), 317-328.

Dhital, S., Dabit, L., Zhang, B., Flanagan, B., and Shrestha, A. K. (2015). In vitro digestibility and physicochemical properties of milled rice. ***Food Chemistry**, 172*, 757-765.

Dias, A. R. G., da Rosa Zavareze, E., Spier, F., de Castro, L. A. S., and Gutkoski, L. C. (2010). Effects of annealing on the physicochemical properties and enzymatic susceptibility of rice starches with different amylose contents. ***Food Chemistry**, 123*(3), 711-719.

Ding, Y., Luo, F., and Lin, Q. (2019). Insights into the relations between the molecular structures and digestion properties of retrograded starch after ultrasonic treatment. ***Food Chemistry**, 294*, 248-259.

Ding, Y., Zheng, J., Xia, X., Ren, T., and Kan, J. (2016). Preparation and characterization of resistant starch type IV nanoparticles through ultrasonication and miniemulsion cross-linking. ***Carbohydrate Polymers**, 141*, 151-159.

Dipnaik, K., and Kokare, P. (2017). Ratio of Amylose and Amylopectin as indicators of glycaemic index and in vitro enzymatic hydrolysis of starches of long, medium and short grain rice. ***International Journal of Research in Medical Sciences**, 5*(10), 4502-4505.

Dupuis, J. H., Liu, Q., and Yada, R. Y. (2014). Methodologies for increasing the resistant starch content of food starches: a review. ***Comprehensive Reviews in Food Science and Food Safety**, 13*(6), 1219-1234.

Elgadir, M. A., Bakar, J., Zaidul, I., Rahman, R. A., Abbas, K., Hashim, D., and Karim, R. (2009). Thermal behavior of selected starches in presence of other food ingredients studied by differential scanning calorimetery (DSC)–Review. ***Comprehensive Reviews in Food Science and Food Safety**, 8*(3), 195-201.

FAO, W. (1997). Carbohydrates in human nutrition (FAO Food and Nutrition paper–66) Chapter 4. ***The role of the glycemic index in food choice. FAO/WHO, Rome***.

Flores-Morales, A., Jiménez-Estrada, M., and Mora-Escobedo, R. (2012). Determination of the structural changes by FT-IR, Raman, and CP/MAS 13C NMR spectroscopy on retrograded starch of maize tortillas. ***Carbohydrate Polymers**, 87*(1), 61-68.

Flores-Silva, P. C., Alvarez-Ramirez, J., and Bello-Perez, L. A. (2018). Effect of Dual Modification Order with Ultrasound and Hydrothermal Treatments on Starch Digestibility. ***Starch-Starke**, 70*(5-6).

Flores-Silva, P. C., Roldan-Cruz, C. A., Chavez-Esquivel, G., Vernon-Carter, E. J., Bello-Perez, L. A., and Alvarez-Ramirez, J. (2017). In vitro digestibility of ultrasound-treated corn starch. ***Starch - Stärke**, 69*(9-10), 1700040.

Frazier, P. J., Donald, A. M., and Richmond, P. (1997). *Starch: structure and functionality* (Vol. 205): Royal Society of Chemistry.

Freeman, J., and Lyons, L. (2008). The use of continuous glucose monitoring to evaluate the glycemic response to food. ***Diabetes spectrum**, 21*(2), 134-137.

Frei, M., Siddhuraju, P., and Becker, K. (2003). Studies on the in vitro starch digestibility and the glycemic index of six different indigenous rice cultivars from the Philippines. ***Food Chemistry**, 83*(3), 395-402.

Gidley, M. J. (1987). Factors affecting the crystalline type (A- C) of native starches and model compounds: a rationalisation of observed effects in terms of polymorphic structures. ***Carbohydrate Research**, 161*(2), 301-304.

Gomes, A. M., da Silva, C. E. M., and Ricardo, N. M. (2005). Effects of annealing on the physicochemical properties of fermented cassava starch (polvilho azedo). ***Carbohydrate Polymers**, 60*(1), 1-6.

Gomes, A. M., da Silva, C. E. M., Ricardo, N. M., Sasaki, J. M., and Germani, R. (2004). Impact of annealing on the physicochemical properties of unfermented cassava starch ("Polvilho Doce"). ***Starch-Stärke**, 56*(9), 419-423.

Gomez, K. (1979). *Effect of environment on protein and amylose content of rice.* Paper presented at the Proceedings of the workshop on chemical aspects of rice grain quality.

Goñi, I., Garcia-Alonso, A., and Saura-Calixto, F. (1997). A starch hydrolysis procedure to estimate glycemic index. ***Nutrition Research**, 17*(3), 427-437.

Granfeldt, Y., Bjorck, I., Drews, A., and Tovar, J. (1992). An in vitro procedure based on chewing to predict metabolic response to. ***European Journal of Clinical Nutrition**, 46*, 649-660.

Gray, G. M. (1970). Carbohydrate digestion and absorption. ***Gastroenterology**, 58*(1), 96-107.

Griglione, A., Liberto, E., Cordero, C., Bressanello, D., Cagliero, C., Rubiolo, P., Bicchi, C., and Sgorbini, B. (2015). High-quality Italian rice cultivars: Chemical indices of ageing and aroma quality. ***Food Chemistry**, 172*, 305-313.

Güemes, M., Rahman, S. A., and Hussain, K. (2016). What is a normal blood glucose? ***Archives of disease in childhood**, 101*(6), 569-574.

Gunaratne, A., and Hoover, R. (2002). Effect of heat–moisture treatment on the structure and physicochemical properties of tuber and root starches. ***Carbohydrate Polymers**, 49*(4), 425-437.

Guo, L., Zhang, J., Hu, J., Li, X., and Du, X. (2015). Susceptibility of glutinous rice starch to digestive enzymes. ***Carbohydrate Polymers**, 128*, 154-162.

Han, X.-Z., and Hamaker, B. R. (2001). Amylopectin fine structure and rice starch paste breakdown. ***Journal of Cereal Science**, 34*(3), 279-284.

Hayakawa, T., SEO, S. W., and IGAUE, I. (1980). Electron Microscopic Observation of Rice Grain. ***Journal of the Japanese Society of Starch Science**, 27*(3), 173-179.

HerCeg, I. L., Jambrak, A. R., ŠubArIĆ, D., BrnČiĆ, M., BrnČiĆ, S. R., Badanjak, M., Tripalo, B., Ježek, D., Novotni, D., and Herceg, Z. (2010). Texture and pasting properties of ultrasonically treated corn starch. ***Czech J. Food Sci**, 28*(2), 83-89.

Hizukuri, S. (1986). Polymodal distribution of the chain lengths of amylopectins, and its significance. ***Carbohydr. Res.**, 147*, 342-347.

Hoover, R., and Vasanthan, T. (1994). Effect of heat-moisture treatment on the structure and physicochemical properties of cereal, legume, and tuber starches. ***Carbohydrate Research**, 252*, 33-53.

Hormdok, R., and Noomhorm, A. (2007). Hydrothermal treatments of rice starch for improvement of rice noodle quality. ***LWT - Food Science and Technology**, 40*(10), 1723-1731.

Hsu, R. J.-c., Chen, H.-J., Lu, S., and Chiang, W. (2015). Effects of cooking, retrogradation and drying on starch digestibility in instant rice making. ***Journal of Cereal Science**, 65*, 154-161.

Hsu, R. J. C., Lu, S., Chang, Y.-h., and Chiang, W. (2015). Effects of added water and retrogradation on starch digestibility of cooked rice flours with different amylose content. ***Journal of Cereal Science**, 61*, 1-7.

Hu, P., Zhao, H., Duan, Z., Linlin, Z., and Wu, D. (2004). Starch digestibility and the estimated glycemic score of different types of rice differing in amylose contents. ***Journal of Cereal Science**, 40*(3), 231-237.

Huang, Q., Li, L., and Fu, X. (2007). Ultrasound effects on the structure and chemical reactivity of cornstarch granules. ***Starch-Stärke**, 59*(8), 371-378.

Huang, Z.-Q., Lu, J.-P., Li, X.-H., and Tong, Z.-F. (2007). Effect of mechanical activation on physico-chemical properties and structure of cassava starch. ***Carbohydrate Polymers**, 68*(1), 128-135.

Huebner, F., Bietz, J., Webb, B., and Juliano, B. (1990). Rice cultivar identification by high-performance liquid chromatography of endosperm proteins. ***Cereal Chem**, 67*(2), 129-135.

Hui, Y. H., and Sherkat, F. (2005). *Handbook of food science, technology, and engineering-4 volume Set*: CRC press.

Isono, Y., Kumagai, T., and Watanabe, T. (1994). Ultrasonic degradation of waxy rice starch. ***Bioscience, biotechnology, and biochemistry**, 58*(10), 1799-1802.

Jacobs, H., and Delcour, J. A. (1998). Hydrothermal modifications of granular starch, with retention of the granular structure: A review. ***Journal of agricultural and food chemistry**, 46*(8), 2895-2905.

Jaggi, N., and Vij, D. (2006). Fourier transform infrared spectroscopy *Handbook of Applied Solid State Spectroscopy* (pp. 411-450): Springer.

Jaisut, D., Prachayawarakorn, S., Varanyanond, W., Tungtrakul, P., and Soponronnarit, S. (2008). Effects of drying temperature and tempering time on starch digestibility of brown fragrant rice. ***Journal of Food Engineering**, 86*(2), 251-258.

Jaisut, D., Prachayawarakorn, S., Varanyanond, W., Tungtrakul, P., and Soponronnarit, S. (2009). Accelerated aging of jasmine brown rice by high-temperature fluidization technique. ***Food Research International**, 42*(5), 674-681.

Jambrak, Herceg, Z., Subaric, D., Babic, J., Brncic, M., Brncic, S. R., Bosiljkov, T., Cvek, D., Tripalo, B., and Gelo, J. (2010). Ultrasound effect on physical properties of corn starch. ***Carbohydrate Polymers**, 79*(1), 91-100.

Jane, J., Chen, Y., Lee, L., McPherson, A., Wong, K., Radosavljevic, M., and Kasemsuwan, T. (1999). Effects of amylopectin branch chain length and amylose content on the gelatinization and pasting properties of starch. ***Cereal Chemistry**, 76*(5), 629-637.

Jane, J. l., Chen, Y., Lee, L., McPherson, A., Wong, K., Radosavljevic, M., and Kasemsuwan, T. (1999). Effects of amylopectin branch chain length and amylose content on the gelatinization and pasting properties of starch. ***Cereal Chemistry**, 76*(5), 629-637.

Jayakody, L., and Hoover, R. (2008). Effect of annealing on the molecular structure and physicochemical properties of starches from different botanical origins–A review. ***Carbohydrate Polymers**, 74*(3), 691-703.

Jeevetha, S., Barakatun-Nisak, M. Y., Ngan, H., Ismail, A., and Azlan, A. (2014). Relationship between amylose content and glycemic index of commonly consumed white rice. ***IOSR-JAVS**, 7*(9), 12-18.

Ji, N., Ge, S., Li, M., Wang, Y., Xiong, L., Qiu, L., Bian, X., Sun, C., and Sun, Q. (2019). Effect of annealing on the structural and physicochemical properties of waxy rice starch nanoparticles: Effect of annealing on the properties of starch nanoparticles. ***Food Chemistry**, 286*, 17-21.

Juhász, R., and Salgó, A. (2008). Pasting behavior of amylose, amylopectin and their mixtures as determined by RVA curves and first derivatives. ***Starch-Stärke**, 60*(2), 70-78.

Juliano, B. (1992). Structure, chemistry, and function of the rice grain and its fractions. ***Cereal Foods World**, 37*, 772-772.

Juliano, B. O. (1977). Rice lipids. ***Brain**, 220*, 25.

Juliano, B. O. (1982). An international survey of methods used for evaluation of the cooking and eating qualities of milled rice.

Juliano, B. O. (1985). Polysaccharides, proteins and lipids of rice. ***Rice: chemistry and technology***, 59-174.

Juliano, B. O. (1993). *Rice in human nutrition*: Int. Rice Res. Inst.

Juliano, B. O., and Bechtel, D. B. (1985). The Rice Grain ant Its Gross Composition. ***CHAMPAGNE ET Rice: Chemistry ant Technology. 3nd. ed. Elaine T. Champagne. American Association of Cereal Chemistry***.

Juliano, B. O., and Hicks, P. A. (1996). Rice functional properties and rice food products. ***Food Reviews International**, 12*(1), 71-103.

Jung, E. Y., Suh, H. J., Hong, W. S., Kim, D. G., Hong, Y. H., Hong, I. S., and Chang, U. J. (2009). Uncooked rice of relatively low gelatinization degree resulted in lower metabolic glucose and insulin responses compared with cooked rice in female college students. ***Nutrition Research**, 29*(7), 457-461.

Kainuma, K., and French, D. (1972). Naegeli amylodextrin and its relationship to starch granule structure. II. Role of water in crystallization of B-starch. ***Biopolymers**, 11*(11), 2241-2250.

Kale, S. J., Jha, S. K., Jha, G. K., Sinha, J. P., and Lal, S. B. (2015). Soaking Induced Changes in Chemical Composition, Glycemic Index and Starch Characteristics of Basmati Rice. ***Rice Science**, 22*(5), 227-236.

Kang, N., Zuo, Y. J., Hilliou, L., Ashokkumar, M., and Hemar, Y. (2016). Viscosity and hydrodynamic radius relationship of high-power ultrasound depolymerised starch pastes with different amylose content. ***Food Hydrocolloids**, 52*, 183-191.

Karim, A. A., Norziah, M., and Seow, C. (2000). Methods for the study of starch retrogradation. ***Food Chemistry**, 71*(1), 9-36.

Keeratiburana, T., Hansen, A. R., Soontaranon, S., Tongta, S., and Blennow, A. (2020). Porous rice starch produced by combined ultrasound-assisted ice recrystallization and enzymatic hydrolysis. ***International Journal of Biological Macromolecules***.

Keetels, C., Oostergetel, G., and Van Vliet, T. (1996). Recrystallization of amylopectin in concentrated starch gels. ***Carbohydrate Polymers**, 30*(1), 61-64.

Kiatponglarp, W., Tongta, S., Rolland-Sabate, A., and Buleon, A. (2015). Crystallization and chain reorganization of debranched rice starches in relation to resistant starch formation. ***Carbohydr Polym**, 122*, 108-114.

Klein, B., Pinto, V. Z., Vanier, N. L., Zavareze, E. d. R., Colussi, R., Evangelho, J. A. d., Gutkoski, L. C., and Dias, A. R. G. (2013). Effect of single and dual heat–moisture treatments on properties of rice, cassava, and pinhao starches. ***Carbohydrate Polymers**, 98*(2), 1578-1584.

Kohyama, K., and Sasaki, T. (2006). Differential scanning calorimetry and a model calculation of starches annealed at 20 and 50 C. ***Carbohydrate Polymers**, 63*(1), 82-88.

Kraithong, S., Lee, S., and Rawdkuen, S. (2018). Physicochemical and functional properties of Thai organic rice flour. ***Journal of Cereal Science**, 79*, 259-266.

Kumar, A., Sahoo, U., Baisakha, B., Okpani, O. A., Ngangkham, U., Parameswaran, C., Basak, N., Kumar, G., and Sharma, S. (2018). Resistant starch could be decisive in determining the glycemic index of rice cultivars. ***Journal of Cereal Science**, 79*, 348-353.

Lan, H., Hoover, R., Jayakody, L., Liu, Q., Donner, E., Baga, M., Asare, E., Hucl, P., and Chibbar, R. (2008). Impact of annealing on the molecular structure and physicochemical properties of normal, waxy and high amylose bread wheat starches. ***Food Chemistry**, 111*(3), 663-675.

Lehmann, U., and Robin, F. (2007). Slowly digestible starch–its structure and health implications: a review. ***Trends in Food Science & Technology***, *18*(7), 346-355.

Lehmann, U., and Robin, F. (2007). Slowly digestible starch – its structure and health implications: a review. ***Trends in Food Science & Technology***, *18*(7), 346-355.

Li, J.-Y., and Yeh, A.-I. (2001). Relationships between thermal, rheological characteristics and swelling power for various starches. ***Journal of Food Engineering***, *50*(3), 141-148.

Li, Y., Ding, G., Yokoyama, W., and Zhong, F. (2018). Characteristics of annealed glutinous rice flour and its formation of fast-frozen dumplings. ***Journal of Cereal Science***, *79*, 106-112.

Liu, H., Bao, J., Du, Y., Zhou, X., and Kennedy, J. F. (2006). Effect of ultrasonic treatment on the biochemphysical properties of chitosan. ***Carbohydrate Polymers***, *64*(4), 553-559.

Liu, H., Xie, F., Yu, L., Chen, L., and Li, L. (2009). Thermal processing of starch-based polymers. ***Progress in Polymer Science***, *34*(12), 1348-1368.

Liu, H., Yu, L., Simon, G., Dean, K., and Chen, L. (2009). Effects of annealing on gelatinization and microstructures of corn starches with different amylose/amylopectin ratios. ***Carbohydrate Polymers***, *77*(3), 662-669.

Liu, H., Yu, L., Xie, F., and Chen, L. (2006). Gelatinization of cornstarch with different amylose/amylopectin content. ***Carbohydrate Polymers***, *65*(3), 357-363.

Liu, J., Liu, X. M., Xiao, S. Y., Tong, C. Y., Tang, D. Y., and Zhao, L. J. (2005). Starch nanoparticle as transgenic vehicle mediated by ultrasound. ***Chemical Journal of Chinese Universities-Chinese***, *26*(4), 634-637.

Lorenz, K., and Kulp, K. (1980). Steeping of Starch at Various Temperatures-Effects on Functional Properties. ***Starch-Stärke***, *32*(6), 181-186.

Lu, S., Chen, L. N., and Lii, C. Y. (1997). Correlations between the fine structure, physicochemical properties, and retrogradation of amylopectins from Taiwan rice varieties. ***Cereal Chemistry***, *74*(1), 34-39.

Luo, Z., Fu, X., He, X., Luo, F., Gao, Q., and Yu, S. (2008). Effect of ultrasonic treatment on the physicochemical properties of maize starches differing in amylose content. ***Starch-Stärke***, *60*(11), 646-653.

Luo, Z., and Lu, J. (2010). Effect of ultrasonic treatment on the thermal properties of maize starches. ***Modern Food Science and Technology***, *26*(7), 666-755.

Maache-Rezzoug, Z., Zarguili, I., Loisel, C., Queveau, D., and Buleon, A. (2008). Structural modifications and thermal transitions of standard maize starch after DIC hydrothermal treatment. ***Carbohydrate Polymers***, *74*(4), 802-812.

Madan, K. C., Wan, R., Bakar, N., Jalil, R., Wan, A., Karrila, T., and Pinkaew, S. (2016). Glycaemic index values and physicochemical properties of five brown rice varieties cooked by different domestic cooking methods. ***Functional Foods in Health and Disease***, *6*(8), 506-518.

Majzoobi, M., Seifzadeh, N., Farahnaky, A., and Mesbahi, G. (2015). Effects of sonication on physical properties of native and cross‐linked wheat starches. ***Journal of Texture Studies***, *46*(2), 105-112.

Manchun, S., Nunthanid, J., Limmatvapirat, S., and Sriamornsak, P. (2012). *Effect of ultrasonic treatment on physical properties of tapioca starch*. Paper presented at the Advanced Materials Research.

Maningat, C., and Juliano, B. (1980). Starch lipids and their effect on rice starch properties. ***Starch‐Stärke***, *32*(3), 76-82.

Martin, M., and Fitzgerald, M. (2002). Proteins in rice grains influence cooking properties! ***Journal of Cereal Science***, *36*(3), 285-294.

Martuscelli, E., and Pracella, M. (1974). Effects of chain defects on the thermal behaviour of polyethylene. ***Polymer***, *15*(5), 306-314.

Mason, T., Lorimer, J., and Bates, D. (1992). Quantifying sonochemistry: casting some light on a 'black art'. ***Ultrasonics***, *30*(1), 40-42.

Minakawa, A. F. K., Faria-Tischer, P. C. S., and Mali, S. (2019). Simple ultrasound method to obtain starch micro-and nanoparticles from cassava, corn and yam starches. ***Food Chemistry***, *283*, 11-18.

Mohan, V., Anjana, R. M., Gayathri, R., Ramya Bai, M., Lakshmipriya, N., Ruchi, V., Balasubramaniyam, K. K., Jakir, M. M., Shobana, S., Unnikrishnan, R., Krishnaswamy, K., Henry, J. K., and Sudha, V. (2016). Glycemic Index of a Novel High-Fiber White Rice

Variety Developed in India--A Randomized Control Trial Study. ***Diabetes Technol Ther**, 18*(3), 164-170.

Monroy, Y., Rivero, S., and García, M. A. (2018). Microstructural and techno-functional properties of cassava starch modified by ultrasound. ***Ultrasonics sonochemistry**, 42*, 795-804.

Morris, V. (1990). Starch gelation and retrogradation. ***Trends in Food Science & Technology**, 1*, 2-6.

Nakamura, Y., Sakurai, A., Inaba, Y., Kimura, K., Iwasawa, N., and Nagamine, T. (2002). The fine structure of amylopectin in endosperm from Asian cultivated rice can be largely classified into two classes. ***Starch-Stärke**, 54*(3-4), 117-131.

Nounmusig, J., Kongkachuichai, R., Sirichakwal, P., Yamborisut, U., Charoensiri, R., and Vanavichit, A. (2018). The effect of low and high glycemic index based rice varieties in test meals on postprandial blood glucose, insulin and incretin hormones response in prediabetic subjects. ***International Food Research Journal**, 25*(2), 835-841.

Nuttall, F. Q. (2015). Body mass index: obesity, BMI, and health: a critical review. ***Nutrition today**, 50*(3), 117.

Ogawa, Y. (2016). Chapter 17 - Quality Evaluation of Rice. In D.-W. Sun (Ed.), *Computer Vision Technology for Food Quality Evaluation (Second Edition)* (pp. 413-437). San Diego: Academic Press.

Panlasigui, L. N., and Thompson, L. U. (2006). Blood glucose lowering effects of brown rice in normal and diabetic subjects. ***International journal of food sciences and nutrition**, 57*(3-4), 151-158.

Panlasigui, L. N., Thompson, L. U., Juliano, B. O., Perez, C. M., Yiu, S. H., and Greenberg, G. R. (1991). Rice varieties with similar amylose content differ in starch digestibility and glycemic response in humans. ***The American journal of clinical nutrition**, 54*(5), 871-877.

Park, D. J., and Han, J. A. (2016). Quality controlling of brown rice by ultrasound treatment and its effect on isolated starch. ***Carbohydrate Polymers**, 137*, 30-38.

Patindol, J. A., Siebenmorgen, T. J., and Wang, Y. J. (2015). Impact of environmental factors on rice starch structure: A review. ***Starch-Stärke**, 67*(1-2), 42-54.

Pérez, S., Baldwin, P. M., and Gallant, D. J. (2009). Structural features of starch granules I *Starch* (pp. 149-192): Elsevier.

Piecyk, M., Druzynska, B., Oltarzewska, A., Wolosiak, R., Worobiej, E., and Ostrowska-Ligeza, E. (2018). Effect of hydrothermal modifications on properties and digestibility of grass pea starch. ***Int J Biol Macromol**, 118*(Pt B), 2113-2120.

Pinto, V. Z., Vanier, N. L., Deon, V. G., Moomand, K., El Halal, S. L., Zavareze Eda, R., Lim, L. T., and Dias, A. R. (2015). Effects of single and dual physical modifications on pinhao starch. ***Food Chemistry**, 187*, 98-105.

Polesi, L. F., Junior, M. D. d. M., Sarmento, S. B. S., and Canniatti-Brazaca, S. G. (2017). Starch Digestibility and Physicochemical and Cooking Properties of Irradiated Rice Grains. ***Rice Science**, 24*(1), 48-55.

Ranawana, D., Henry, C., Lightowler, H., and Wang, D. (2009). Glycaemic index of some commercially available rice and rice products in Great Britain. ***International journal of food sciences and nutrition**, 60*(sup4), 99-110.

Rashmi, S., and Urooj, A. (2003). Effect of processing on nutritionally important starch fractions in rice varieties. ***International journal of food sciences and nutrition**, 54*(1), 27-36.

Reed, M. O., Ai, Y., Leutcher, J. L., and Jane, J. l. (2013). Effects of cooking methods and starch structures on starch hydrolysis rates of rice. ***Journal of food science**, 78*(7).

Remsen, C. H., and Clark, J. P. (1978). A visosity model for a cooking dough 1 ***Journal of Food Process Engineering**, 2*(1), 39-64.

Rewthong, O., Soponronnarit, S., Taechapairoj, C., Tungtrakul, P., and Prachayawarakorn, S. (2011). Effects of cooking, drying and pretreatment methods on texture and starch digestibility of instant rice. ***Journal of Food Engineering**, 103*(3), 258-264.

Ritudomphol, O., and Luangsakul, N. (2019). Optimization of Processing Condition of Instant Rice to Lower the Glycemic Index. ***Journal of food science**, 84*(1), 101-110.

Robin, J. (1974). Lint-nerized starches. Gel filtration and enzymatic studies of insoluble residues from prolonged acid treatment of potato starch. ***Cereal Chem.**, 51*, 389-406.

Samarakoon, E., Waduge, R., Liu, Q., Shahidi, F., and Banoub, J. (2020). Impact of annealing on the hierarchical structure and physicochemical properties of waxy starches of different botanical origins. ***Food Chemistry**, 303*, 125344.

Setiawan, S., and Jane, J.-l. (2010). Department of Food Science and Human Nutrition, Iowa State University, Ames, IA 50011. ***Improving feed quality by proper processing of raw materials***, 41.

Sevenou, O., Hill, S., Farhat, I., and Mitchell, J. (2002). Organisation of the external region of the starch granule as determined by infrared spectroscopy. ***International Journal of Biological Macromolecules**, 31*(1-3), 79-85.

Sevenou, O., Hill, S. E., Farhat, I. A., and Mitchell, J. R. (2002). Organisation of the external region of the starch granule as determined by infrared spectroscopy. ***International Journal of Biological Macromolecules**, 31*(1), 79-85.

Shin, S. I., Kim, H. J., Ha, H. J., Lee, S. H., and Moon, T. W. (2005). Effect of Hydrothermal Treatment on Formation and Structural Characteristics of Slowly Digestible Non‐pasted Granular Sweet Potato Starch. ***Starch‐Stärke**, 57*(9), 421-430.

Shin, S. I., Lee, C. J., Kim, M. J., Choi, S. J., Choi, H. J., Kim, Y., and Moon, T. W. (2009). Structural characteristics of low-glycemic response rice starch produced by citric acid treatment. ***Carbohydrate Polymers**, 78*(3), 588-595.

Shu, X., Jia, L., Ye, H., Li, C., and Wu, D. (2009). Slow digestion properties of rice different in resistant starch. ***J Agric Food Chem**, 57*(16), 7552-7559.

Sievert, D., and Pomeranz, Y. (1989). Enzyme-resistant starch. I. Characterization and evaluation by enzymatic, thermoanalytical, and microscopic methods. ***Cereal Chem**, 66*(4), 342-347.

Sievert, D., and Wuesch, P. (1993). Amylose chain association based on differential scanning calorimetry. ***Journal of food science**, 58*(6), 1332-1335.

Sitch, L. A. (1990). Incompatibility barriers operating in crosses of Oryza sativa with related species and genera *Gene Manipulation in Plant Improvement II* (pp. 77-93): Springer.

Sittipod, S. (2014). *Changes in rice kernel and starch during parboiling process.* Kansas State University.

Slade, L., and Levine, H. (1987). Recent advances in starch retrogradation. ***Industrial polysaccharides***, 387-430.

Slade, L., and Levine, H. (1988). Non-equilibrium melting of native granular starch: Part I. Temperature location of the glass transition associated with gelatinization of A-type cereal starches. ***Carbohydrate Polymers***, *8*(3), 183-208.

Sowbhagya, C., and Bhattacharya, K. (1979). Simplified determination of amylose in milled rice. ***Starch=Stärke***, *31*(5), 159-163.

Srichuwong, S., Sunarti, T. C., Mishima, T., Isono, N., and Hisamatsu, M. (2005). Starches from different botanical sources I: Contribution of amylopectin fine structure to thermal properties and enzyme digestibility. ***Carbohydrate Polymers***, *60*(4), 529-538.

Sujka, M. (2017). Ultrasonic modification of starch - Impact on granules porosity. ***Ultrason Sonochem***, *37*, 424-429.

Sujka, M., and Jamroz, J. (2013). Ultrasound-treated starch: SEM and TEM imaging, and functional behaviour. ***Food Hydrocolloids***, *31*(2), 413-419.

Sun, L., Ranawana, D. V., Tan, W. J. K., Quek, Y. C. R., and Henry, C. J. (2015). The impact of eating methods on eating rate and glycemic response in healthy adults. ***Physiology & behavior***, *139*, 505-510.

Takeda, Y., Shibahara, S., and Hanashiro, I. (2003). Examination of the structure of amylopectin molecules by fluorescent labeling. ***Carbohydrate Research***, *338*(5), 471-475.

Tester, R., Debon, S., and Sommerville, M. (2000). Annealing of maize starch. ***Carbohydrate Polymers***, *42*(3), 287-299.

Tester, R. F., Karkalas, J., and Qi, X. (2004). Starch—composition, fine structure and architecture. ***Journal of Cereal Science***, *39*(2), 151-165.

Thirumdas, R., Saragapani, C., Ajinkya, M. T., Deshmukh, R. R., and Annapure, U. S. (2016). Influence of low pressure cold plasma on cooking and textural properties of brown rice. ***Innovative Food Science & Emerging Technologies***, *37*, 53-60.

Tirosh, A., Shai, I., Tekes-Manova, D., Israeli, E., Pereg, D., Shochat, T., Kochba, I., and Rudich, A. (2005). Normal fasting plasma glucose levels and type 2 diabetes in young men. ***New England Journal of Medicine***, *353*(14), 1454-1462.

Trung, P. T. B., Ngoc, L. B. B., Hoa, P. N., Tien, N. N. T., and Hung, P. V. (2017). Impact of heat-moisture and annealing treatments on physicochemical properties and digestibility of starches from different colored sweet potato varieties. ***International Journal of Biological Macromolecules,*** *105*(Part 1), 1071-1078.

Truong, T. H., Yuet, W. C., and Hall, M. D. (2014). Glycemic index of American-grown jasmine rice classified as high. ***International journal of food sciences and nutrition,*** *65*(4), 436-439.

Tsutsui, K., Katsuta, K., Matoba, T., Takemasa, M., Funami, T., Sato, E., and Nishinari, K. (2013). Effects of time and temperature of annealing on rheological and thermal properties of rice starch suspensions during gelatinization. ***Journal of Texture Studies,*** *44*(1), 21-33.

Ulbrich, M., Bai, Y., and Flöter, E. (2020). The supporting effect of ultrasound on the acid hydrolysis of granular potato starch. ***Carbohydrate Polymers,*** *230*, 115633.

Ulloa, J. A., Enríquez López, K. V., Contreras Morales, Y. B., Rosas Ulloa, P., Ramírez Ramírez, J. C., and Ulloa Rangel, B. E. (2015). Effect of ultrasound treatment on the hydration kinetics and cooking times of dry beans (Phaseolus vulgaris). ***CyTA - Journal of Food***, 1-9.

Vamadevan, V., and Bertoft, E. (2018). Impact of different structural types of amylopectin on retrogradation. ***Food Hydrocolloids,*** *80*, 88-96.

van Soest, J. J. G., and Vliegenthart, J. F. G. (1997). Crystallinity in starch plastics: consequences for material properties. ***Trends in Biotechnology,*** *15*(6), 208-213.

Vandeputte, G., Derycke, V., Geeroms, J., and Delcour, J. (2003). Rice starches. II. Structural aspects provide insight into swelling and pasting properties. ***Journal of Cereal Science,*** *38*(1), 53-59.

Varavinit, S., Shobsngob, S., Varanyanond, W., Chinachoti, P., and Naivikul, O. (2003). Effect of amylose content on gelatinization, retrogradation and pasting properties of flours from different cultivars of Thai rice. ***Starch=Stärke,*** *55*(9), 410-415.

Waduge, R., Hoover, R., Vasanthan, T., Gao, J., and Li, J. (2006). Effect of annealing on the structure and physicochemical properties of barley starches of varying amylose content. ***Food Research International,*** *39*(1), 59-77.

Waduge, R. N., Hoover, R., Vasanthan, T., Gao, J., and Li, J. (2006). Effect of annealing on the structure and physicochemical properties of barley starches of varying amylose content. ***Food Research International**, 39*(1), 59-77.

Waigh, T. A., Jenkins, P. J., and Donald, A. M. (1996). Quantification of water in carbohydrate lamellae using SANS. ***Faraday Discussions**, 103*, 325-337.

Walter, M., Marchezan, E., and Avila, L. A. d. (2008). Rice: composition and nutritional characteristics. ***Ciência Rural**, 38*(4), 1184-1192.

Wang, H., Xu, K., Ma, Y., Liang, Y., Zhang, H., and Chen, L. (2020). Impact of ultrasonication on the aggregation structure and physicochemical characteristics of sweet potato starch. ***Ultrasonics sonochemistry**, 63*, 104868.

Wang, S., Li, C., Copeland, L., Niu, Q., and Wang, S. (2015). Starch retrogradation: A comprehensive review. ***Comprehensive Reviews in Food Science and Food Safety**, 14*(5), 568-585.

Wang, S., Wang, J., Wang, S., and Wang, S. (2017). Annealing improves paste viscosity and stability of starch. ***Food Hydrocolloids**, 62*, 203-211.

Wang, W., Powell, A., and Oates, C. (1997). Effect of annealing on the hydrolysis of sago starch granules. ***Carbohydrate Polymers**, 33*(2-3), 195-202.

Wani, A. A., Singh, P., Shah, M. A., Schweiggert-Weisz, U., Gul, K., and Wani, I. A. (2012). Rice Starch Diversity: Effects on Structural, Morphological, Thermal, and Physicochemical Properties-A Review. ***Comprehensive Reviews in Food Science and Food Safety**, 11*(5), 417-436.

Warren, F. J., Gidley, M. J., and Flanagan, B. M. (2016). Infrared spectroscopy as a tool to characterise starch ordered structure—a joint FTIR–ATR, NMR, XRD and DSC study. ***Carbohydrate Polymers**, 139*, 35-42.

Webb, B. (1991). Rice quality and grades *Rice* (pp. 508-538): Springer.

Wolever, T. M., and Jenkins, D. J. (1986). The use of the glycémie index in predicting the blood glucose response to mixed meals. ***The American journal of clinical nutrition**, 43*(1), 167-172.

Wolever, T. M., Jenkins, D. J., Jenkins, A. L., and Josse, R. G. (1991). The glycemic index: methodology and clinical implications. ***The American journal of clinical nutrition***, *54*(5), 846-854.

Wordu, G., and Banigo, E. (2013). Evaluation of the glycemic index of some cooked variety of rice products in Nigeria. ***Net Journal of Agricultural Science***, *1*(2), 38-41.

Xu, M., Saleh, A. S., Gong, B., Li, B., Jing, L., Gou, M., Jiang, H., and Li, W. (2018). The effect of repeated versus continuous annealing on structural, physicochemical, and digestive properties of potato starch. ***Food Research International***, *111*, 324-333.

Xu, M., Saleh, A. S. M., Liu, Y., Jing, L., Zhao, K., Wu, H., Zhang, G., Yang, S. O., and Li, W. (2018). The Changes in Structural, Physicochemical, and Digestive Properties of Red Adzuki Bean Starch after Repeated and Continuous Annealing Treatments. ***Starch - Stärke***, *70*(9-10), 1700322.

You, S. Y., Oh, S. G., Han, H. M., Jun, W., Hong, Y. S., and Chung, H. J. (2016). Impact of germination on the structures and in vitro digestibility of starch from waxy brown rice. ***Int J Biol Macromol***, *82*, 863-870.

Zavareze, E. d. R., and Dias, A. R. G. (2011). Impact of heat-moisture treatment and annealing in starches: A review. ***Carbohydrate Polymers***, *83*(2), 317-328.

Zavareze Roa, E., Storck, C. R., de Castro, L. A. S., Schirmer, M. A., and Dias, A. R. G. (2010). Effect of heat-moisture treatment on rice starch of varying amylose content. ***Food Chemistry***, *121*(2), 358-365.

Zeng, F., Ma, F., Kong, F., Gao, Q., and Yu, S. (2015). Physicochemical properties and digestibility of hydrothermally treated waxy rice starch. ***Food Chem***, *172*, 92-98.

Zhang, S., Li, Z., Lin, L., Zhang, L., and Wei, C. (2019). Starch Components, Starch Properties and Appearance Quality of Opaque Kernels from Rice Mutants. ***Molecules***, *24*(24), 4580.

Zheng, J., Li, Q., Hu, A. J., Yang, L., Lu, J., Zhang, X. Q., and Lin, Q. Q. (2013). Dual-frequency ultrasound effect on structure and properties of sweet potato starch. ***Starch-Starke***, *65*(7-8), 621-627.

Zhong, Y., Xiang, X., Zhao, J., Wang, X., Chen, R., Xu, J., Luo, S., Wu, J., and Liu, C. (2020). Microwave pretreatment promotes the annealing modification of rice starch. ***Food Chemistry****, 304*, 125432.

Zhou, Z., Robards, K., Helliwell, S., and Blanchard, C. (2002). Composition and functional properties of rice. ***International Journal of Food Science & Technology****, 37*(8), 849-868.

Zhu, F. (2015). Impact of ultrasound on structure, physicochemical properties, modifications, and applications of starch. ***Trends in Food Science & Technology****, 43*(1), 1-17.

Zhu, J., Li, L., Chen, L., and Li, X. (2012). Study on supramolecular structural changes of ultrasonic treated potato starch granules. ***Food Hydrocolloids****, 29*(1), 116-122.

Zhu, L.-J., Liu, Q.-Q., Wilson, J. D., Gu, M.-H., and Shi, Y.-C. (2011). Digestibility and physicochemical properties of rice (Oryza sativa L.) flours and starches differing in amylose content. ***Carbohydrate Polymers****, 86*(4), 1751-1759.

Zhu, L., Zhang, Y., Wu, G., Qi, X., Dag, D., Kong, F., and Zhang, H. (2020). Characteristics of pasting properties and morphology changes of rice starch and flour under different heating modes. ***International Journal of Biological Macromolecules***.

Zuo, J. Y., Knoerzer, K., Mawson, R., Kentish, S., and Ashokkumar, M. (2009). The pasting properties of sonicated waxy rice starch suspensions. ***Ultrasonic Sonochemistry****, 16*(4), 462-468.

Zuo, Y. Y., Hebraud, P., Hemar, Y., and Ashokkumar, M. (2012). Quantification of high-power ultrasound induced damage on potato starch granules using light microscopy. ***Ultrason Sonochem****, 19*(3), 421-426.

# APPENDIX A

## A1. Determination of Amylose content (Juliano, 1970)

### 1.1 Equipment

1.1.1 100 ml volumetric flasks

1.1.2 Cylinders, etc.

1.1.3 Hot plate

1.1.4 Pipettes

1.1.5 Spectrophotometer

### 1.2 Chemical and reagents

1.2.1 Acetic acid, 1.0 N

1.2.2 Amylose, from potato

1.2.3 Ethanol, 95%

1.2.4 Hydrochloric acid

1.2.5 Iodine solution, 0.2% I2 and 2% KI in distilled water

1.2.6 Sodium hydroxide, 0.09 N

1.2.7 Sodium hydroxide, 1.0 N

### 1.3 Procedure

100 mg of ground rice was weighed and transferred to 100 ml volumetric flask. Then, added 1 ml of 95% ethanol, carefully washing down any samples adhering to side of the flask. After that, 9 ml of 1 N sodium hydroxide was added to each sample and heat in a boiling water for 10 min and then cooling at room temperature. Solution was made to 100 ml volume with distilled water and then vortex vigorously and obtain 1 mg/ml solution. The solution was stand for at least 2 h. before continuing next step. This solution was pipetted 5 ml into 100 ml volumetric flask containing 50 ml distilled water. Next, added 1.0 ml of 1 N acetic acid and mixed together and then added 2 ml of iodine solution. Added distilled water to make volume up to 100 ml and let stand for 20 min for measuring an absorbance at 620 nm.

### 1.4 Procedure for standard curve preparation

Potato amylose was wight 40 mg into 100 ml volumetric flask. Then, added 1 ml of 95% ethanol, carefully washing down any samples adhering to side of the flask. Pipette 1, 2, 3, 4, and 5 ml of solution into 100 ml volumetric flask with 50 ml of distilled water. After that, 9 ml of 1 N sodium hydroxide was added to each sample and heat in a boiling water for 10 min and then cooling at room temperature. Solution was made to 100 ml volume with distilled water and then vortex vigorously and obtain 1 mg/ml solution. The solution was stand for at least 2 h. before continuing next step. This solution was pipetted 5 ml into 100 ml volumetric flask containing 50 ml distilled water. Next, added 1.0 ml of 1 N acetic acid and mixed together and then added 2 ml of iodine solution. Added distilled water to make volume up to 100 ml and let stand for 20 min for measuring an absorbance at 620 nm. The amylose content expressed as the percentage of dry matter calculating by using the linear equation from standard amylose (Figure A-1).

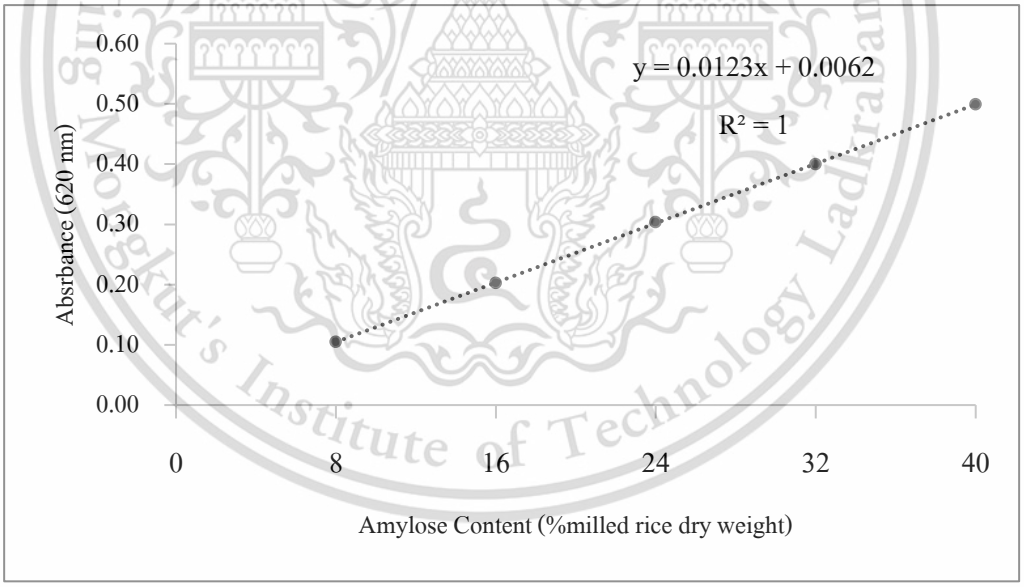


**Figure A-1** Standard curve for amylose determination

## A2. Determination of moisture content

### 2.1 Equipment

2.1.1 Hot air oven

2.1.2 Desiccator

2.1.3 Aluminum can

### 2.2 Procedure

2.2.1 Dry the empty aluminum cans and cover in the hot air oven at 105°C for 3 h and transfer to a desiccator at room temperature to cool. Weigh the empty aluminum pans.

2.2.2 The samples are weighted about 3.00±0.05 g into aluminum can.

2.2.3 Place the aluminum can with sample into the hot air oven for 4 h at 105°C.

2.2.4 After drying, the aluminum can to a desiccator to cool. Reweigh the dish and its dried sample. The moisture content was calculated following the equation as below:

$$\text{Moisture content (\%)} = \frac{(W1 - W2) \times 100}{W1}$$

Where: W1 = weight of sample before drying (g)

W2 = weight of sample after drying (g)

# APPENDIX B

## B-1. FTIR patterns of three rice cultivars

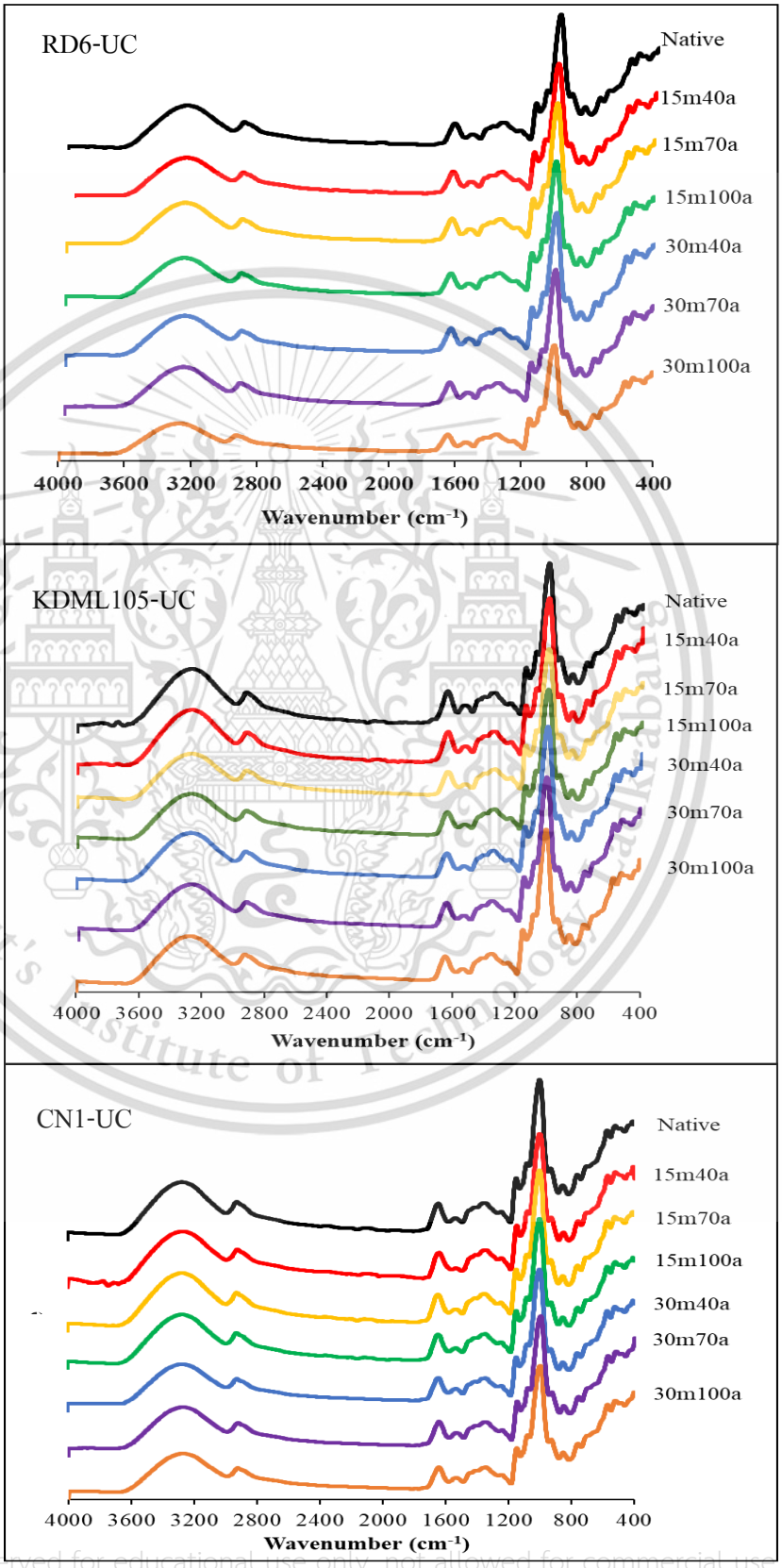


**Figure B.1** The FTIR patterns of natives, and ultrasound – chilling treatments of three rice cultivars

**B-2. Examples of native, and ultrasound treated RD6 rice grains.**

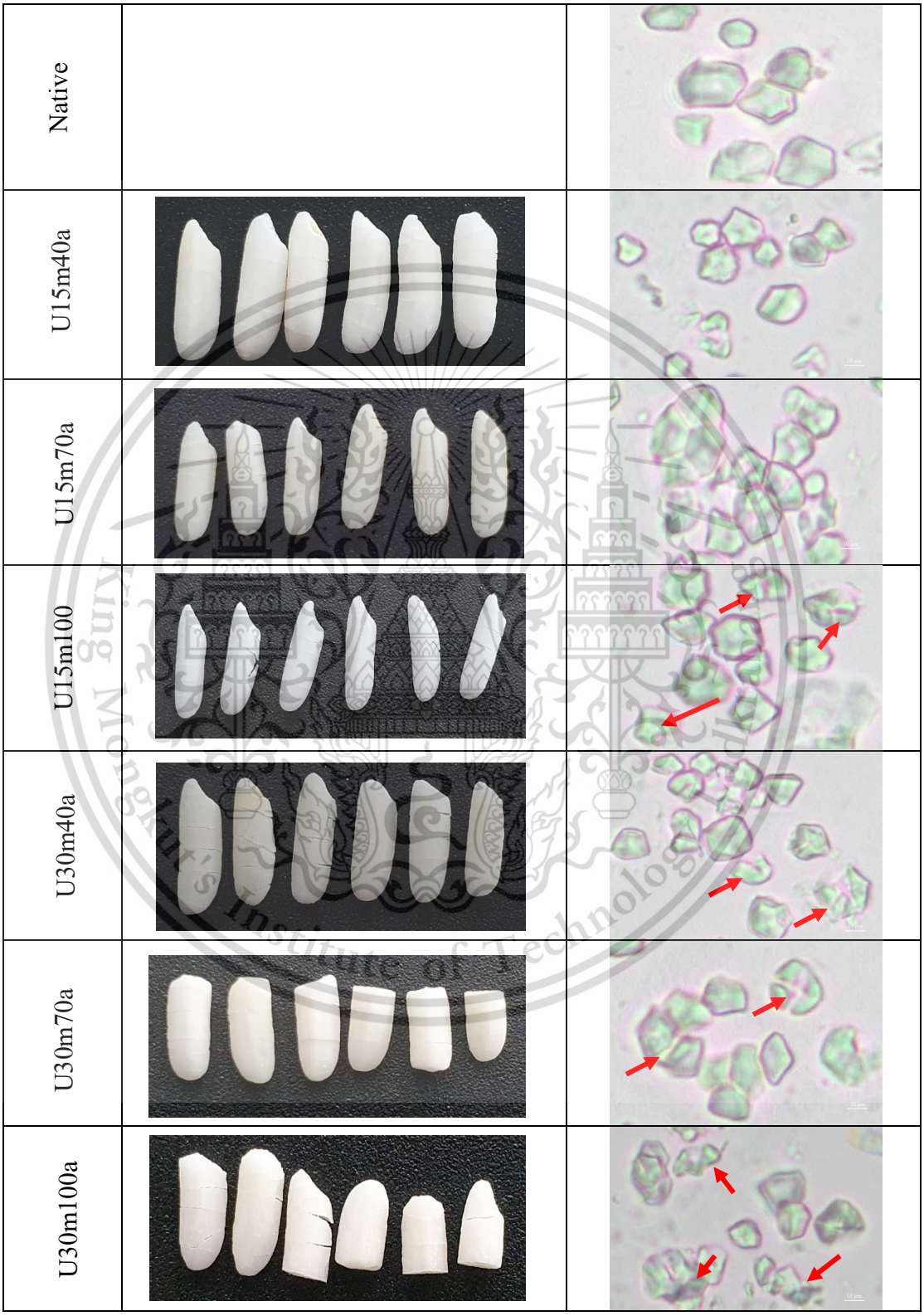


**Figure B.2** Rice grain photographs and rice powder granules of native and ultrasound treatments observed under normal light with 40× magnification.

**B-3. Examples of native, and ultrasound treated KDML105 rice.**

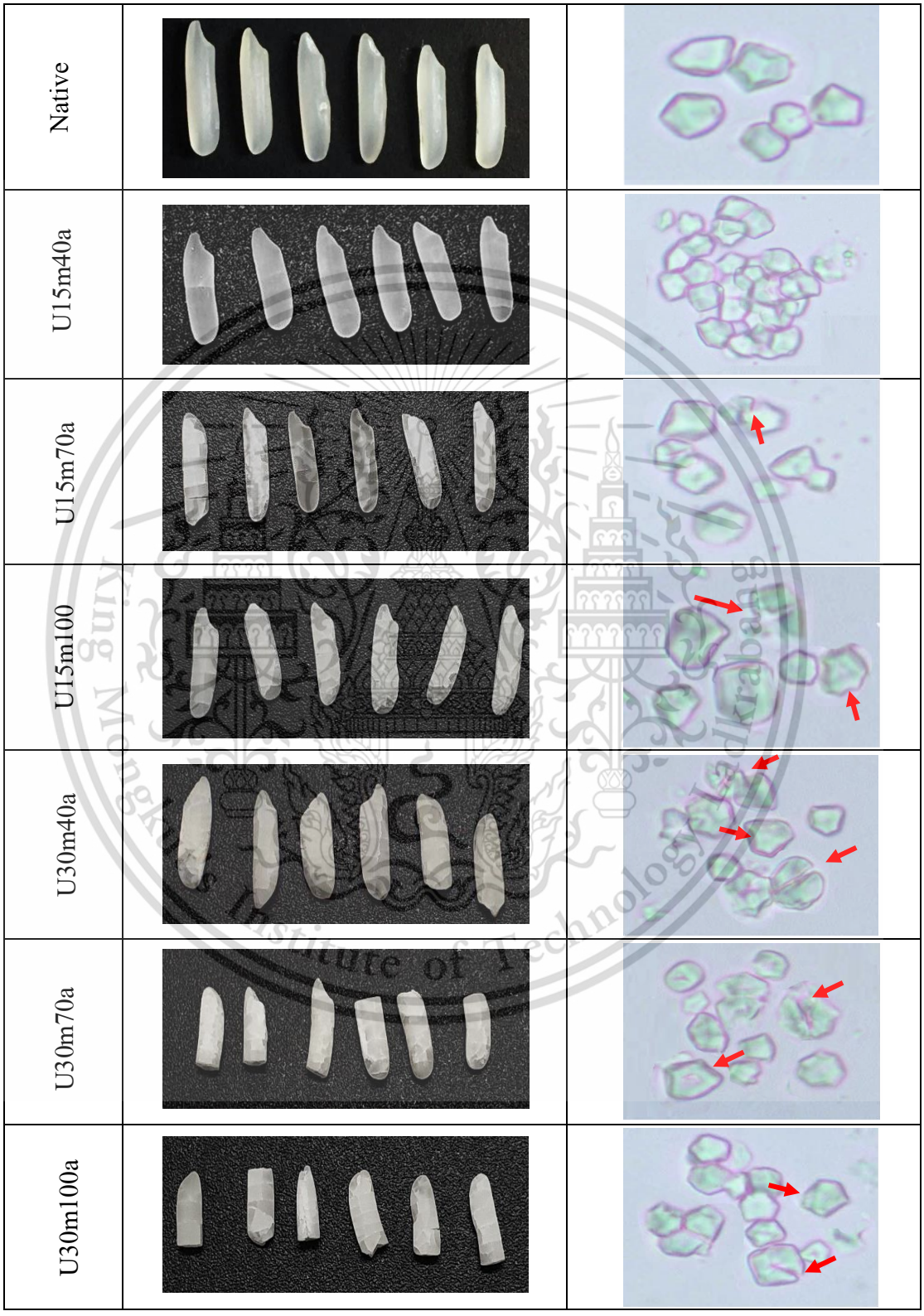


**Figure B.3** Rice grain photographs and rice powder granules of native and ultrasound treatments observed under normal light with 40× magnification.

**B-4. Examples of native, and ultrasound treated CN1 rice grains.**

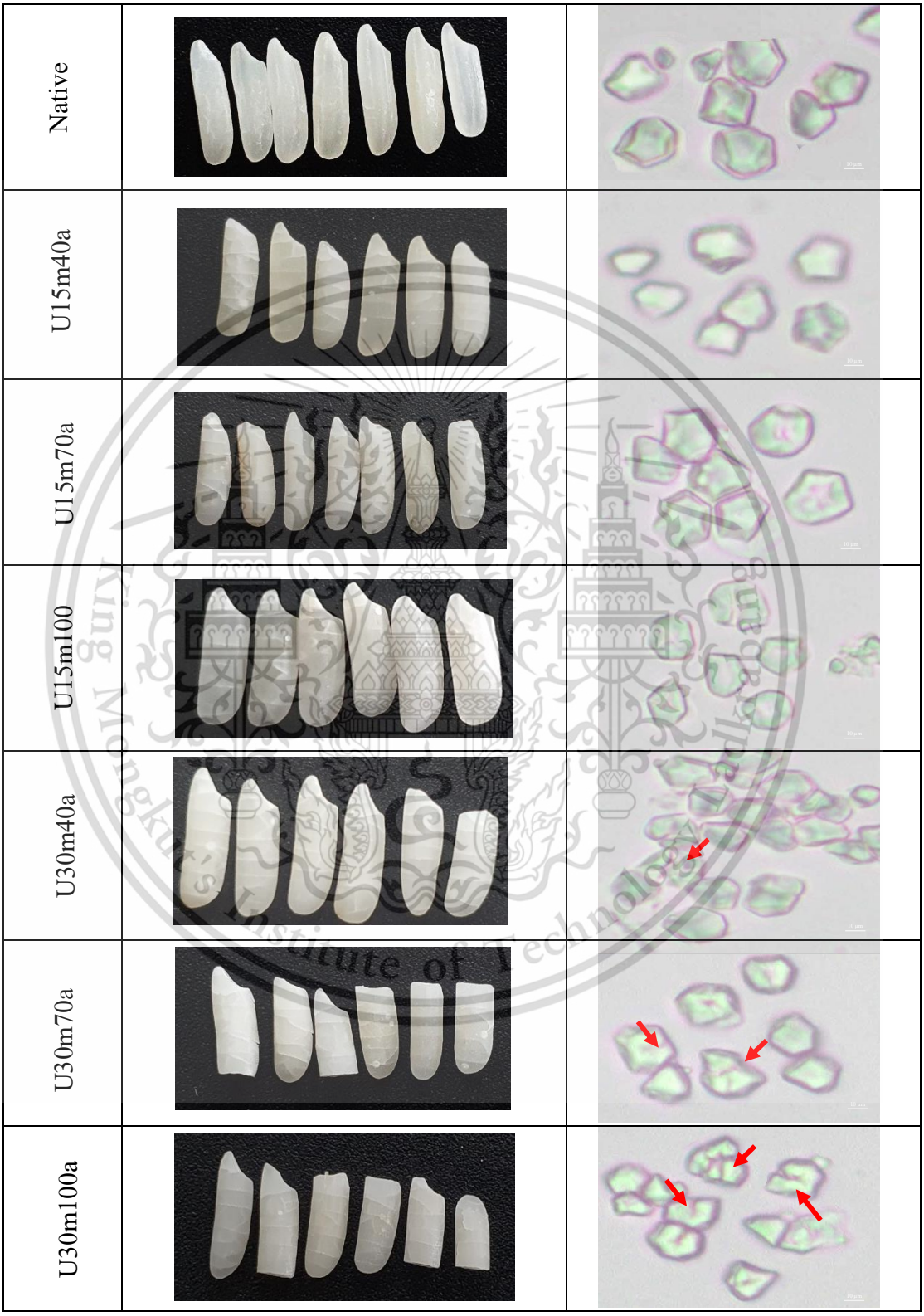


**Figure B.4** Rice grain photographs and rice powder granules of native and ultrasound treatments observed under normal light with 40× magnification.

**B-5. Examples of native, ultrasound-chilling and ultrasound-chilling and annealing treated rice grains for three rice cultivars.**

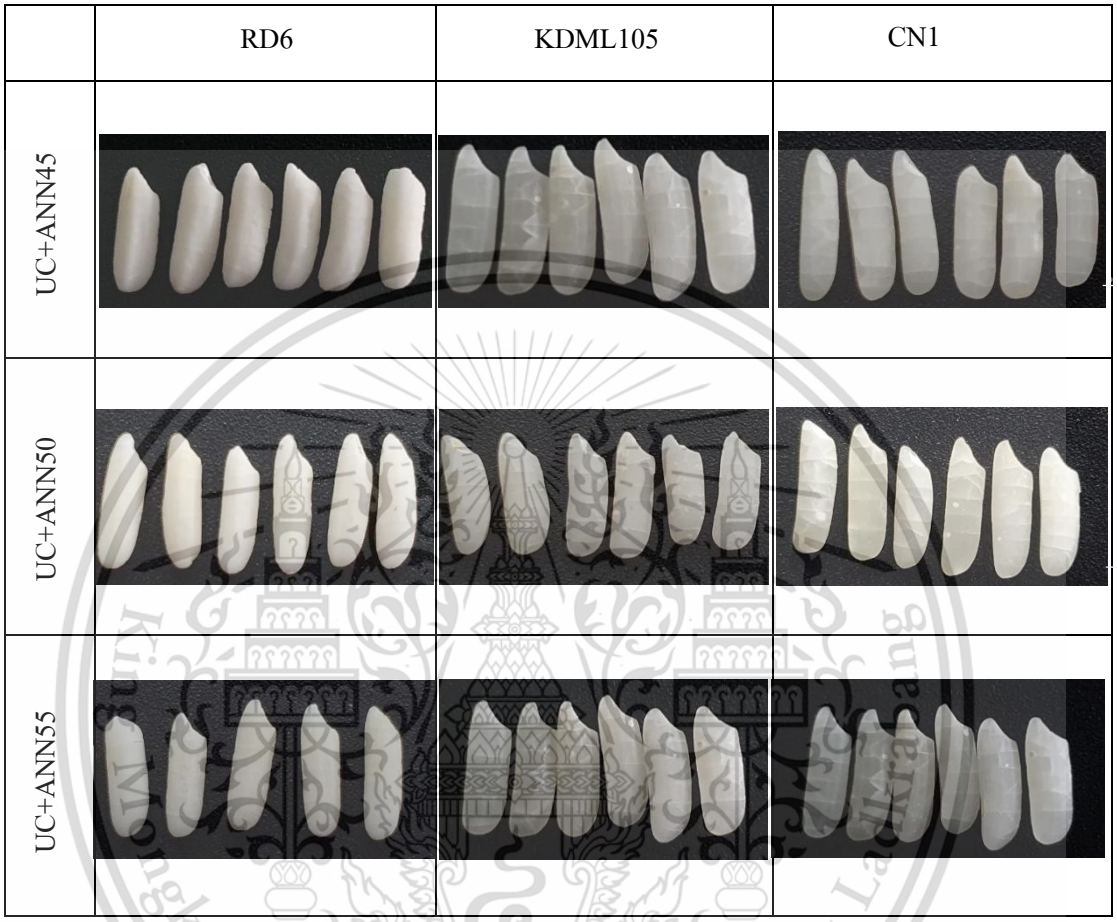


**Figure B.5** Rice grain photographs of native, ultrasound-chilling (UC) and ultrasound-chilling followed annealing treatments (UC+ANN).

# AUTHOR BIOGRAPHY

**Name** Miss Kannika Kunyanee

**Educations**

B.Sc. (Food Science), King Mongkut's Institute of Technology Ladkrabang.

M.Sc. (Food Science and Technology), Burapha University.

Ph.D. (Food Science) King Mongkut's Institute of Technology Ladkrabang.

**Awards**

The best oral presentation at the 7th International Conference on Integration of Science and Technology for Sustainable Development (7th ICIST) held on 26-29 November 2018, Bali, Indonesia.

The best oral presentation at the 8th International Conference on Integration of Science and Technology for Sustainable Development (8th ICIST) held on 19-22 November 2019, Anhui province, PR China.

**Publications**

Kunyanee K. and Luangsakul N. (2020). The effects of ultrasound - assisted recrystallization followed by chilling to produce the lower glycemic index of rice with different amylose content. ***Food Chemistry***. 323, 1-9.

Kunyanee K. and Luangsakul N. (2019). The effects of dual modification with ultrasound and annealing treatments on the properties and glycemic index of the Thai glutinous rice cultivar 'RD6'. ***International Journal of Agricultural Technology***. 15(6), 933-946.

Kunyanee K. and Luangsakul N. (2018). The utilization of ultrasound and chilling treatment to reduce GI in Thai glutinous rice (RD6). ***International Journal of Agricultural Technology***. 14(7), 1365-1378.